2019-09-08

Investigation of Therapeutic Immune Cell Metabolism

Josephine Anna Tueller
Brigham Young University

Investigation of Therapeutic Immune Cell Metabolism

Josephine Anna Tueller

A thesis submitted to the faculty of
Brigham Young University
in partial fulfillment of the requirements for the degree of

Master of Science

K. Scott Weber, Chair
Julianne H. Grose
Kim L. O'Neill

Department of Microbiology and Molecular Biology

Brigham Young University

ABSTRACT

Investigation of Therapeutic Immune Cell Metabolism

Josephine Anna Tueller
Department of Microbiology and Molecular Biology, BYU
Master of Science

This thesis addresses multiple approaches to investigating mechanisms of immune linked disease. There are four projects outlined below which describe the work of these investigations.

First, educating students about techniques to study disease and therapies is an important area of research. Flow cytometry is a common technique in immunology and its versatility and high throughput abilities can be applied to many fields. While it is very useful, flow cytometry is a complex technique that requires training to operate and understand, and there are very few reports about administering effective training. This thesis outlines the first report of a full semester university course about flow cytometry. Students who completed the course reported increased confidence in their skill levels in conceptual, technical and analytical areas.

Second, in the fight against cancer, immunotherapies may provide the necessary adaptability to successfully combat many cancer types. By strengthening and educating the immune system, clinicians can help patients fight cancer without resorting to harmful chemotherapeutics, or immunotherapies can be used in tandem with current treatments. Chimeric antigen receptor (CAR) T cells and checkpoint blockade are two of the most successful immunotherapies. CAR T cells combine the extraordinary binding ability of an antibody with T cell signaling molecules via genetic engineering, for a faster and more efficient cancer killing version of the patient's own T cells. These have been remarkably successful, but results depend on the specific signaling co-receptors that are included in the design. Increased understanding of co-receptor function could help in making CAR T cell design more specific, and enable CAR T cells to be effective against more types of cancers. Metabolic function is crucial in understanding T cell therapeutics because T cells need to use energy efficiently enough to compete with ravenous cancer cells. This thesis outlines an ongoing investigation into a co-receptor's effect on CAR T cell metabolism, suggesting that co-receptors can alter CAR T cell metabolism by increasing maximal respiration.

Third, CD5 is a negative regulatory co-receptor on T cells that can modulate T cell activation. Related inhibitory co-receptors (PD-1 and CTLA-4) are currently being effectively blocked as checkpoint therapies to reactivate T cells towards cancerous cells. This thesis outlines ongoing work investigating CD5's impact on cellular metabolism. We have found that T cells without CD5 are hypermetabolic as compared to normal naïve T cells. CD5 deficient T cells also have higher maximal respiration, higher basal respiration and higher glycolytic capacity. These differences are also present transiently after non-specific activation. Thus, CD5 significantly regulates the ability of a T cell to use energy, suggesting that CD5 may be a good target for creating more efficient T cell immunotherapies.

Fourth, in a separate project, this thesis examines environmental causes of disease. Asthma and allergies are common and growing problems in children and adults. Evaporative cooling can be a less expensive alternative to central cooling, but its effects on allergens and other bioaerosols in the home remains unclear. This project examines the relationship between evaporative cooling and bioaerosols (dust mites, bacterial endotoxin, and fungal β-(1→3)-D-glucans) in low income homes in Utah. We report significantly higher levels of these bioaerosols, particularly fungi in homes with evaporative cooling after adjusting for home-specific factors.

Keywords: T cells, Flow cytometry, CAR T cells, metabolism, CD5, asthma

ACKNOWLEDGEMENTS

Thank you to the College of Life Sciences Teaching Enhancement Grant for funding to improve the flow cytometry class, and a deep thank you to the Simmons Center for Cancer Research for invaluable support for early and late research on this project.

Thank you to Dr. Weber for all of your mentoring, and for helping me to learn to be a scientist. Thanks as well to Dr. Andersen, Dr. Grose, and Dr. O'Neill for invaluable advice and questions along the way.

I am immensely grateful to Claudia Freitas for handing me a microcentrifuge tube and the motivation to start. This was all your idea—thank you for believing that I could do it. Thank you also to Kiara Whitley and Deborah Johnson for teaching me from the beginning. Somewhere between all of my many questions, you've become true friends.

Thank you to Graceaphine, Isa, Oli, Mo, thanks for being the best role models a big sister could have, to Mom and Dad, thank you for believing in this dream of mine, and helping me to make it happen, and the biggest thank you to Michael who listened to every presentation more times than anyone should, and has supported me through all of it.

TABLE OF CONTENTS

LIST OF TABLES

LIST OF FIGURES

CHAPTER 1: INTRODUCTION

1.1 Introduction

A more complete understanding of the causes and means to treat disease is obtained by investigating it from multiple angles. The immune system is a remarkably complex network of cells and organs that protect bodies from the most complex diseases [1]. Examination of the interaction between the immune system and foreign and self-antigens can provide critical insights for fighting diseases more effectively.

Scientists often use complex tools to gain information about biological processes. One valuable tool in the scientific toolbox is called flow cytometry. It is a very common technique in immunological research, but it is a versatile technology with possible applications in many fields [2]. Flow cytometry is a high throughput technique, meaning it can measure large amounts of valuable data in a short amount of time, but it is also complex and highly technical, requiring a high level of training to properly use it. Educating students with the conceptual, technical, and analytical skills needed to use this technique enable scientists to make important discoveries at universities, hospitals and in industry [3]. Chapter 2 of this thesis describes a novel class started here at Brigham Young University to better educate undergraduate and graduate students on how to design, run and analyze flow cytometry experiments.

Understanding the basic science behind the immune system has led to incredible new solutions to some of the most difficult problems. Cancer is a terrible, multifaceted disease, and the current standard of chemotherapy and radiation can be brutally harmful for a patient, albeit effective in many cases [4]. Immunotherapy is a powerful possible alternative, which uses a patient's own immune system to target, kill and suppress cancer [5]. By giving immune cells

extra abilities to recognize and remove cancer cells using genetic engineering, these engineered immune cells can more effectively compete against cancer [6].

T cells direct the immune system, so creating T cells with optimized receptors, known as chimeric antigen receptors (CAR), can have a positive effect on the entire immune system. These therapies have been very effective in clinical trials and were recently approved for certain types of leukemia [7-9]. However, CAR T cells are generally ineffective in solid tumors, due to numerous factors [10]. One of these factors is the lack of nutrients in the tumor microenvironment, because the cancer cells have used up all available resources, leaving immune cells unable to do their job effectively [11-14]. Understanding how CAR T cells utilize energy could be useful in tailoring CAR T cell therapy to the patient and their individual disease progression. Chapter 3 of this thesis outlines work I have done to understand how different generation of CAR constructs alter T cell metabolic function.

Recent breakthroughs in immunotherapy have enabled clinicians to stop the function of also molecules that inhibit the immune system. The Nobel prize in medicine in 2019 was awarded to James P. Allison and Tasuku Honjo for their discovery of negative regulatory molecules known as checkpoints (PD-1, CTLA-4) that can stop immune cells from working [15]. These are very useful normally to prevent an overreaction by the immune system, especially in preventing autoimmunity. Unfortunately, tumor cells often use this mechanism to their advantage by signaling through these negative regulatory pathways to stop immune cells from attacking [16]. Checkpoint inhibitor therapies work simply by blocking the checkpoint molecule with an antibody, allowing the immune cells to remain active in a suppressive tumor environment. These therapies have been very effective for certain types of cancers [17, 18], and open the door for immune modulation in cancer. The known mechanisms work through very

distinct pathways and scenarios, suggesting that characterizing additional negative regulatory molecules can allow for more fine-tuned and diverse treatment of cancers that are not responding to current checkpoint inhibitor therapies [19, 20]. CD5 is a negative regulatory molecule found on the surface of T cells that is primarily known for its role in T cell development [21-23]. Understanding how CD5 can affect normal T cell function could aid in immunotherapy, and a better knowledge of how the immune system monitors the health of the body. Chapter 4 of this thesis describes my work to understand the role of CD5 in T cell metabolic function and how altering CD5 may alter T cell function.

In a separate project, the role of environmental causes of disease in the home was also studied. Asthma is prevalent in 5% of children and has risen dramatically in recent years, causing major quality of life burdens and increased health care costs for these individuals and their families [24, 25]. This research focused on a major potential source of asthma, the quality of air inside the home and exposure to potential allergens. A growing body of literature suggests that evaporative coolers have the potential to significantly alter the microbiological and bioaerosol profile of homes in dry climates. Evaporative coolers have recently been incentivized as an environmentally conscious option for cooling in arid environments, but the health effects of using an evaporative cooler compared to central air conditioners remains unclear [26, 27]. To address this question, dust was collected from low income homes with evaporative coolers or with central air, and then tested for dust mite allergens, bacterial endotoxin, and β-(1→3)-D-glucans. Chapter 5 of this thesis describes the results of this study which found that homes with evaporative coolers have significantly higher levels of potential asthma triggers.

CHAPTER 2: FLOW CYTOMETRY EDUCATION

This work described in this chapter has been submitted to a scientific journal and is under review. It has been formatted for this thesis but is otherwise unchanged.

A Full Semester Flow Cytometry Course Improves Graduate and Undergraduate Student Confidence and Interest

Josie A. Tueller, Kiara V. Whitley, and K. Scott Weber

Department of Microbiology and Molecular Biology,
Brigham Young University, Provo, Utah, United States of America

2.1 Abstract

Flow cytometry is a versatile and high throughput technique for rapid and efficient biological testing. It requires a high level of conceptual, technical, and analytical skills to properly design experiments, effectively operate flow cytometry machines, and analyze the data. A lack of training and development of any of these three skills can result in underutilization and improper use of flow cytometric machines that can impede research progress. Often students develop these conceptual, technical, and analysis skills from trial and error, but many students either do not use this powerful flow cytometry technology, use it improperly or ineffectively, or give up using it without proper training and support. Here we report on a course which teaches flow cytometry skills to undergraduate and graduate students. The design of this course is unique in that it teaches conceptual, technical, and analytical skills related to flow cytometry in a full semester format. Undergraduate and graduate students reported significant increases in their confidence levels over the course of the semester. Here we provide our findings and resources for others who may want to implement a similar course.

2.2 Introduction

Flow cytometry is a technique that can be used to simultaneously quantify multiple markers on a single cell and analyze thousands of cells in a matter of seconds [28-30]. It is remarkably powerful and useful for many different disciplines [31]. The field itself is rapidly expanding and there is an important need for effective training [29]. Numerous novel applications of flow cytometry are being identified and developed, increasing the versatility of its use [32]. Academic interest of both faculty and students in using this technology has risen, increasing the need for student training so this technology and innovative uses can be understood and utilized.

To effectively utilize flow cytometry in academic settings, undergraduate and graduate students need to be competent in understanding proper experimental setup and design, executing effective machine usage and data acquisition, and performing appropriate data analysis [33, 34]. Lack of education in flow cytometry conceptual, technical, and analytical skills often leads to student learning by trial and error, which can result in expensive machine repair or waste of costly resources [2]. We have also seen that lack of education on the university level has resulted in underutilization of flow cytometric machinery. These two issues highlight the need for more education in flow cytometry in academic settings where students are actively involved in learning how to perform research.

In addition to improving research efficiency and productivity, flow cytometry education can also provide a useful skill set to students for future career opportunities in academics or industry [35]. Very few papers have been published outlining flow cytometry education efforts. Here we provide a brief summary of the published papers describing flow cytometry education efforts in a classroom setting (Table 1).

Table 2-1: A brief review of existing flow cytometry education papers

Audience/Purpose	Time	Takeaway	Reference
Undergraduate students and research trainees	Three hour tutorial and a three day program	An active and collaborative approach aids learning	[36]
Undergraduate teaching lab to learn about phagocytosis	Five to six hours (One module)	Applying flow cytometry can be the ideal method in a classroom.	[37]
Undergraduate teaching lab about microbial growth curves	Three weeks (One lab module)	Comparison of various methods benefits students	[38]
Undergraduate teaching lab about immunology (T	One quantitative exercise	New generation flow cytometers are an excellent	[3]

cells)		classroom tool	
Undergraduate teaching lab for immunology skills	Half semester	Students are interested and engaged in flow cytometry skills	[39]
High School students laboratory experience	One month summer apprenticeship	Younger students can benefit from access to the technique	[40]

Education research can provide evidence based reports of better ways to teach specific topics [41, 42]. Many have called for more of this evidence-based educational research and better alignment of teaching with successful practices [43]. Personal investment in the material and use of novel technologies can be very useful for learning [44-46]. There are important lessons from evidence-based research in flow cytometry, especially in the development of applicable instruction and student participation yielding better learning. Fuller *et al.* reported the success of two short flow cytometry courses targeted to different audiences [36]. The first reported on students which had direct applications for flow cytometry in their research, so the three-day course focused mainly on technical skills and data interpretation. The second course consisted of a three-hour tutorial for undergraduate pathology students which focused on establishing a more basic understanding of flow cytometry through active learning. By utilizing real flow cytometry data in a computer learning center, the researchers were able to see student engagement and improved skills in both their three-day and three-hour courses [36]. Ott *et al.* report about a course with an in-depth study of immunological tools, including half of a semester focused on flow cytometry. By delving deeper into flow cytometry, the students were able to develop expertise and were exposed to numerous applications [39]. The undergraduate students reported increases in confidence across the board and had high satisfaction with the half semester flow cytometry course.

Others have described the successful use of flow cytometry as a tool in a laboratory course. Flow cytometry does not have to be a technique only used in large research projects; it can be very effective for classroom education of students about biotechnology techniques [3]. Boothby *et al.* emphasized flow cytometry as a tool to visualize phagocytosis in a teaching laboratory setting [37]. A similar paper teaches about the value of advancing technology by comparing microbial cell counting with a hemocytometer to the accuracy and speed of a flow cytometer [38]. Even high school students can gain skills from the flow cytometry educational experiences as reported by the leaders of a summer biotechnology internship program, again showing that a diverse range of students can benefit from learning this technology [40].

Flow cytometry education can also help students feel more comfortable and encourage undergraduate research. However, a solid understanding of the physical technology, the biological principles, and the data processing is necessary for students to effectively gather data with a flow cytometer [47]. One previous publication detailing the effectiveness of an eight week course cites student feedback that due to the complexity of the topic they wanted the course to be an entire semester [39].

Here we seek to address the need for a more comprehensive and expanded flow cytometry course by outlining a successful semester-long course. This paper aims to help science educators as no full semester course has been previously presented in the literature. This course provides hands-on experience, in-depth conceptual understanding, and development of proficiency for students. This class is also designed to make students aware of the possibilities of the technology, address limitations such as the initial price investment, and provide ideas for helping students wrestle with highly technical data and machine complexity. This paper focuses primarily on course content and student confidence and interest, while future studies will focus

on measuring student proficiency.

2.3 Materials and methods

2.3.1 Subjects

This report uses data from a flow cytometry course offered at Brigham Young University (MMBio 522, Flow Cytometry) in the fall of 2018. The course is designed for graduate students and for undergraduates who are heavily involved with research. The target student typically has a research project that uses or will need to use flow cytometry, making the class highly applicable for the students. In recent years, the course has also become a class commonly taken by brand new graduate students who have not chosen a lab yet, leading to a wider variability in student abilities, interest, and skills. The course has also expanded and evolved to include and support students in fields beyond biology, specifically chemistry and engineering. The course currently supports training for 24 students.

2.3.2 Course outline

This two-credit course is intended to teach students how to design and run flow cytometry experiments tailored to the two instruments in the Research Instrumentation Core Facility (RIC) at the Brigham Young University College of Life Sciences: the BD Accuri C6+, which has two lasers and can measure six parameters, and the Beckman Coulter Cytoflex, which has four lasers and can measure thirteen parameters. The course consists of hour-long biweekly lectures or labs designed to teach conceptual, technical and analytical skills, which build upon each other, increasing in difficulty level (Figure 1A). These skills are practiced and assessed throughout the course with variable associated point values (Figure 1B and Table 2). Table 2 can provide an outline for others interested in a developing a similar course.

A

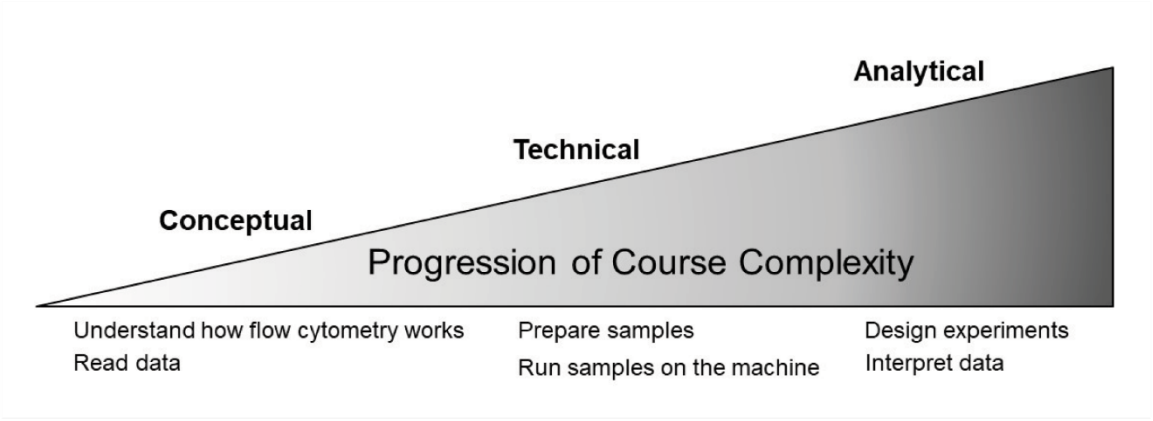

B

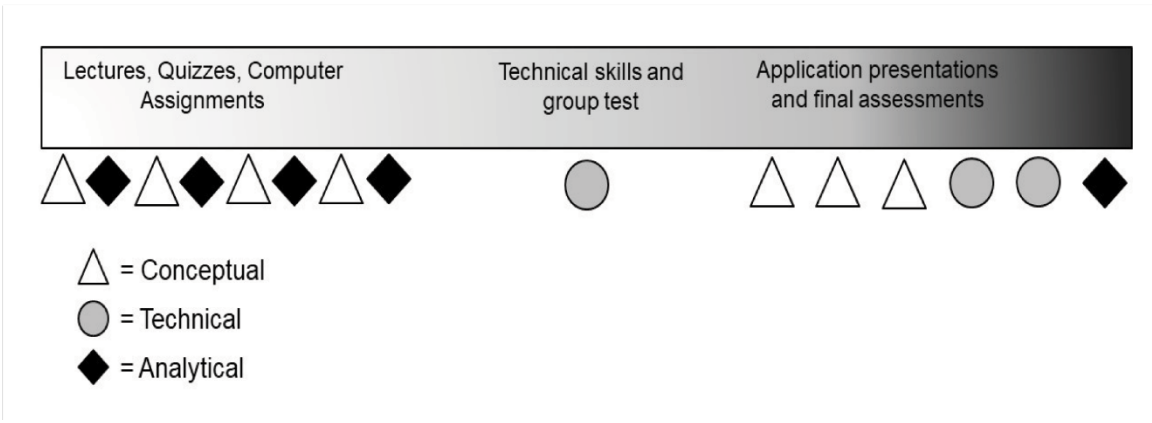

Figure 2-1: Progression of complexity in the course. The course is organized to allow skills to build upon each other. (A) This depicts the conceptual framework for the course, where learning conceptual skills builds the foundation for learning technical skills followed by analytical skills, culminating with student skill tests and individual application presentations. (B) This outlines the assessment pattern in the course. Students have multiple opportunities to practice and demonstrate competency in these skills sets.

Table 2-2: Outline of course, detailing assignments and assessments

Date	Topic	Reading
Sept 4 (Tues)	1.1 Introduction to flow cytometry and course overview	Syllabus Principles of the flow cytometer
Sep 6 (Thur)	1.2 Theory: Basics of flow cytometry – Quiz #1	Givan Chapters 1 & 2 Flow cytometry: An introduction
Sep 11 (Tues)	Computer lab: Software overview and practice Computer lab assignment #1	Data analysis
Sep 13 (Thur)	1.3 Theory: Components of flow cytometers and data analysis 1.4 Quiz #2	Givan Chapters 3 & 4
Sep 18 (Tues)	Computer lab: Data set analysis – Computer lab assignment #2	Compensation tutorial
Sep 20 (Thur)	1.5 Theory: Fluorescence absorption, emission, and compensation Quiz #3	Givan Chapter 5 Principles of Fluorescence
Sep 25 (Tues)	Computer lab: Data set analysis – Computer lab assignment #3	
Sep 27 (Thur)	Theory: Staining proteins outside and inside of cells. – Quiz #4	Givan Chapters 6 & 7
Oct 2 (Tues)	Computer lab: Data set analysis – Computer lab assignment #4	
Oct 4 (Thur)	1.6 Theory: Flow analysis of cell cycle, apoptosis, and cell sorting Quiz #5	Givan Chapters 8 & 9
Oct 9 (Tues)	Computer lab: Data set analysis quiz – Computer lab assignment #5	
Oct 11 (Thur)	1.7 Theory: Clinical flow labs, and modern flow– Quiz #6	Givan Chapter 10 Modern flow cytometry
Oct 16 (Tues)	RIC flow cytometer overview and training by Dr. Sandra Hope	
Oct 18 (Thur)	2.1 Hands on training: Accuri and CytoFlex operation overview Quiz #7	Multicolor panel building
Oct 23 (Tues)	2.2 Hands on training: Sample preparation lab	Controls in Flow Cytometry Optimizing your experiment Troubleshooting
Oct 25 (Thur)	2.3 Hands on training: Small group flow cytometry sample runs and data analysis	
Oct 30 (Tues)	2.4 Hands on training: Small group flow cytometry sample runs and data analysis	
Nov 1 (Thur)	2.5 Hands on training: Small group flow cytometry sample runs and data analysis	
Nov 6 (Tues)	2.6 Hands on training: Flow cytometer operation skill exam	
Nov 8 (Thur)	2.7 Current applications of flow cytometry – Quiz #8	Givan Chapter 11 & 12 Common applications, new technology, protocols
Nov 13 (Tues)	3.1 Student Flow Cytometry Technique Presentations	
Nov 15 (Thur)	3.2 Student Flow Cytometry Technique Presentations	
Nov 27 (Tues)	3.3 Student Flow Cytometry Technique Presentations	
Nov 29 (Thur)	3.4 Student Flow Cytometry Technique Presentations – Quiz #9	
Dec 4 (Tues)	4.1 Cell sample preparation and staining practical	
Dec 6 (Thur)	4.2 Independent flow cytometry practical	
Dec 11 (Tues)	4.3 Data analysis practical	
Dec 13 (Thur)	4.4 Cell sorting demonstration – Quiz #10	

2.3.3 Course sections

The following main sections of the course help students gain a theoretical and technical understanding of how flow cytometry works and then to apply that knowledge in hands-on experiments and data analysis.

- **Conceptual quizzes:** The students read one to two chapters from "Flow Cytometry: First Principles" by Givan to prepare for class. Quizzes are comprised of 7 questions which cover material from the previous class to assess understanding of concepts taught in lecture and 3 questions about the reading assignment in order to assess lecture preparation.
- **Computer lab assignments (Figure 2):** The course utilizes a student computer laboratory in which each computer is equipped with software from two flow cytometric machines, the BD Accuri C6+ and the Beckman Coulter Cytoflex, in order to provide data analysis practice. FlowJo data analysis software is also used in a month-long academic license for data analysis in a couple of the labs. Integrating technology into courses can be very useful for student engagement and future success in the technique [48, 49].
- **Hands-on machine training:** This course provides technical cytometric machine training in the Research Instrumentation Core Facility (RIC) at Brigham Young University with help from the director and technicians. Two cytometric machines are available in the RIC: A BD Accuri C6+ that can measure 6 parameters and a Beckman Coulter Cytoflex that can measure 13 parameters.

Accuri Software

Case scenario: You are an intern working in a pathology unit of the hospital. Your supervisor hands you some blood samples isolated from patients that he suspects have been infected with methicillin-resistant *Staphylococcus aureus* (MRSA). He trusts you to use flow cytometry to label and analyze the samples to correctly identify which patients are positive for two proteins (SpA and ClfA) on the surface of *S. aureus*. You label the cells with fluorescent antibodies specific for these two markers, SpA [PE (FL2)] and ClfA **[**APC (FL4)**]**, which will bind to *S. aureus* infected cells in the blood; if a patient is positive for *S. aureus*, the sample will be double positive for both colors.

Download the "**MRSA screening data**". Go to File and click on "Open Workspace". Find the MRSA screening data folder and open the "MRSA screen template.c6" workspace file (it's the first file you see when you open the folder, not in the folder labeled MRSA screen data files).

1) (1 point) Select the Collect tab. Click on sample A1 and set quadrant gates on each of the dot plots except for the top left plot so that nearly all of the cells are **very tightly gated** in the left bottom quadrant. Select sample A3. Perform compensation to correct bleeding of PE into APC.

What compensation value did you input for APC-%PE? _____

2) (1 point) Select the Analyze tab. Click on the middle plot (plot #8). Find a sample that has a population that is positive for both PE and APC. The positive control sample is A6 so use this as a reference. List the names of three samples that are double positive for PE and APC other than A6 below (there are more than 3 samples that are double positive).

1_____ 2_____ 3_____

3) (1 point) Click on plot #10 (far right plot). Click on those 3 samples that you selected and make a histogram gate (M2) over the positive population. Look at the table at the bottom of the screen and find the column that reads "Mean APC-A" and record the values that are for **only the histogram (M2) gate** for those three samples below.

1_____ 2_____ 3_____

4) (1 point) Import the "**HPB_4_Color_example**" data set into the BD Accuri software. Click on the Collect tab and select sample A4. Insert a dot plot. Change the axis on this dot plot so it is CD3/FITC and CD8/APC. Add a quadrant gate to discriminate between negatives, single positives, and double positives. What is the **number** of cells that are CD8 positive and CD3 negative? _____

5) (1 point) In the "**HPB_4_Color_example**" data set in the BD Accuri software, continue analyzing sample A4 and add a histogram plot. Change the histogram axis so it is CD45 PE-Cy7A. How many **separate** peaks can you see? _____

Add a histogram gate to the most positive CD45 peak (the peak with the most fluorescence). What **percentage** of the plot is the most positive CD45 (PE-Cy7A) peak? _____

Figure 2-2: Example of computer lab assignment. This section of the assignment was designed to test the student's knowledge in analyzing data in the BD Accuri C6+ software package. Questions focused on enhancing flow cytometry principles such as color compensation, gating, making graphs, and population identification. Similar questions were asked across multiple data sets to reinforce student knowledge and skill acquisition by analyzing different data.

- **Sample preparation training:** Preparation of flow cytometry samples (e.g. isolation of T cells and staining with antibodies) is demonstrated to the students followed with practice by the students. This exercise helps students familiarize themselves with sample preparation work and benefit by improving technique. The example demonstration is done with mouse splenocytes (Supplemental Figure 1).
- **Current applications:** Students choose a paper with a flow cytometry application of interest and present the technique to the class. Quizzes are given to assess basic understanding of the techniques presented. Recent research shows benefits to learning when students read current literature [50].
- **Machines and programs:** This course used FlowJo analysis software on an academic license as well as BD Accuri C6+ and Cytoflex data software. The student BD Accuri and the Cytoflex machines were used for technical skill practice.

2.3.4 Survey instrument

For this study, students were given a ten-question survey one week into the semester and one week before the end of the semester (Table 3). The survey was based on a published survey used by Ott *et al.* in their class evaluating flow cytometry and ELISA laboratory modules. The survey was granted exempt status by the Brigham Young University IRB (#E18387). Students were asked to rate their perceived knowledge and skill level on a scale of 1 to 5, with 1 = strongly disagree, 2 = disagree, 3 = neither agree or disagree, 4 = agree, and 5 = strongly agree.

Table 2-3: Ten question survey administered to students . Assessment of student attitudes was measured by agreement with statements on a 5-point Likert scale (1 = strongly disagree, 2 = disagree, 3 = neither agree or disagree, 4 = agree, 5 = strongly agree), and results are displayed as the mean. Question numbers here are referred to in subsequent figures by Q1, Q2, etc.

Students rated their perceived knowledge and skill level from "strongly disagree" to "strongly agree" (score 1 through 5).

I am able to:	**Skill**
1. Describe in basic terms how a flow cytometer works	Conceptual
2. Design properly controlled flow cytometry experiments to address research questions and troubleshoot as needs arise	Analytical
3. Explain how flow cytometry data is generated and presented in histogram or dot plots	Conceptual
4. Understand how the fluidics and optics systems enable multi-color analysis of a single cell	Conceptual
5. Identify current applications of flow cytometry	Conceptual
6. Compensate fluorescence cross talk on a flow cytometer	Technical
7. Analyze and interpret flow cytometry data	Analytical
8. Stain membrane bound antigens for flow cytometric analysis	Technical
9. Quantify cell viability on a flow cytometer	Technical
10. Design and run a multicolor flow cytometry experiment	Analytical

2.3.5 Data analysis

Data analysis was performed on responses from students who had completed both the pre- and post-surveys. A 5-point Likert scale was used to access student attitudes and data comparisons between groups were performed using a Wilcoxon ranked test. Statistics were performed using Prism 7 software (GraphPad).

2.3.6 Data availability

All data from this study are either included in this published article (and its Supplementary Information files) or available upon request.

2.4 Results

These students were all self-selecting students enrolled in the Flow Cytometry Course at Brigham Young University during fall semester of 2018. Fourteen students completed the pre- and post-surveys. Only students who completed both the pre- and post-surveys were included in this data analysis.

Students report a significant increase in confidence from the pre-survey to the post-survey with relation to these skills targeted in the course (Figure 3). This method of data assignment emphasizes the specific goals of the course. The increase in student confidence scores is consistently improved across the three types of questions (conceptual, technical, and analytical). It is interesting to note that students had higher pre-survey confidence in conceptual skills, yet the increase in the post-survey confidence levels for the conceptual questions is similar to those seen with the technical and analytical. The analytical and technical skills can be classified as more difficult skills to master and students entered with less confidence in these topics.

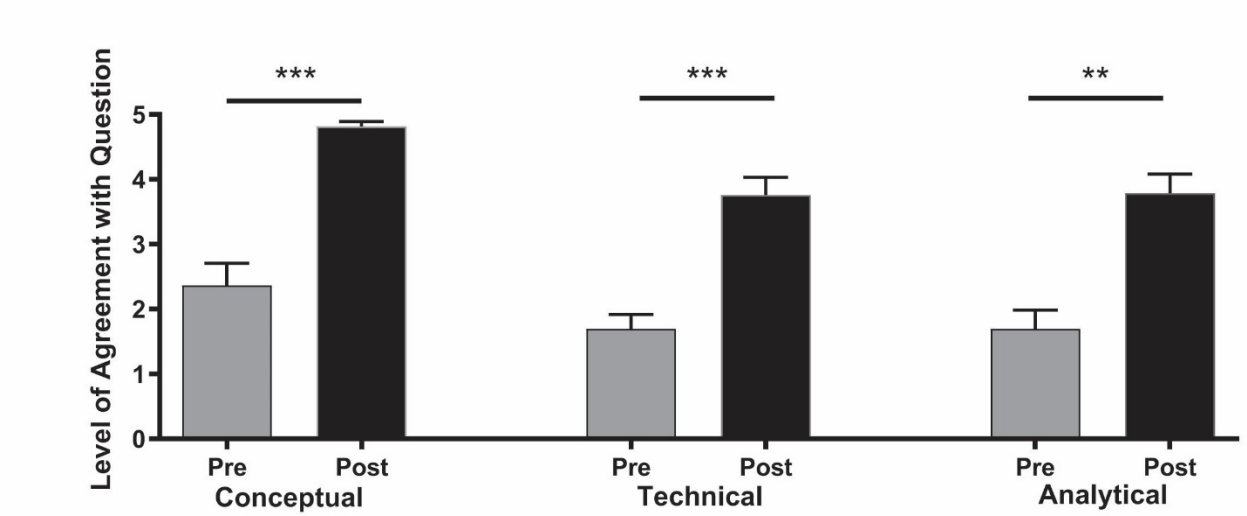

Figure 2-3: Self-assessment organized by skills. Questions from the ten-question survey, grouped by skill type as indicated above in Table 3. These represent the mean responses for each set of skills before and after the course. Students report a significant gain of confidence in the skills in each category. Grey represents responses from the survey given at start of the course (pre-survey) and black represents responses from the survey given at the end of the course (post-survey).

Upon examination of individual questions, some other trends appear. In Figure 4A (conceptual questions), question 1 asked about the most basic knowledge of flow cytometry, and students rated themselves relatively highly. Many students coming into this course have some knowledge of flow cytometry via exposure in a research laboratory setting, or even use of a student flow cytometer which requires a two-hour training to operate. The other conceptual questions (Questions 3-5; histograms, fluidics, and applications) have similar responses and increases, where students report high confidence in these skills at the end of the course.

When looking at the technical questions (Figure 4B), question 6 shows the lowest average starting score. This question referred to compensation, an advanced flow cytometry technique which many of the students did not have any exposure to before the course. The two other technical skills (Questions 8 and 9; cell staining, and viability analysis) show similar increases to most other skills. The analytical questions (Figure 4C) include the actual design of proper controls, data interpretation and multi-color experiment design (Questions 2, 7, and 10).

Students report medium levels of confidence in these difficult skills in the pre-survey and had similar increases in the post-survey.

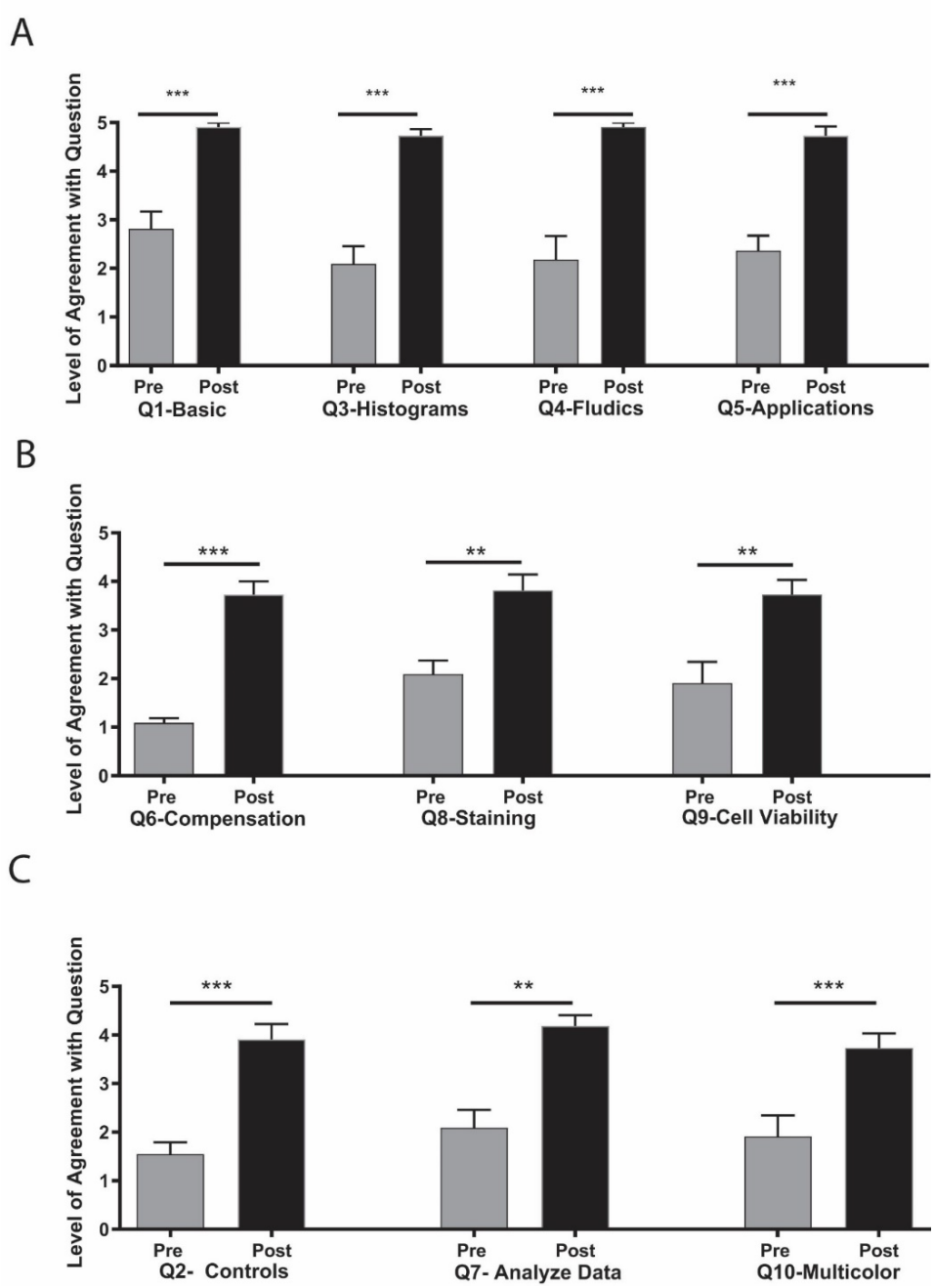

Figure 2-4: Individual question analysis of changes in student pre and post survey responses . Questions are grouped into (A) Conceptual, (B) Technical, and (C) Analytical questions. Results are displayed as mean and assessed using a Wilcoxon ranked pairs test. Grey represents responses from the survey given at start of the course (pre-survey) and black represents responses from the survey given at the end of the course (post-survey).

This survey did not reveal any differences in confidence levels between undergraduate and graduate students or male or female students (data not shown). This may be due to the course effectiveness for many types of students or small sample size. It should be noted that these results represent a self-assessment of skills, so they measure student confidence and not actual ability. This course is designed as a launching ground for students to do their own research projects, so confidence and willingness are a necessary first step. Future studies are planned to formally examine student proficiency at the end of the course.

2.5 Discussion

Flow cytometry skills are increasingly important in today's competitive job and research market [35]. Creating opportunities to learn marketable skills is a major goal for many university programs [51]. While others have reported educational opportunities for exposure to flow cytometry, this report outlines a comprehensive semester long course dedicated to teaching flow cytometry skills. Students reported significant increases in their confidence level in relation to essential flow cytometry skills. Building complex skills on top of simple skills can be an effective way to teach and this course outline may prove useful for other educators wishing to implement similar programs.

This course seeks to help students become independent users of flow cytometers, but that can be variable depending on the students' abilities and motivation. As mentioned previously, a wide range of students have taken this course. For some students, flow cytometry is an immediately necessary skill for their research, while others are merely interested in future career options. This wide array of students may require additional customization of the course, possibly adding additional technical and specific training for those wanting to become proficient at more

complex applications. Alternatively, this course could narrow or split in focus, as seen in Fuller *et al.* and focus on the specific needs of the various groups.

Early iterations of the course did not include any sample preparation training, but students provided feedback that this was proving to be a barrier for student use. Many students wanted to learn flow cytometry skills before investing in the costly reagents in order to assess if the flow cytometer would fit with their project. Other students had very little wet lab background, so preparing cells on their own and without instruction was an intimidating prospect. After student feedback, a cell staining element was incorporated for the first time and was received well.

This year also provided a unique challenge after two Attune machines were swapped for one Cytoflex machine. While this allowed for more complex multicolor experiments, it limited the technical practice time for each student on the machine with more parameters. Despite this challenge, students reported that they had increased confidence in their conceptual, technical, and analytical skills and proficiency. Interestingly, students also reported a desire to have more focus on technical skills. This may reflect a practical approach to learning, but it may also signal a possible barrier to future expansion with a limited number of flow cytometry machines. This specific course was complicated by a downsize in the number of machines available for course use, and that may be reflected in students' answers. In the future, this could be addressed by having students work with teaching assistants or technicians on the machines during times they signed up for outside of the regularly scheduled class time. Students were generally satisfied with the addition of a day to practice cell preparation which is useful for future teaching of this course.

One shortcoming to note is that the confidence levels reported by students may or may not translate to true proficiency. While all students did pass a proficiency test at the end of the semester administered by the course teaching assistants, this does not necessarily lead to successful data collection and analysis, especially when considering that students may not use these skills regularly and may forget them. The goal of this course is to provide a background for students to design their own experiments, but they may need to review these technical and analytical points in order to be successful in the future.

In a thematic analysis of student comments, it was apparent that students had high interest in gaining a conceptual understanding of flow cytometry. That was the most common answer category in response to the question, "What are you looking to gain from this course?" This may be because students didn't have a framework for what kinds of technical or analytical skills they may need. However, near the end of the course, students were most satisfied with their knowledge in conceptual and analytical skills. They were less satisfied with the technical skills gained, perhaps reflecting an inadequate amount of time operating the machines to internalize the technical skills.

Traditional flow cytometry training has often been informal, short and largely self-directed. However, this is a complex technique with many subtleties that need to be learned to be an effective user. For some users, a short training is sufficient for their purposes, but for others, a deeper understanding could yield efficient and interesting research. This course could be a welcome addition for universities looking to expand the range of skills for their students, and for instrument cores aiming to maximize student usage and research productivity. This paper aims to give educators a basis for their own course development. Additional variations of this course may include a lecture class with an accompanying laboratory class to emphasize and help

students internalize technical skills, or a unit in other related courses. By promoting student skills, this course could aid student research productivity and increase marketability, while providing a unique and valuable educational experience.

2.6 Supporting information

Mouse Spleen Sample Flow Cytometry Preparation Protocol

Reagents	Antibodies:	Supplies:
PBS – 1% BSA	CD4 Pe-Cy7	15ml conical tubes
RBC Lysis Buffer	CD8 PE	Microscope slides
2% paraformaldehyde	CD11b APC	FACS tubes
Fc Block (CD16/32)	B220 FITC	Petri dishes
		Fabric filters
		Pipettes

Sample Prep Steps

1. Prepare a 15mL conical tube with 5mL PBS – 1% BSA
2. Euthanize mouse and remove the spleen.
3. Dump the spleen into a petri dish and mash the spleen in one half of a petri dish with the frosted end of two microscope slides.
4. Filter the liquid back into the conical vial using filter fabric.
5. Wash the lid and slides with 5mL PBS – 1% BSA, filter back into 15 ml conical tube.
6. Spin at 1200 rpm for 5 minutes.
7. Resuspend in 3mL RBC Lysis buffer. Wait 3 minutes, aliquot cells into FACs tubes (unstained, single color, and sample), then spin at 1200rpm for 5 minutes.
8. Resuspend in 500uL of PBS – 1% BSA. Add 1ul Fc Block (CD16/32). Stain 10 minutes at 4°C. While you wait, prepare your antibody master mix in the dark. We have 2 sample that will be labeled with the master mix so you'll add 3ul of each antibody into 600uL of PBS – 1% BSA.
9. Spin at 1200 rpm for 5 minutes.
10. Add 200ul of 1x PBS – 1% BSA to the unstained and single color controls. Add 1uL of the designated stain for each single-color control tube. Resuspend the designated samples in 200uL of master mix. Stain IN THE DARK for 15-30 minutes.
12. Spin at 1200 rpm for 5 minutes. Wash with 2mL of PBS – 1% BSA. Spin again.
13. Resuspend in 250uL PBS – 1% BSA and 250uL 2% paraformaldehyde.
14. Filter the samples using the filter fabric. You are now ready to run your samples!

Supplemental Figure 1. Example of mouse splenocyte staining protocol

CHAPTER 3: CAR T CELL METABOLISM

The following chapter is a work in progress and will be submitted for scientific review upon completion. Current data and future directions for this project are presented here.

3.1 Introduction

3.1.1 Cancer immunotherapy treatment is an important treatment option

Cancer is the second leading cause of disease in the US, yet many aspects of this disease such as the causes and best treatment options remain unclear. Current treatment involves chemotherapy, radiation, and surgery; which leave patients weak, sick and immunosuppressed for extended periods of time [52]. Immunotherapy approaches intend to strengthen the immune system to fight against the tumor cells rather than suppress the immune system like traditional approaches [53]. Additionally, the ability of the immune system to specifically target cancerous cells provides a potentially less invasive path for patient treatment.

T cells are the core elements of the adaptive immune system. Helper T cells coordinate the entire immune response, and cytotoxic T cells are efficient killing cells [54]. When a single T cell recognizing a foreign antigen as a threat to the body, it can launch a full immune response which can have the threat contained within days. This makes T cells the ideal candidate for agents in immunotherapy [55]. Vaccines effectively harness these strengths of the immune system by priming the immune system to generate memory cells that will respond rapidly to the antigen upon re-exposure, resulting in quick containment with no symptoms. Unfortunately, with cancer there is not always a clear foreign antigen recognized by the immune system, because cancer cells begin as normal cells that mutate to a state of uncontrolled growth.

Cancer cells disguise themselves using various means, most importantly by downregulating MHC which would normally present intracellular peptides as danger signals. Cancer looks normal from the outside except for the subtle presence of unique mutated biomarkers. Some biomarkers are specific to cancer, known as tumor specific antigens, while others are often present in low levels normally but are upregulated significantly in cancer, known as tumor associated antigens [56]. The native immune system will not always respond to these tumor-associated peptides, but T cell therapy hinges on the idea of engineering immune cells so that they are able to more effectively recognize and respond to these tumor biomarkers, enabling the immune system to better differentiate between cancerous and healthy tissue.

3.1.2 CAR T cell therapy combines antibody specificity with T cell killing capacity

T cells can recognize, attack and kill foreign cells or infected host cells. They can do this by recognizing foreign antigen on major histocompatibility complex proteins (MHC). Infected cells will display antigen continuously and if the T cell receptor (TCR) binds and recognizes it as foreign, it will kill the cell before the infection can spread. Unfortunately, this approach often times does not work in cancer because the T cell may not recognize cancer peptides as foreign. Cancer cells are self, with a few alterations, so they will not always be recognized and removed. To add to the confusion, cancer cells will often down-regulate MHC proteins to get around T cell recognition [56]. Cancerous cells can be undetected and unregulated for long periods of time.

CAR T cell therapy is a potential solution to that cancer cell recognition problem. A chimeric antigen receptor (CAR) bypasses the need for a TCR and MHC by using an antibody as the antigen recognition molecule. A CAR combines the antibody binding region with the signaling capacity of a TCR, enabling it to trigger T cell effector functions and to kill cancer cells directly. A CAR can also activate memory T cell formation to prevent future metastasis.

The antibody binding domain allows the CAR to bind antigen even if it is not presented on MHC. It also allows researchers to specify which molecules will be bound by the CAR by the antibody that is selected.

The signaling portion of a CAR is also very important. Early design CARs use the CD3ζ domain of the TCR complex to initiate signaling. It is the native intracellular protein associated with the T-cell receptor that initiates T cell activation signals, so it is used as part of CAR constructs to amplify the native T cell signaling pathway. These were known as first generation CARs and were largely ineffective because T cells require two signals for full activation [57]. One reason T cells need a second signal to become fully activated is to prevents autoimmunity. This is most commonly accomplished by CD28 binding to B7 on an antigen presenting cell, which when done in coordination with TCR binding to antigen T cell activation is initiated [58]. The second-generation CARs added a co-stimulatory domain in addition to CD3ζ, providing two T cell activation signals upon the binding of the CAR antibody to its antigen. Thus, second generation CAR designs began to reflect this basic biology by including various domains in between the antibody binding domain and the final CD3ζ signaling molecule. An overview of relevant CAR designs is shown in Figure 1. Researchers have found that the second generation CAR with CD28 activates a quick response in CAR T cells with high proliferation and cytokine production [59]. CD28 is the natural second signal for T cell activation, and binding activates the NFAT pathway triggering Glut1 increasing access to glycolysis [60]. 4-1BB or CD137 is another co-stimulatory domain in activated T cells which was first used in early CAR therapy to provide this second signal [9]. Binding of 4-1BB results in enhanced mitochondrial capacity and activates PGC1α-mediated pathways through a MAP kinase [61].4-1BB sends a slower activation signal initially, but the 4-1BB CAR T-cells actually have better longevity and memory

responses that those with CD28 [62]. A third generation CAR sought to create the "best of both worlds" by combining all three of the domains (CD28, 4-1BB, and CD3ζ). There are promising early results with this third generation design, but its effectiveness remains unproven [63, 64]. Other types of CAR domains exist, but these three (CD28 and 4-1BB second generation CARs and the third generation CAR) are the focus of this study because they are the most widely used.

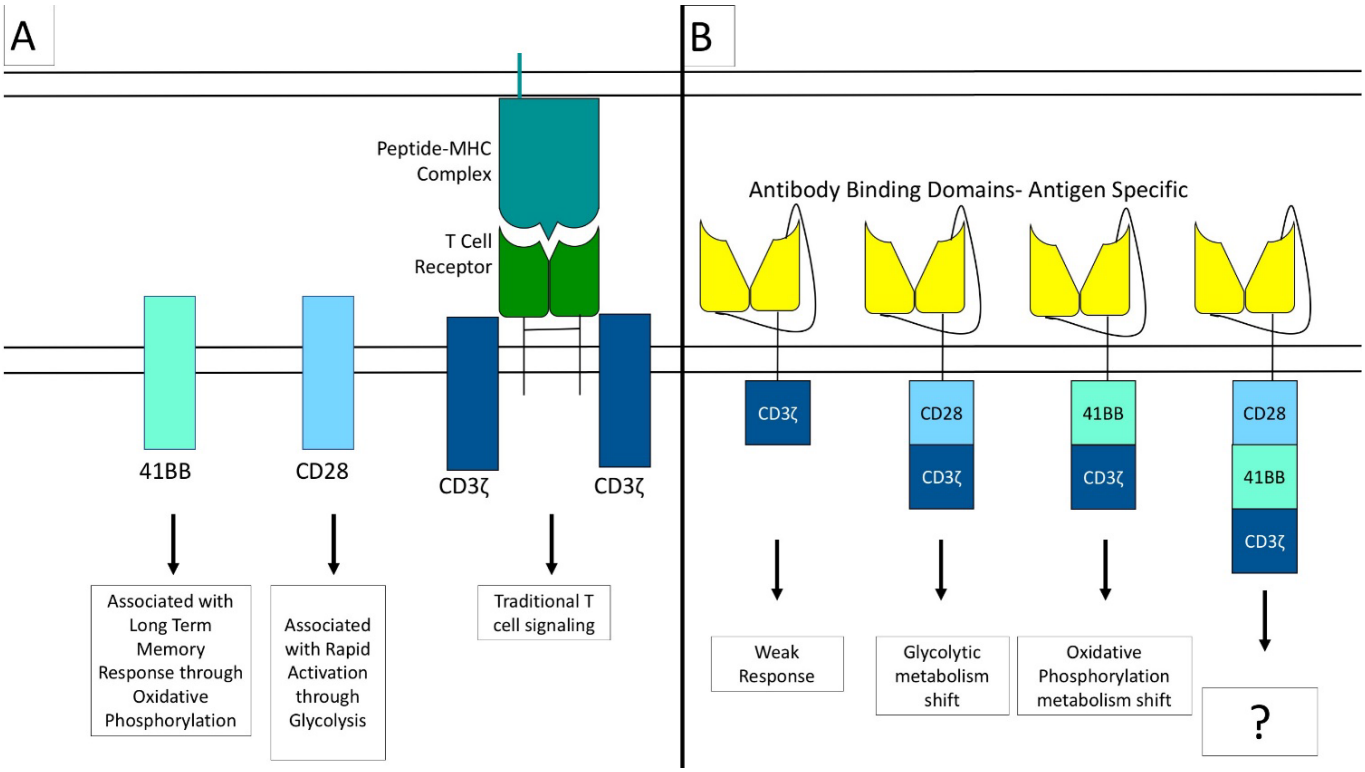

Figure 3-1: CAR T cell mechanism. (A) Native T cell receptor (TCR) uses peptide MHC from diseased cell complexing with TCR to send one signal and then co-stimulatory molecules to send a second signal. (B) The CAR constructs use antibodies to bind antigen instead of the TCR and then various signaling domains have been engineered to initiate an activation response. The signaling differences between these CAR constructs form the basis of the scientific question for this project.

CD28 and 4-1BB CAR T cells have been the focus of many clinical trials. CD28 CAR T cells targeting B cell malignancies were recently approved by the FDA as a standard best practice method of care for leukemias, with the indication that CAR T cells can be a viable

therapy [7-9, 65, 66]. Early clinical trials showed success and remission rates of over 90% in total [67]. 4-1BB CARs have recently received attention because of their prolonged response and better memory, meaning that a patient may only need one injection instead of multiple invasive procedures [68, 69]. CAR therapy is working well in hematological cancers but there are additional obstacles to before CAR therapy is effective in treating solid tumors.

3.1.3 T cell dysfunction is an obstacle to effective CAR therapy

As mentioned previously, there are multiple barriers to entering the tumor. Once T cells get into the tumor, they still face many obstacles including exhaustion, inhibitory signals, antagonist immune cells and more [14, 70]. One major problem in the tumor microenvironment is resource depletion. Cancerous cells grow quickly and use up many resources, often causing cell death and damage around the tumor site. Recent studies suggest that this competition for resources is a major component of immunosuppression in the tumor [11, 13]. T cells, even CAR T cells, often can't get energy in this depleted environment so they become exhausted and ineffective. The careful selection of co-stimulatory domains may ameliorate this problem by altering T cell metabolism [71].

3.1.4 Cancer metabolism and T cell metabolism compete for resources

Cancer also has a unique metabolic signature which makes immunotherapy difficult [52, 53, 72]. Known as the Warburg effect, cancer cells switch from oxidative phosphorylation, which is more efficient, to glycolysis, which is less efficient but much faster [72]. For these high proliferating cells, producing 2 ATP immediately from repeated glycolysis is worth more than 36 ATP that can be generated by the slower process of oxidative phosphorylation. Especially in glucose rich environments, tumor cells will undergo this metabolic switch. By switching to

glycolysis, the tumor cell can get quick access to all the energy it needs. There are many implications of this effect, some of which complicate T cell metabolism [13].

T cells can also undergo this sort of Warburg metabolic reprogramming to expand rapidly in some situations. An active effector killer or coordinating helper T cell needs to switch to glycolytic metabolism to have enough energy [59]. However, this is not anaerobic respiration or fermentation. Phosphoenol pyruvate is the byproduct of glycolysis, but in this aerobic setting, it is not converted to lactic acid. Instead, it is used as a building block for cellular components and a signal to the T cell that activation is happening [73]. This switch is crucial to T cell activation and the function of the immune system [74].

This kind of energy usage in cells affects initial cytotoxicity and longevity of treatment. A shift to glycolytic metabolism marks T cell activation, and an increased capacity to use glycolysis would enable greater activation. On the other hand, memory T cells shift away from anaerobic to aerobic respiration to maintain longevity, enabling them to control any future tumor growth. Memory cells have more mitochondrial biomass than effector cells, providing us physiological evidence for this phenomenon. However, the tumor microenvironment can suppress mitochondrial growth making these switches difficult [75]. This evidence suggests that altering CAR T cell energy metabolism may play an important role in their effectiveness.

3.1.5 Modifying CAR metabolism to overcome challenges with T cell exhaustion

CAR T cells have all the properties of normal T cells, but with added capabilities from additional co-stimulatory domains. Some researchers suggest using cells without inhibitory signals such as PD-1 because the lack of inhibition should lead to better activation [11, 76]. Others advocate for selecting only the most active cell populations [70]. The prevailing opinion is in favor of modifying the naïve T cells to the appropriate response. This modulation is

dependent on the co-stimulatory domains selected for inclusion. It has been shown that CD28 added as a co-stimulatory domain predisposes the T cell toward glycolysis, allowing for better initial activation, while 4-1BB increases oxidative phosphorylation, allowing for greater longevity [77]. Currently, nothing is known about the energy metabolism of the combined construct, or of the effect differing environmental energy scenarios have on the metabolism of second generation CAR T cells. [78-80]. By studying the energy metabolism of CAR T cells, this project aimed to understand their basic biology and provide a basis for understanding therapy recommendations.

CAR T cells offer a promising alternative to chemotherapy and radiation. A better understanding of the mechanism of CAR T cell energy usage will allow for specific therapeutic recommendations. Additionally, these constructs provide a great way to observe the basic biology of T cell activation in a clinically relevant alteration. Specifically, investigation of the glycolytic switch in CAR T cells dependent on their co-stimulatory domain could elucidate this mechanism [81].

3.2 Materials and methods

3.2.1 Constructs

This work was performed using retroviral plasmid pMSCV-IRES-GFP II (pMIG II) from AddGene. Retroviral work was necessary because lentiviruses (the preferred viral backbone in human CAR T cell creation) do not efficiently infect murine T cells [81]. Constructs were created to target murine CD19 using sequence reported by Kochenburd 2019 [82]. The CD8 hinge, and the signaling domains (CD28, 41BB and CD3zeta) were generously shared by the Kranz lab after their murine optimization [83].

Plasmids were grown in *E. coli* and isolated with Zymo Maxi Prep kit to yield high enough concentrations.

3.2.2 Viral transfection

PlatE packaging cells (293T variant) were cultured overnight in six well plates to approximately 80% confluency. The plasmids were placed in serum free media along with Mirus Bio VirusGen transfection reagent and allowed to incubate to form complexes for 12.5 minutes. Then the solution was applied dropwise to the packaging cells and allowed to incubate for 48 hours.

The viral supernatant can be harvested and filtered through a 0.45 micron filter, and then applied to freshly activated T cells.

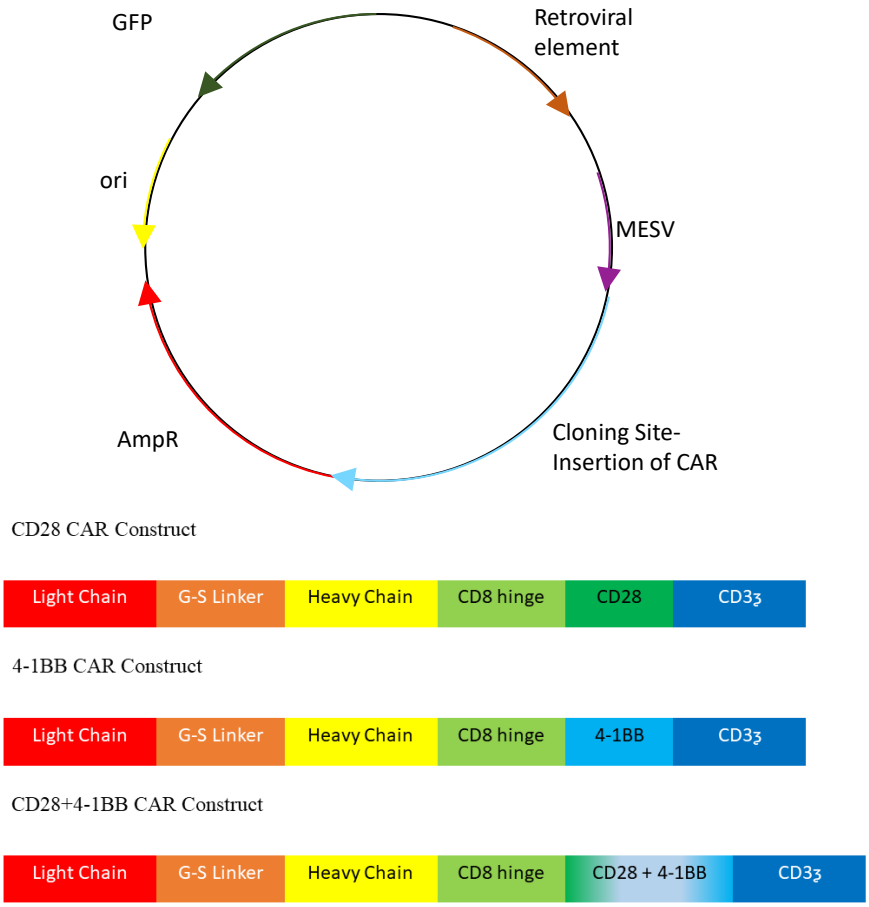

Figure 3-2: Construct Design. (A) pMIGII vector for insertion of the plasmid. (B): An outline of the essential portions of each of these CAR T cells. This was the basis for the plasmid engineering section of this project.

3.2.3 T cell isolation

T cells were isolated from the spleens of the mice above, immediately after CO_2 euthanization. A single cell suspension of splenocytes mixed with magnetic beads was applied to magnetic columns to isolate CD4+ T cells by negative selection (Miltenyi Biotech). Cells were placed in RPMI complete 1640 media[81] and cultured along with 30 U/ml IL2 and CD28/CD3 Dynabeads to allow the cells to activate and proliferate. After 24 hours, the cells were separated from the Dynabeads, and then placed in a Percoll gradient (35% vs 65%), which allows for separation of the activated cells from the non-activated cells.

3.2.4 T cell transduction

Fresh virus was applied to activated CD4+ T cells along with 10μg/ml polybrene into 24 well plates. Plates are centrifuged for 1-2 hours to encourage transduction, and then incubated for at least 4 hours. Polybrene is removed, and cells were incubated for another 36 hours at 37°C with 5% CO_2. CAR expression can be confirmed via flow cytometry.

3.2.5 Metabolic profiling

T cells were assayed using an Extracellular Flux Analyzer XFp, which measures extracellular acidification rate (ECAR) (mpH/min) and oxygen consumption rate (OCR) (picomoles/min). These metrics can serve as proxies for real time glycolytic and mitochondrial respiration, respectively. 150,000 cells were plated into a poly-D-lysine coated eight-well plate, which allows the cells to adhere properly in a single cell layer. The plate was incubated at 37° C with no CO_2 for 2 hours to foster the optimum environment for measuring metabolic activity.

For the mitochondrial stress assay, OCR and ECAR were measured while cells were subjected to real time injections of compounds that stretch the cells to the metabolic limits. At basal conditions and after each injection, these measurements were taken 3 times for each well. The injections were 1 μM oligomycin, 1.5 μM fluorocarbonyl cyanide phenylhydrazone (FCCP), and 0.5 μM rotenone/antimycin A (XFp mito stress test kit; cat#103010-100; Agilent Technologies).

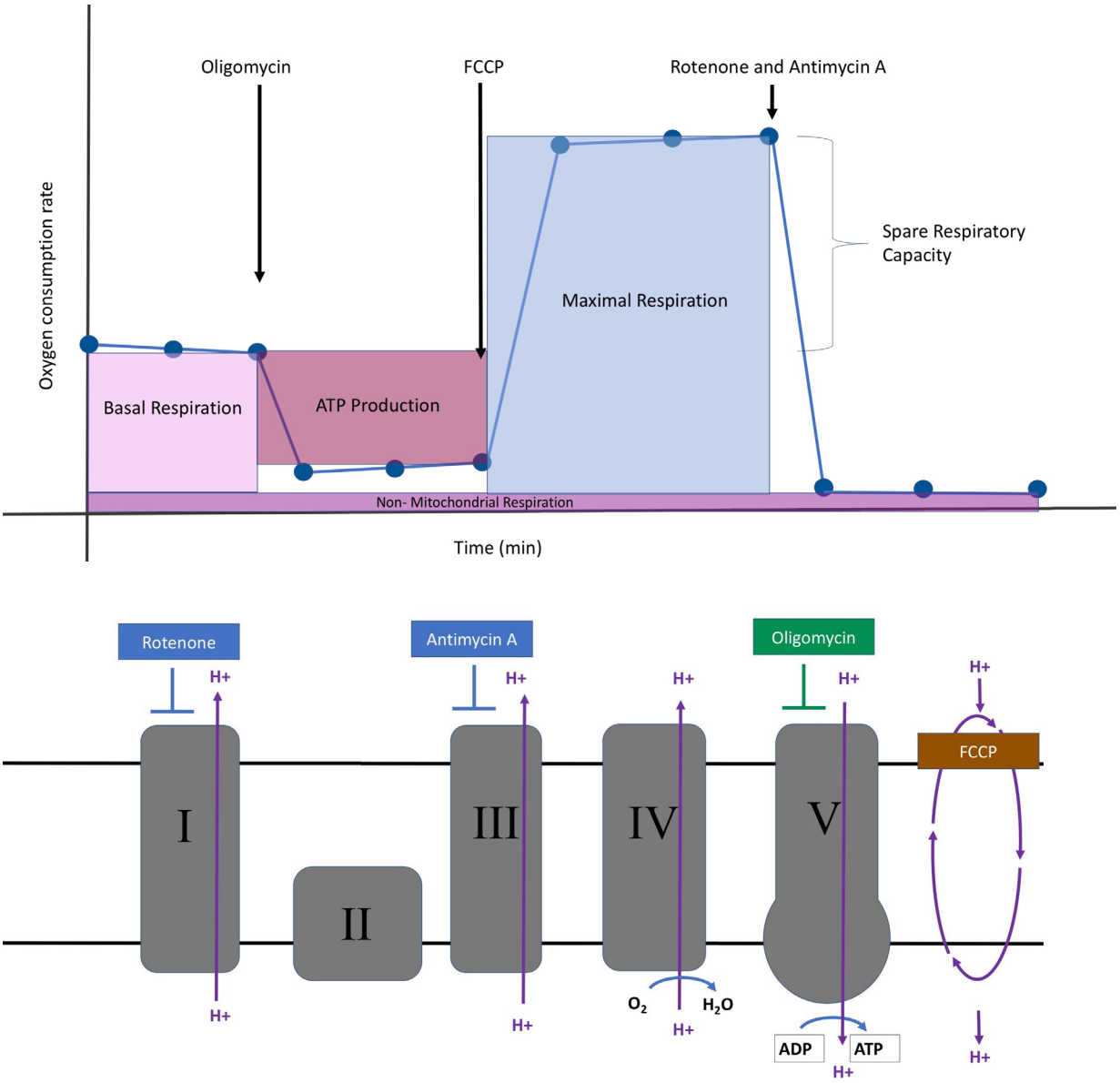

Figure 3-3: Metabolic Assay explained mechanistically. (A): This figure outlines the data that can be extracted from using the seahorse machine. By adding compounds that inactivate various parts of the electron transport chain (as shown in Figure 3b), the cells are stretched to their metabolic limits (B): An outline of the targets of the compounds added in Figure 3a and where they modulate the electron transport chain.

3.3 Results

This project is ongoing, with data continuing to be collected. The following describes our findings for others continuing this project and the results of optimization of this on-going project.

3.3.1 Procedural findings

First, CD4 T cells were better maintained and activated by Dynabeads than antibodies in non-specific activation in our experiments. Lee et al found that CD3/CD28 antibody activation worked best for CD8+ T cells, but a direct comparison consistently showed that for CD4+ T cells the CD3/CD28 Dynabead method of activation works better (Figure 3-4A). Interestingly, in this data, the control with no activation performs similarly to the Dynabeads, while the antibodies perform worse. Essentially, Dynabeads were able to keep the cells alive at the same level for the 24 hours between tests, while the antibodies could not (Figure 4-4B).

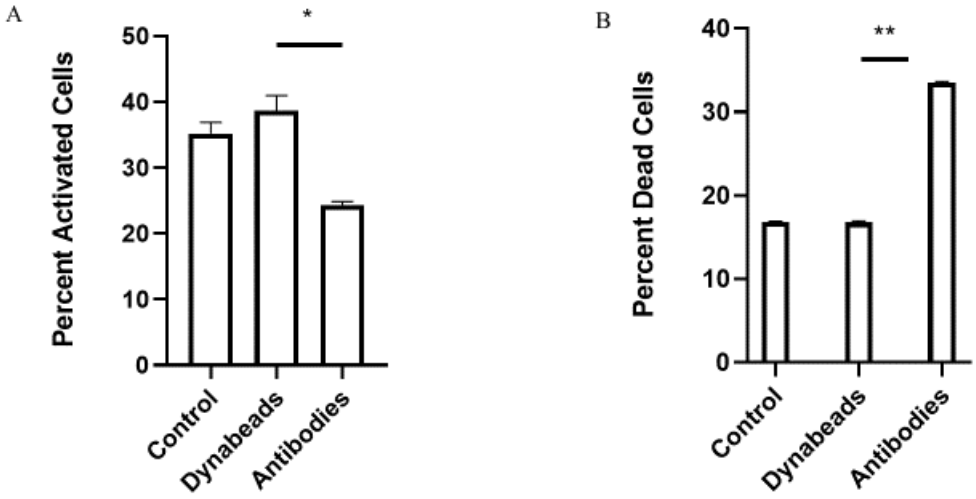

Figure 3-4: Non-specific activation of CD4+ T cells works better with Dynabeads than with CD3/CD28 antibodies. (A) Percentage of activated cells measured by flow cytometry, gating on the activated cell population using activation marker CD44 and forward scatter. Control represents cells that were cultured without the activation reagents. (B) Percentage of dead cells, calculated using PI stain and flow cytometry.

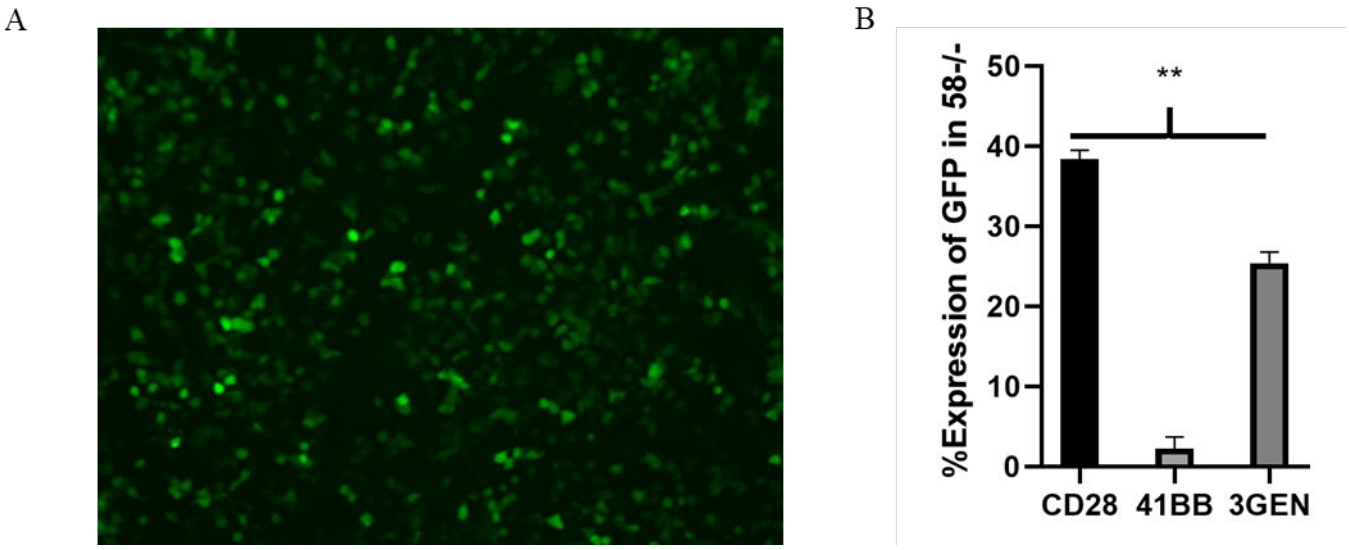

Figure 3-5: Viruses are infecting some cell types. (A) 3GEN virus on PlatE cells displaying GFP fluorescence. (B) Quantification of GFP expression in 58-/- T cell hybridomas.

The plasmids for the CD28 CAR and the third generation (CD28+4-1BB) CAR are performing well. They have high viral titer, as evidenced by high fluorescence of the packaging cells (Figure 3-5A) and the transduction efficiency of a T cell hybridoma line, 58-/- cells (Figure 3-5B). The 4-1BB CAR vector does not have high transduction efficiency in the T cell hybridoma (data not shown), determining the reason for this will require further investigation.

3.3.2 Negative results

Currently, CAR T cell production has not made it possible to accurately measure the metabolism of the various CAR T cells (Figure 3-6). Cell death and transient expression of the CAR on T cell surface makes this a difficult process which has not been optimized fully. Measuring OCR levels results shows levels which are too low to be analyzed meaningfully, indicating extensive cell death at some point in the process.

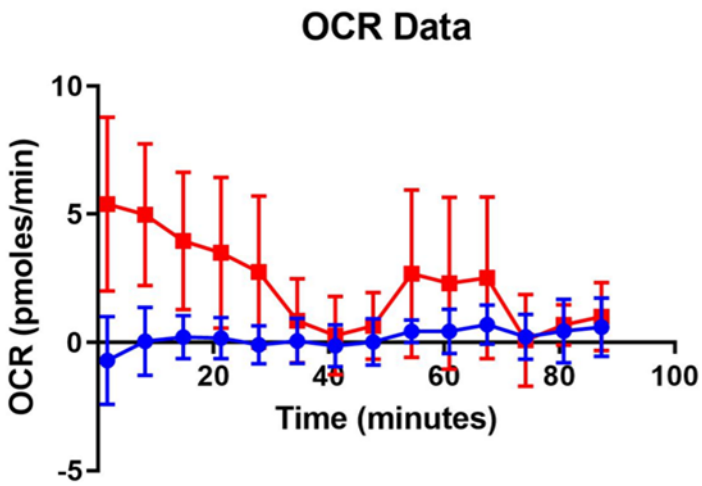

Figure 3-6: CAR T cell metabolism has not been able to be measured. Cells are not surviving the CAR T cell creation process. Red represents third generation (3GEN) and blue represents the CD28 CAR. Note the scale of the oxygen consumption rate, which is much lower than it should be.

3.4 Conclusions and future directions

Understanding the metabolism of CAR T cells could allow for fine-tuned approaches to cancer immunotherapy. Even more simply, the basic biology of these altered T cells also can shed light on normal T cell function.

In the future, to continue this project, the metabolism of the CAR T cells can be looked at in a few ways. The mitochondrial stress test and glycolysis stress test are best used as overview assays, and then investigation can proceed from there. Adding inhibitors of enzymes that prepare materials for respiration while measuring oxygen consumption can identify where the cell is obtaining its glucose for respiration. Metabolomic assays could also shed light on the nutrients used by CAR T cells. Measuring mitochondrial mass would be another important step in understanding the course of altered metabolism.

Studying the synergy of CAR T cells and checkpoint inhibitors metabolically also would be an interesting direction. Checkpoint inhibitors alter metabolism and can be used in conjunction with CAR T cells, but that realm is relatively new [10].

CHAPTER 4: THE ROLE OF CD5 ON T CELL METABOLISM

The following chapter is a work in progress and will be submitted for scientific review upon completion. Current data and future directions for this project are presented here.

4.1 Introduction

T-cell function is highly specific and sensitive to small changes to the cellular composition [84]. This chapter provides an investigation of T-cells with varying levels of a specific co-receptor called CD5. Energy use is particularly crucial to T cell activation and survival, making T-cell metabolism an important potential therapeutic target.

T cell activation is initiated by an antigen binding strongly to the T-cell receptor (TCR), making this interaction crucial to the entire immune system. Various co-receptors mediate antigen-TCR binding, and different co-receptors can trigger diverse responses. As discussed in chapter 3, co-receptors have been shown to have a large impact on the metabolic program of a T cell [77]. CD5 is a co-receptor that plays a negative regulatory role in thymic development of T cells [22]. As T cells develop, their unique receptors are tested for strength of binding; they must recognize the MHC molecule well enough to interact with it, but they cannot bind too tightly to self MHC, or there would be a risk of autoimmunity. If a receptor's binding strength falls above a certain threshold, it will be given a signal to trigger apoptosis. CD5 appears to module T cell receptor binding to MHC, and fine tune the sensitivity of the interaction in order to prevent cells with a binding capacity at the higher end of the range from dying. CD5 abundance correlates with the strength of the self peptide-TCR reaction, providing a means to control thymic selection more specifically [22].

Recently, it has been suggested that CD5 may act as a negative regulator in multiple circumstances, making it similar to common negative co-receptors like PD-1 or CTLA4 [85].

These co-receptors effectively block the activation signal of TCR binding from progressing in the cell. CD5 is believed to perform a similar inhibition of activation [23]. It is believed to do this through calcium mobilization and regulation of metabolic genes. The inhibition of the activation signal can be valuable when the immune response needs to be slowed or stopped, or to prevent autoimmunity or a cytokine storm [86]. However, this "stop signal" has also been co-opted by cancer cells to prevent immune cells from removing some cancer cells and enabling some cancer to grow unabated [17, 87]. Checkpoint inhibitor therapies bind to negative co-receptors and prevent them from inhibiting T cell activation, thus allowing for greater immune activity, and better cancer outcomes.

CD5 is a similar negative regulator, suggesting that it could also be useful in immunotherapy. Previously, it has been shown that CD5 modulates calcium signaling, a crucial second messenger involved with a number of cell processes [23]. Calcium is specifically involved in triggering the transcriptional factors needed for T cell activation, especially activation of glucose transporter Glut-1. CD5 signals to IP3R which decreases calcium activation of the nuclear factor of activated T cells (NFAT), presumably influencing metabolism. In a gene analysis of B cells, metabolic genes were some of the main genes activated differentially when CD5 is absent. This project looks to characterize the metabolism of T cells when the CD5 co-receptor is knocked out.

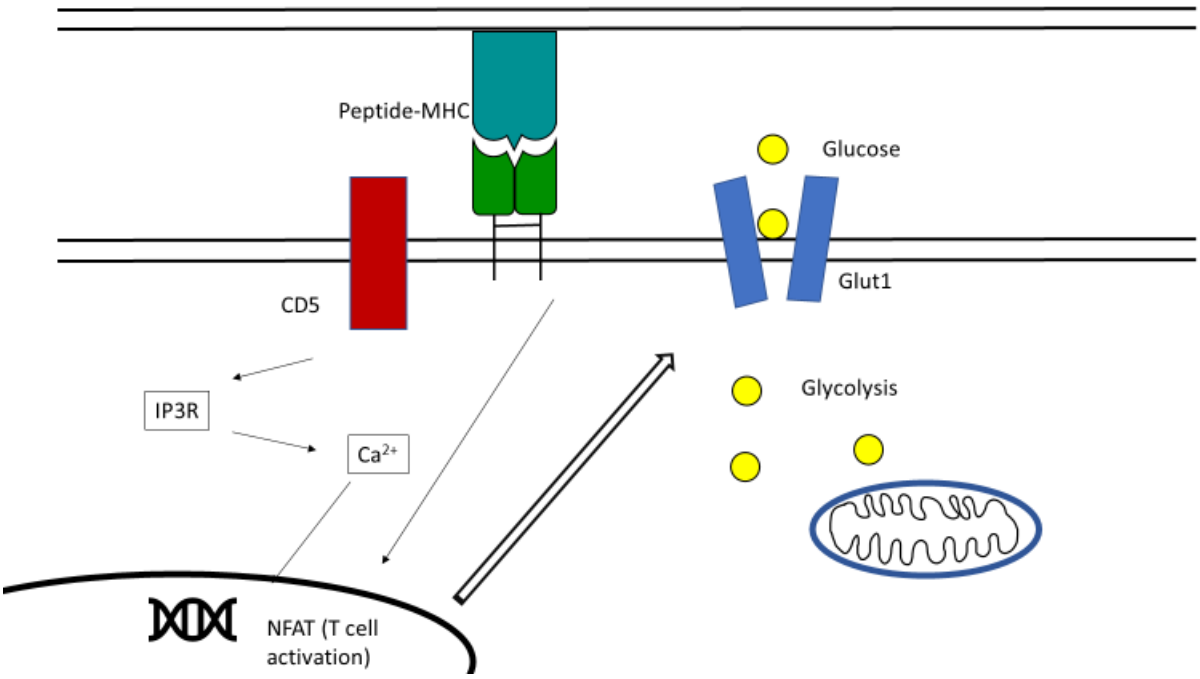

Figure 4-1: The interaction of CD5 with T cell activation and metabolism. The T cell receptor interaction is depicted which is modulated in turn by CD5. This pathway activates IP3R to mobilize calcium which triggers the T cell activation transcription factor. One effect of this transcription cascade is the activation of the Glut1 glucose transporter to upregulate intake of glycolysis.

4.2 Materials and methods

4.2.1 Mice

The mice used all have a C57/BL6 background and were housed in standard conditions on site in the BYU vivarium and fed with normal chow. The strains used were wild type (WT) C57/BL6 and CD5 knock out (KO).

4.2.2 T cell isolation

T cells were isolated from the spleens of the mice above, after CO_2 euthanization. A single cell suspension of splenocytes mixed with magnetic beads was applied to magnetic columns to isolate CD4+ T cells by negative selection (Miltenyi Biotech). Cells were placed in RPMI 1640 media with added 25 mM glucose, 2 mM L-glutamine and 1 mM sodium pyruvate (Agilent Technologies).

4.2.3 Metabolic assays

T cells were assayed using an Extracellular Flux Analyzer XFp, which measures extracellular acidification rate (ECAR) (mpH/min) and oxygen consumption rate (OCR) (pmoles/min). These metrics can serve as proxies for real time glycolytic and mitochondrial respiration, respectively. 150,000 cells were plated into a poly-D-lysine coated eight-well plate, which allows the cells to adhere properly in a single cell layer. The plate was incubated at 37° C with no CO_2 for 2 hours to foster the optimum environment for measuring metabolic activity.

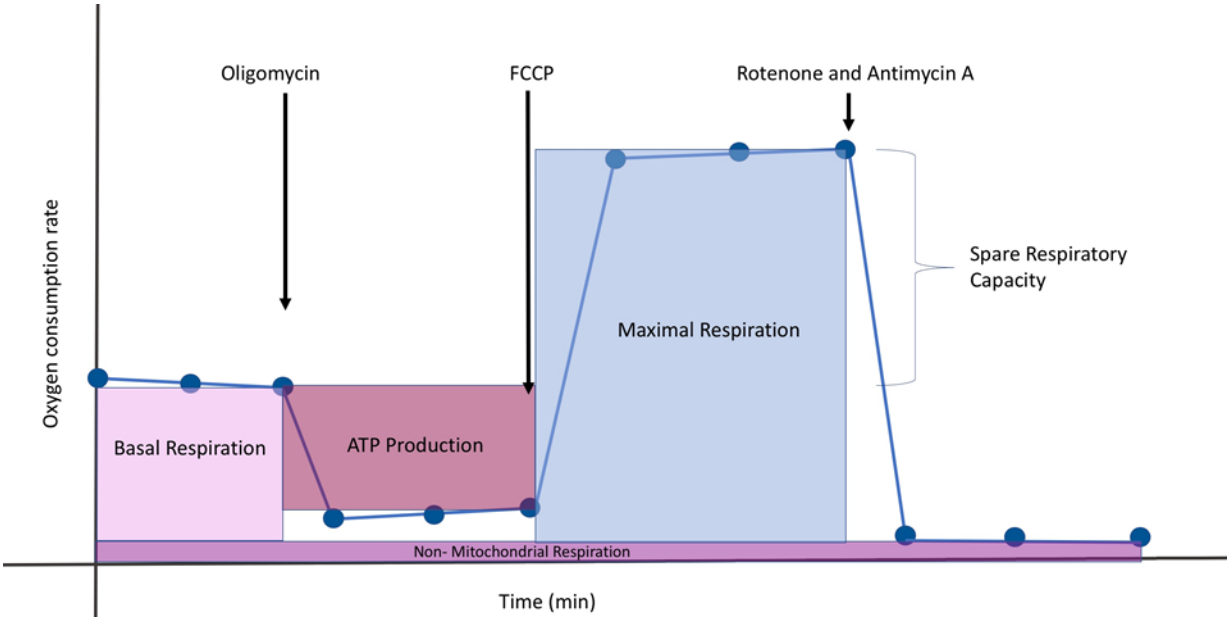

Figure 4-2: Mitochondrial Stress Test Data template. This is a sample of what data output would look like from the Seahorse mitochondrial stress test, displaying the theoretical changes in oxygen consumption over time with the addition of the various chemicals. The colored boxes represent the metrics that can be obtained from this test.

For the mitochondrial stress assay, OCR and ECAR were measured while cells were subjected to real time injections of compounds that stretch the cells to the metabolic limits. At basal conditions and after each injection, these measurements were taken 3 times for each well. The injections were 1 μM oligomycin, 1.5 μM fluorocarbonyl cyanide phenylhydrazone (FCCP),

and 0.5 µM rotenone/antimycin A (XFp mito stress test kit; cat#103010-100; Agilent Technologies). The time frame and template of results can be seen in Figure 4-2.

For the glycolysis stress test, OCR and ECAR are measured similarly, but in response to 10 mM glucose, 1 µM oligomycin and 50 mM 2-DG (XFp glycolysis stress test kit; cat#103017-100; Agilent Technologies). All chemicals were purchased from Seahorse Bioscience (North Billerica, MA). Calculations for individual parameters represents the average of individual well calculations for each assay group. Error bars are calculated based on the individual well calculation for each parameter (Report Generator User guide, Agilent Seahorse). A timeframe and results template can be seen in Figure 4-3.

The naïve cells were kept and activated with CD3/CD28 stimulation beads, as recommended by the manufacturers. The metabolic assays were then repeated at 24 hours, 96 hours, and 120 hours.

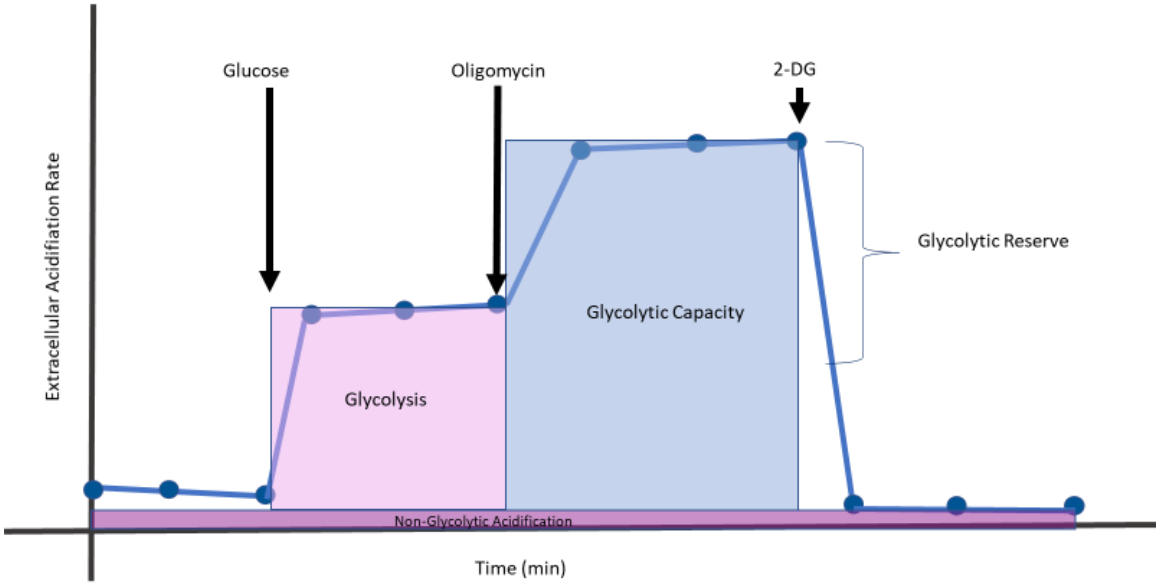

Figure 4-3: Glycolysis stress test data template.This is a sample of what data output would look like from the Seahorse glycolysis stress test, displaying the theoretical changes in the extracellular acidification rate

over time with the addition of the various chemicals. The colored boxes represent the metrics that can be obtained from this test.

4.3 Results

To understand the role of CD5 in metabolism, we isolated naïve T-cells from wild type mice and CD5 knockout mice. Based on the negative regulatory role of CD5, we expected CD5 KO T cells to have a higher activation profile, but it was unknown if that activation pattern was mediated by metabolic processes.

We ran a cell mitochondrial stress test and found that CD5 KO T cells have significantly higher levels of mitochondrial respiration (Figure 4-4). This test measure oxygen consumption rate in real time as drugs are added to inhibit specific parts of the oxidative phosphorylation process (Figure 4-2).

The basal level of activity of CD5KO T cells differs significantly after normalization (Figure 4-4B), indicating that the normal high sensitivity of CD5 KO cells may be due to a more active metabolism, even without stimulation. Adding oligomycin blocks ATP synthetase, so difference between the pre-injection and post-injection levels can give an estimate of oxygen consumption being used for ATP production (Figure 4-4C). The levels after oligomycin did not differ significantly (data not shown), so the difference in ATP production mirrors the basal level discrepancy. These differences repeated consistently over five assays, suggesting a biological change here, instead of something procedural.

Another important measure is the capacity of the cell to use energy. Basal levels often correlate with maximum respiration, but not always. Adding FCCP bypasses the previously blocked ATP synthetase and allows all the hydrogen ions to flow freely back into the

mitochondrial matrix, consuming the maximum amount of oxygen. This measure is much higher in CD5KO T cells, suggesting that they have a larger spare respiratory capacity.

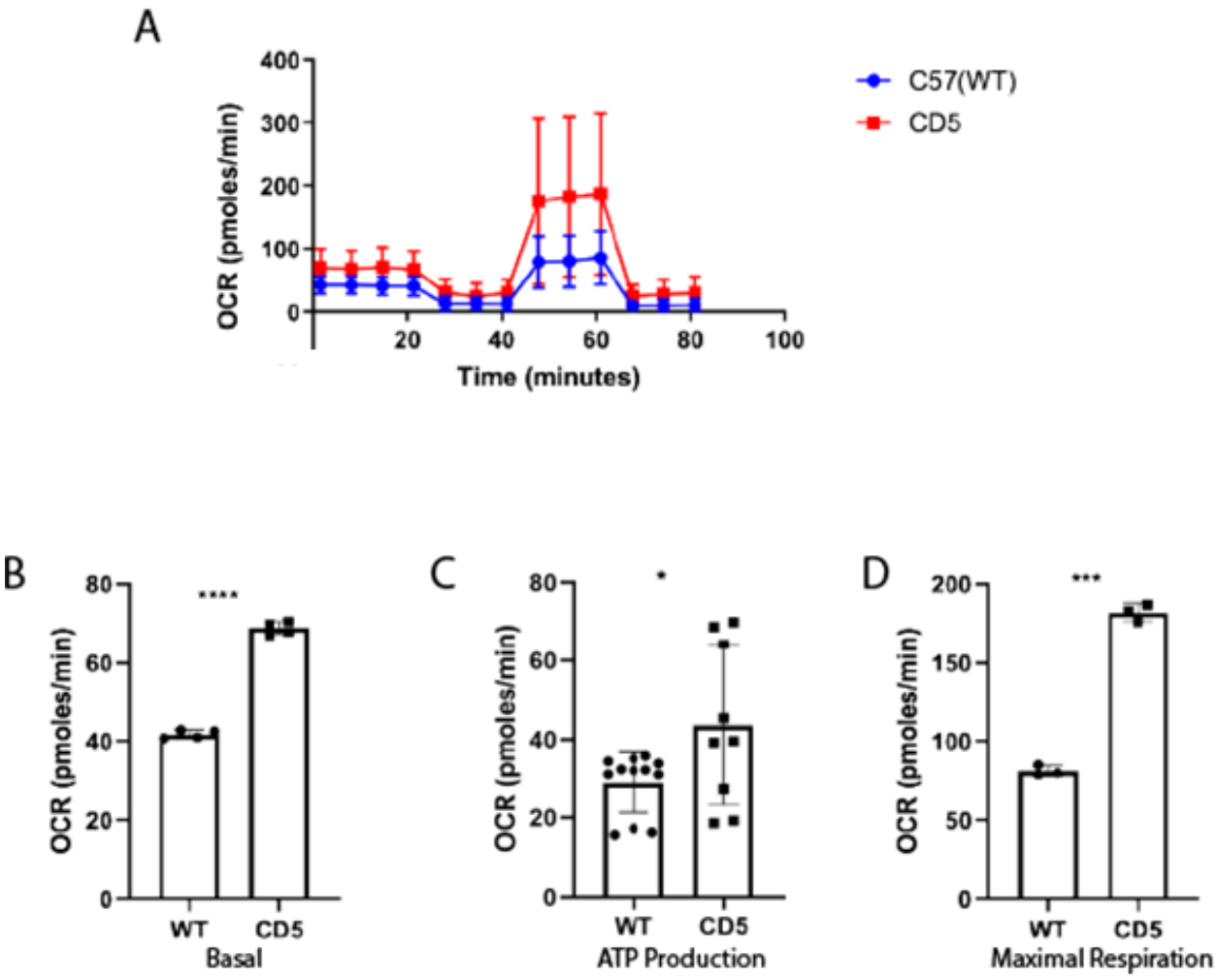

-

Figure 4-4: CD5 KO T cells have higher mitochondrial oxygen consumption as compared to WT T cells. (A) Mitochondrial stress test results indicate that CD5 KO T cells are higher at all points of the test, indicating a hypermetabolic state. The following figures show the breakdown of those differences at each point in the test. (B) The basal levels of oxygen consumption differ between the CD5 KO and the WT T cells. (C) The levels of ATP production as measured by oxygen consumption differ between the CD5 KO and the WT T cells. (D) The maximal respiration capacity as measured by oxygen consumption after the addition of an uncoupler differ between the CD5 KO and the WT T cells. (N=5) (*=P<0.05, **=P<0.01, ***= P<0.001, ****=P<0.00001)

The glycolysis stress test measures the extracellular acidification rate (ECAR), which can be a good indicator of how much glycolysis is ongoing inside of the cells, because glycolysis creates extra hydrogen ions. First, glucose is added to cause that spike, and CD5 KO cells had higher acidification, suggesting higher rates of glycolysis. This makes sense considering that glycolysis is the first step leading to mitochondrial respiration which was shown to be higher previously (Figure 4-4B). Figure 4-4C shows the difference after the addition of oligomycin. As mentioned above, oligomycin blocks ATP synthetase, which should lead to maximum glycolysis, because the cell is getting all of its energy from glycolysis. Interestingly, in these cells, the rate goes down after blocking ATP synthetase, possibly indicating that that extracellular acidification has contributions from other sources. Regardless, the difference between the ability to utilize glycolysis is significantly higher in CDKO cells.

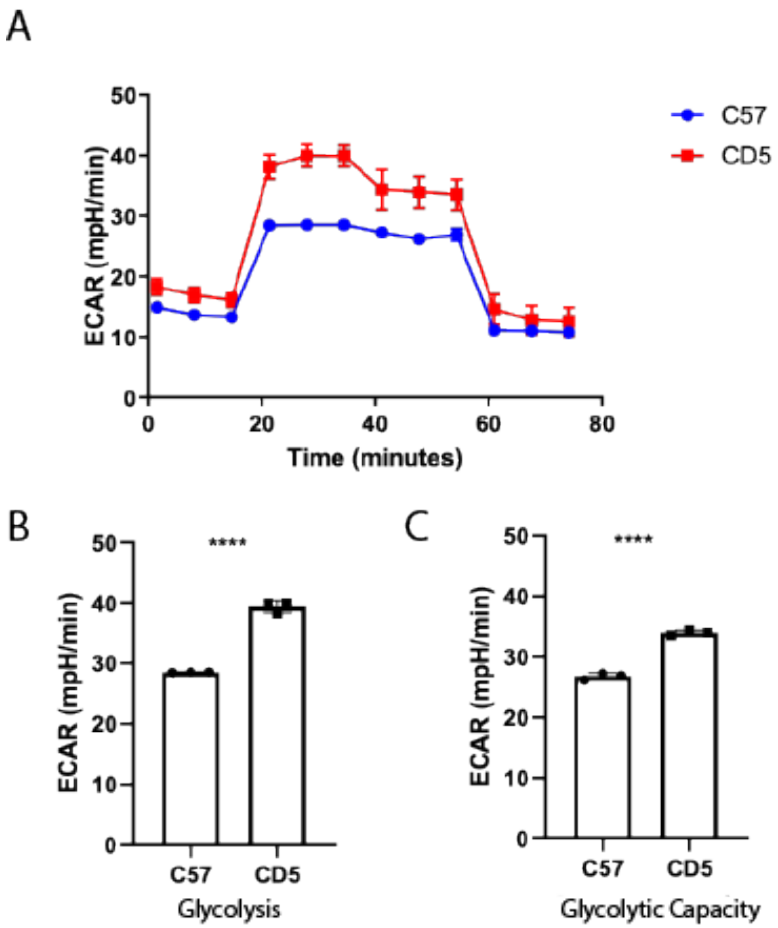

Figure 4-5: CD5 KO T cells have a higher glycolytic energy profile than WT T cells. (A) Glycolytic stress test for CD5 KO T cells versus WT T cell indicates high glycolysis usage after the addition of glucose, oligomycin and 2-DG to measure maximum and minimum levels. (N=3). (B) Comparison of basal glycolysis between the two. (C) Comparison of maximum glycolytic capacity. (N=5) (*=P<0.05, **=P<0.01, ***= P<0.001, ****=P<0.00001)

The metabolic differences are maintained transiently over time. Work done with Claudia Freitas indicates that the same difference in mitochondrial capacity is only significantly displayed at 96 hours after activation with CD3/CD28 Dynabeads (Figure 4-6 E, F). More tests could lead to a significant result since the trend remains the same, but that is ongoing work.

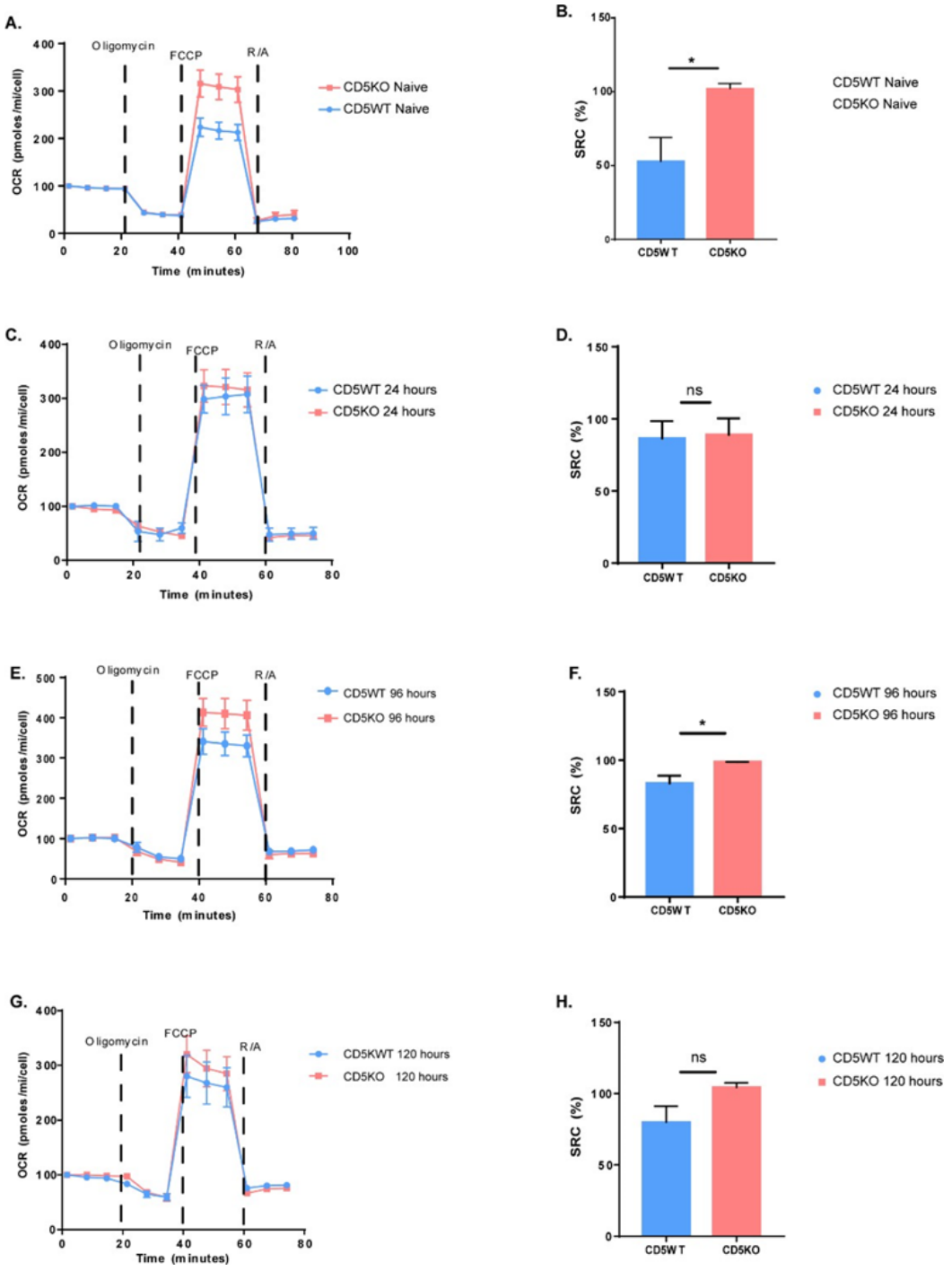

Figure 4-6: CD5KO T cells display higher mitochondrial respiration across time points. (A) CD5 KO cells compared to the WT counterpart in a mitochondrial stress test in naïve cells. Cells were isolated from mouse splenocytes and added to the plates, then subjected to the listed blockers of the electron transport chain. (B) Comparison of spare respiratory capacity (SRC) at this time point. (C, E, G) Mitochondrial stress test at 24, 96 and 120 hours, respectively. Isolated cells were cultured for the appropriate time before testing. (D, F, H) SRC at 24, 96 and 120 hours respectively. (*=P<0.05) (Work done with Claudia Freitas and Tyler Cox.)

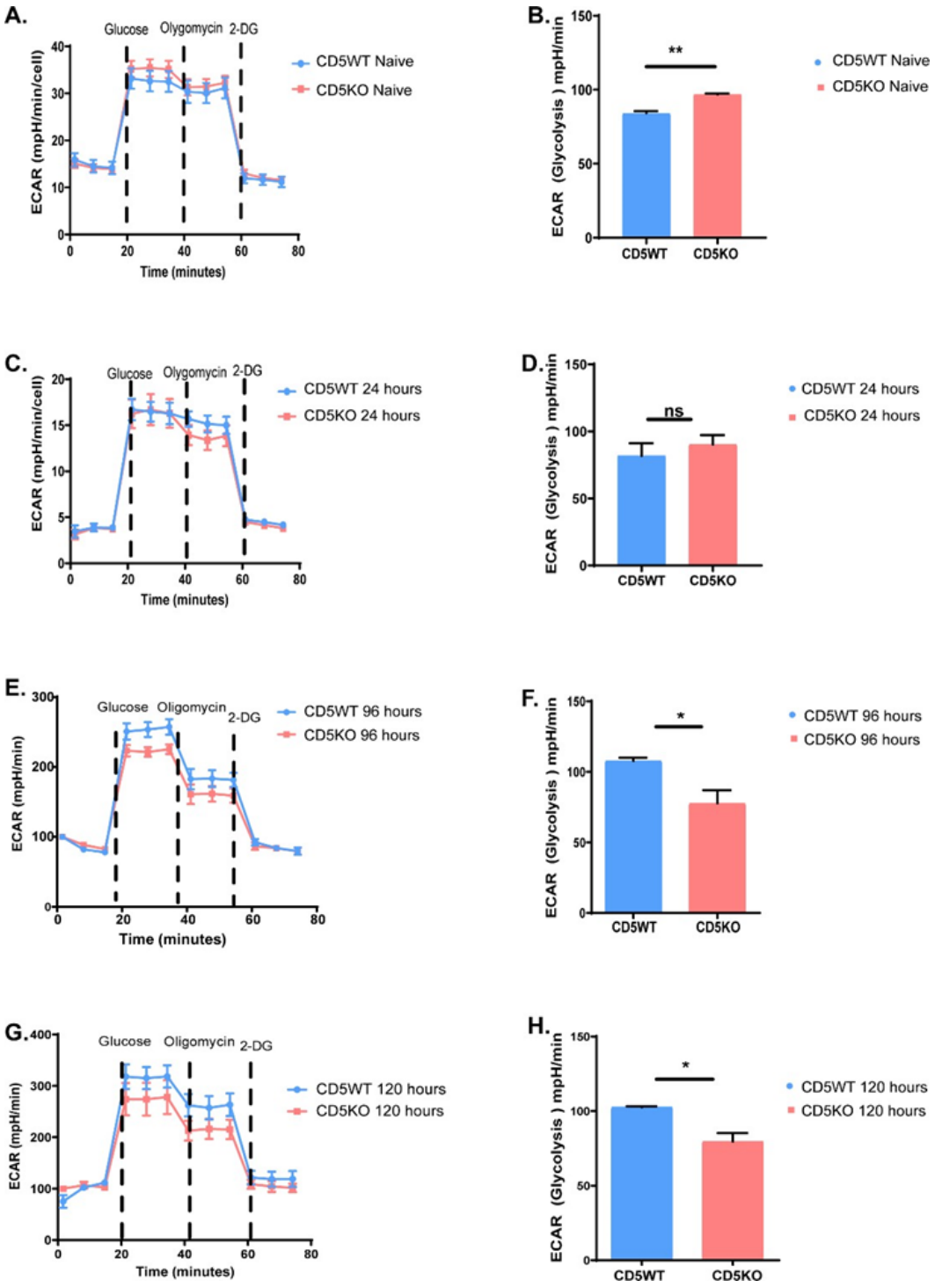

Figure 4-7: CD5KO T cells display higher glycolytic respiration across time points. (A)CD5 KO cells compared to the WT counterpart in a glycolytic stress test in naïve cells. Cells were isolated from mouse splenocytes and added to the plates. (B) Comparison of glycolysis at this time point. (C, E, G) Mitochondrial stress test at 24, 96 and 120 hours, respectively. Isolated cells were cultured for the appropriate time before testing. (D, F, H) Glycolysis at 24, 96 and 120 hours respectively. (*=P<0.05, **=P<.01)(Work done with Claudia Freitas and Tyler Cox.)

4.4 Conclusions and future directions

This preliminary data suggests that CD5 KO T cells have significantly different energy demands than wild type T cells in the naïve state. The profiles of both glycolysis usage and mitochondrial capacity indicate that naïve CD5 KO T cells have a higher energy capacity.

A more metabolically active T cell could be useful for certain immunotherapies. Cancer often outcompetes immune cells for resources, and more metabolic capacity could be very useful. The tumor microenvironment is often immunosuppressive in multiple ways, but one of the simplest is nutrient availability [11, 13, 75, 80]. By engineering a T cell with hypermetabolism, it may be able to compete more effectively against rapidly dividing cancer cells.

In the future, the differences in CD5 KO metabolism can be investigated further, at more time points, and with different energy substrates. A metabolomics assay would be able to identify the relative abundance of different nutrients in the two cell types, which could give insight into what metabolic pathways are being altered [88]. Metabolic differences could also be mediated by the microbiome, as shown by the interaction of PD-1, a similar negative regulatory molecule with the microbiome of mice [89].

The next step for application would be testing WT T cells, treated with an anti-CD5 antibody in order to prevent CD5 from signaling. This could give some indication of whether the metabolic differences are mediated directly or indirectly. Further, creating CAR T cells from CD5 KO T cells could provide this increased metabolic output for competition with cancer cells.

CHAPTER 5: EVAPORATIVE COOLER USE AND BIOAEROSOLS

The work described in this chapter has been submitted to a scientific journal and is under review. It has been formatted for this thesis, but it is otherwise unchanged.

Associations between evaporative cooling and dust mite allergens, endotoxins, and β-(1→3)-D-glucans in house dust: A study of low-income homes

James D. Johnston[1*], Ashlin E. Cowger[2*], Robert J. Graul[1], Ryan Nash[1], Josie A. Tueller[2], Nathan R. Hendrickson[1], Daniel R. Robinson[1], John D. Beard[1], K. Scott Weber[2]

[*] Co-first author

[1] Brigham Young University

Department of Public Health

4103 Life Sciences Building

Provo, Utah 84602

[2] Brigham Young University

Department of Microbiology & Molecular Biology

4007 Life Sciences Building

Provo, Utah 84602

5.1 Abstract

Recent work suggests that evaporative coolers increase the level and diversity of bioaerosols, but this association remains understudied in low-income homes. We conducted a cross-sectional study of metropolitan, low-income homes in Utah with evaporative coolers (n = 20) and central air conditioners (n=28). Dust samples (N = 147) were collected from four locations in each home, and analyzed for dust mite allergens Der p 1 and Der f 1, endotoxins, and β-(1→3)-D-glucans. In all sample locations combined, Der p 1 or Der f 1 was significantly higher in evaporative cooler versus central air conditioning homes (OR = 2.29, 95% CI = 1.05 – 4.98). Endotoxin concentration was significantly higher in evaporative cooler versus central air conditioning homes in furniture (geometric mean (GM) = 8.05 vs. 2.85 EU/mg, $P < 0.01$) and all samples combined (GM = 3.60 vs. 1.29 EU/mg, $P = 0.03$). β-(1→3)-D-glucan concentration and surface loads were significantly higher in evaporative cooler versus central air conditioning homes in all four sample locations and all samples combined ($P < 0.01$). Our study suggests that low-income, evaporative cooled homes have higher levels of immunologically-important bioaerosols than central air-conditioned homes in dry climates, warranting studies on health implications and other exposed populations.

5.2 Practical implications

A growing body of literature suggests that evaporative coolers have the potential to significantly alter the microbiological and bioaerosol profile of low-income homes in dry climates. Our focus on low-income homes was valuable, in that higher occupant densities appeared to be a significant factor influencing dust mite allergen concentrations. In addition to evaporative cooler use, sample location was a significant determinant of endotoxin levels. Evaporative cooler use, home age, number of residents, and bedroom carpet age, were significant

determinants of β-(1→3)-D-glucan levels. Indoor environmental quality professionals should consider air conditioning type and these housing factors when trying to understand or mitigate bioaerosols in low-income homes.

5.3 Introduction

Residential exposure to bioaerosols (i.e. inhalable particles of microbial, plant, or animal origin) appears to be responsible, paradoxically, for both protection against and initiation of serious allergic diseases. Early-life bioaerosol exposures play a key role in shifting the immune system either toward or away from a T helper cell 2 (TH2) imbalance and associated atopy [90, 91]. Conversely, exposure to residential bioaerosols can lead to sensitization with multiple allergy-type symptoms in asthmatic and non-asthmatic individuals [92]. Children spend approximately 60 – 80% of their time [93], and adults spend approximately 70% of their time indoors at home [94, 95], making the home a key microenvironment for bioaerosol exposure. The bioaerosol profile of an individual home varies widely based on multiple housing factors, including geographical location [96-101], presence of indoor or outdoor animals [96-105], living on a farm [96, 102], number of occupants [97-100, 103], cleanliness and presence of cockroaches [97, 104], presence of carpeting or rugs [99, 102], and other factors. A few studies also suggest that evaporative coolers may significantly alter the bioaerosol profile in homes for immunologically important exposures such as house dust mite (HDM) allergens Der p 1 and Der f 1, bacterial endotoxins, and β-(1→3)-D-glucans [106-109].

Evaporative coolers are predominantly used in climates with low relative humidity (RH) and seasonally high outdoor temperatures [27] such as the Rocky Mountain States in the U.S. Residential evaporative coolers remove heat from dry ambient air by drawing the air across a wetted filter media, resulting in lower indoor air temperature, but higher RH [109, 110]. The

higher RH from evaporative coolers may create an ecological niche for HDMs to survive in arid and semi-arid climates [106, 109], potentially exposing home occupants to mite allergens [111]. Furthermore, untreated evaporative cooler sump water provides a growth medium for Gram-negative bacteria during summer months [112], and may be a significant source of residential endotoxin load in homes [107, 108]. Early-life exposure to endotoxins, the lipopolysaccharide portion of the cell wall in Gram-negative bacteria, may confer protection against the development of allergic diseases, including asthma [24, 113-116], while simultaneously causing airway inflammation and asthma symptoms in children and adults [117-120]. Finally, fungi are more common, and fungal species associated with allergies are more prevalent, in homes with evaporative coolers compared to homes with other forms of air conditioning [26, 108]. β-(1→3)-D-glucans, polysaccharides found in the cell wall of fungi, plants, and some bacteria, are important immunologically because they are associated with airway inflammation and decreased lung function [121-125]. We hypothesized that evaporative coolers may also be associated with higher levels of mold-related bioaerosols such as β-(1→3)-D-glucans, although we are not aware of any prior studies reporting this.

Although a growing body of research shows that evaporative coolers are associated with higher levels and varying types of immunologically important bioaerosols in homes, most prior studies on this topic do not report socioeconomic factors related to their study homes. Lower socioeconomic status is associated with increased asthma incidence and morbidity in affluent countries [25, 126, 127], and factors such as household income and occupant density may be important modifying factors for indoor bioaerosol loads. The purpose of this study, therefore, was to compare bioaerosol levels specifically in low-income households based on use of evaporative coolers or central air conditioners.

5.4 Methods

5.4.1 Study design

We conducted a cross-sectional study which included homes (N=48) that were identified by recruiting individuals exiting the Woman, Infants, and Children (WIC) office at the Utah County Health Department (UCHD). Research assistants were stationed at a booth outside of the WIC office, where they contacted potential participants in English and Spanish as they exited the office. Participants in the study were given study flyers in either English or Spanish, and a screening questionnaire to determine if their home met criteria for the study. Exclusion criteria for the study were (1) use of humidifiers or vaporizers, (2) previous water damage covering more than 9.29 m^2 (100 ft^2), (3) home newer than 5 years old, and (4) household income ≥ 100% of the 2017 Federal Poverty Guidelines. All participating homes were in Utah County, Utah. We recruited only central air and evaporative cooling homes for this study. However, when study personnel arrived at the homes for sample collection they verified the type of air conditioning used in the home. This verification step found that 4 of the homes did not actually have air conditioning of any type, resulting in the following sample sizes: evaporative cooling (N=20), central air conditioning (N=24), or no air conditioning (N=4). Due to the small number of homes with no air conditioning, the four homes with no air conditioning were combined with the 24 homes that had central air conditioning for analyses (hereafter referred to as central air conditioning homes), as was done in a previous study [106].

Home visits were conducted between July and October 2017. At each home visit, study personnel collected dust samples and measured indoor temperature and relative humidity (RH). Brigham Young University's Institutional Review Board approved this study (IRB #X17261).

5.4.2 Reservoir dust collection

Dust was collected from four different areas in each home. These areas included the primary adult resident's mattress, the floor in the same room as the mattress, upholstered furniture in the living room, and the living room floor. All bedding was removed from the mattress before sampling to allow a direct sample from the mattress to be taken. A $1m^2$ area of the surface to be sampled was measured and then vacuumed continuously for 3 minutes. Each sample was taken using a Eureka (Bloomington, IL, USA) "Mighty Mite" vacuum (model 3684F) attached to a Duststream® dust collector extension and 40 μm nylon mesh filter (Indoor Biotechnologies, Charlottesville, VA, USA). Prior to sample collection, all research assistants were trained on sampling procedures. Following sample collection, the dust was sieved using a #50 wire mesh (300μm) and then moved to a 15 ml polypropylene conical tube. Samples were then stored at approximately -20° C until they were analyzed for dust mite allergens Der p 1 and Der f 1, endotoxins, and β-(1→3)-D-glucans.

5.4.3 Der p 1 and Der f 1 extraction and analysis

Der p 1 (*D. pteronyssinus*) and Der f 1 (*D. farinae*) allergens were extracted by suspending 100 mg of dust in 2 mL of phosphate-buffered saline with 0.05% Tween-20 (PBS-T). Samples were agitated for 2 hours at room temperature then centrifuged for 20 minutes at 2,500 RPM and 4°C. Allergen levels were detected using a two-site monoclonal antibody-based enzyme-linked immunosorbent assay (ELISA) kit (Indoor Biotechnologies, Charlottesville, VA, USA). Sample extracts (200 mL) were added in triplicate to each plate, and a 10-point curve was made using sequential 2-fold dilutions of a known standard in PBS-T with 1% BSA. Samples were read with an optical density plate reader at wavelength 405 nm. Prism 8 software (GraphPad Software, La Jolla, CA, USA) was used to extrapolate allergen concentrations from

the standard curve for each plate. The limit of detection (LOD) for both Der p 1 and Der f 1 assays was 0.04 mg/g of dust.

5.4.4 Endotoxin and β-(1→3)-D-glucan extraction and analysis

Extraction of endotoxin and β-(1→3)-D-glucan from dust samples was performed by suspending 100 mg of dust in 2 mL of sterile, pyrogen-free LAL water containing 0.05% Tween-20 (LAL-T), followed by agitation at room temperature for 1 hour. After agitation, samples were centrifuged at 2500 RPM at 4°C for 20 minutes and supernatants were collected and stored at −20°C. For endotoxin testing, sample extracts were diluted in LAL endotoxin-free water and were added in triplicate to each plate. A seven-point curve was made using four sequential 1:10 dilutions of a known standard in LAL endotoxin-free water. Endotoxin levels were measured using a Kinetic-QCL™ assay (Lonza, Walkersville, MD, USA). Samples were read with an optical density plate reader at wavelength 405 nm. Plate reader software was set up to measure time of onset at 0.200 O.D. units. Excel was used to extrapolate allergen concentrations from the onset times for each standard. The LOD for endotoxin was 0.0001 EU/g.

For β-(1→3)-D-glucan testing, sample extracts were heat treated at 100°C for one hour and diluted in pyrogen-free water as previously described [120, 128, 129]. Samples were added in triplicate to each plate. A five-point standard curve was made using sequential 2-fold dilutions. β-(1→3)-D-glucan levels were measured using (1,3)-β-D-Glucan Detection Glucatell® kit based on the Kinetic Onset Time protocol according to manufacturer's specifications (Associates of Cape Cod Incorporated, East Falmouth, MA, USA). Samples were read with an optical density plate reader at wavelength 405 nm. Plate reader software was set up to measure time of onset at 0.03 O.D. units. Excel was used to extrapolate β-(1→3)-D-glucans concentration from a log-log standard curve. The LOD for β-(1→3)-D-glucan was 0.0000625 µg/mg dust.

5.4.5 Indoor temperature and RH measurement

Indoor air temperature and RH measurements were collected as described in the Supporting Information (Supplemental Methods, Indoor Temperature and RH Measurement).

5.4.6 Housing questionnaire

The research team obtained written consent and administered a 40-item housing survey at the beginning of each in-home visit. The survey included items regarding the type, age, and size of the home, number of persons and pets living in the home, possible sources of humidity, such as unvented bathrooms or water damaged areas, age and type of mattresses, flooring, and other furniture, and frequency of vacuuming/cleaning.

5.4.7 Statistical techniques

All analyses were conducted using SAS version 9.4 (SAS Institute Inc., Cary, NC). Geometric means (GM), geometric standard deviations (GSD), minimums, maximums and p-values from t-tests were calculated for continuous characteristics of single-family homes and frequencies, percentages and p-values from χ^2 tests were calculated for categorical characteristics according to air conditioning type (central air conditioning vs. evaporative cooler). Occupant density, age of living room furniture and age of bedroom carpet were right skewed, so these variables were natural logarithm transformed.

When possible, analyses for house dust analytes were conducted for concentration and surface load to evaluate the robustness of the results to choice of outcome definition. All of the house dust analytes (Der f 1, Der p 1, and combined Der f 1 or Der p 1 concentration; endotoxin concentration and surface load, β-(1→3)-D-glucan concentration and surface load) were right

skewed, so these variables were natural logarithm transformed and GMs, GSDs or 95% confidence intervals (CI), minimums, and maximums were calculated.

Following previous authors [130, 131] , linear regression models were used for analyses when 100% of samples had concentrations or surface loads above detection limits, Tobit regression models were used for analyses when greater than 30 to 99% of samples had concentrations or surface loads above detection limits, and unconditional exact or large sample/asymptotic approximate logistic regression models were used for analyses when greater than 10 to 30% of samples had concentrations or surface loads above detection limits. To be specific, unconditional exact or large sample/asymptotic approximate logistic regression models were used to calculate unadjusted exact or large sample/asymptotic approximate odds ratios (OR) and 95% CI that estimated associations between air conditioning type or housing characteristics and the odds of Der f 1, Der p 1 and combined Der f 1 or Der p 1 above detection limits for individual sample locations and all sample locations combined (23% of samples had Der f 1 or Der p 1 concentrations above detection limits). Tobit regression models were used to calculate unadjusted GM ratios, 95% CI, and p-values that estimated associations between air conditioning type or housing characteristics and endotoxin concentration or surface load for individual sample locations and all sample locations combined (94% of samples had endotoxin concentrations or surface loads above detection limits). Linear regression models were used to calculate unadjusted GM ratios, 95% CI, and p-values that estimated associations between air conditioning type or housing characteristics and β-(1→3)-D-glucan concentration or surface load for individual sample locations and all sample locations combined (100% of samples had β-(1→3)-D-glucan concentrations or surface loads above detection limits).

Stepwise variable selection was used to develop unconditional logistic or linear regression models that included housing characteristics that were associated with Der f 1, Der p 1, and combined Der f 1 or Der p 1 concentration, and β-(1→3)-D-glucan concentration and surface load. Entry and exit significance levels were set at $\alpha = 0.15$. SAS does not have an option to conduct stepwise variable selection for Tobit regression models, so all housing characteristics were included in multiple Tobit regression models for endotoxin concentration and surface load and housing characteristics that had p-values less than $\alpha = 0.15$ were identified. Unconditional logistic, Tobit, or linear regression models were then used to calculate associations between air conditioning type and Der f 1, Der p 1, and combined Der f 1 or Der p 1 concentration, endotoxin concentration and surface load, and β-(1→3)-D-glucan concentration and surface load adjusting for housing characteristics that were identified via stepwise variable selection (or multiple Tobit regression models for endotoxin concentration and surface load).

Statistical techniques used to analyze 72-hour mean RH and temperature data and unadjusted associations between 72-hour mean RH and temperature, Der f 1, Der p 1, and combined Der f 1 or Der p 1 concentration, endotoxin concentration and surface load, and β-(1→3)-D-glucan concentration and surface load are described in the Supporting Information (Supplemental Methods, Statistical Techniques).

5.5 Results

5.5.1 Home characteristics

The geometric mean age of homes was 38.58 years and the geometric mean size was 92.26 m^2 (Table 1). The percentages of homes that were apartment, single story, two story, or other styles of homes were 25, 17, 27, and 31, respectively. The arithmetic mean number of residents was 4.79 and the geometric mean occupant density was 4.79 residents per 100 m^2. The

geometric mean ages of the bedroom carpet, bedroom mattress, living room carpet, and living room furniture were 94.62, 35.33, 61.47, and 53.29 months, respectively. Home age was the only characteristic that was statistically significantly different ($P < 0.01$) among homes with central air conditioning (31.70 years) and homes with evaporative coolers (51.53 years).

5.5.2 Der f 1 and Der p 1 allergen concentration

Overall, 34 (23%) dust samples were positive (i.e., above detection limits) for either Der f 1 or Der p 1 (Supplemental Table 1). Of the 28 homes with central air conditioning, 10 (36%) were positive for combined Der p 1 or Der f 1 in at least one location. Of the 20 homes with evaporative coolers, 11 (55%) were positive for combined Der p 1 or Der f 1 in at least one location. Only two homes were found with allergen concentrations (Der f 1 for both) that would be considered clinically significant for sensitization (i.e., > 2.0 µg/g dust). These samples were from a living room carpet (2.08 µg/g dust) and bedroom carpet (2.50 µg/g dust).

The odds of combined Der f 1 or Der p 1 concentrations above the detection limit were higher in homes with evaporative coolers compared to homes with central air conditioning for all sample locations combined (OR = 2.29; 95% CI: 1.05, 4.98; P = 0.04) (Figure 1, Supplemental Table 1). Number of residents, occupant density and bedroom carpet age were significantly positively associated with combined Der f 1 or Der p 1 concentration (Figure 1, Supplemental Table 2). Stepwise variable selection for combined Der f 1 or Der p 1 selected home size, number of residents and bedroom carpet age. Adjusting the odds ratio for air conditioning type and combined Der f 1 or Der p 1 for home size, number of residents and bedroom carpet age weakened the association (OR = 1.83; 95% CI: 0.70, 4.75; P = 0.22).

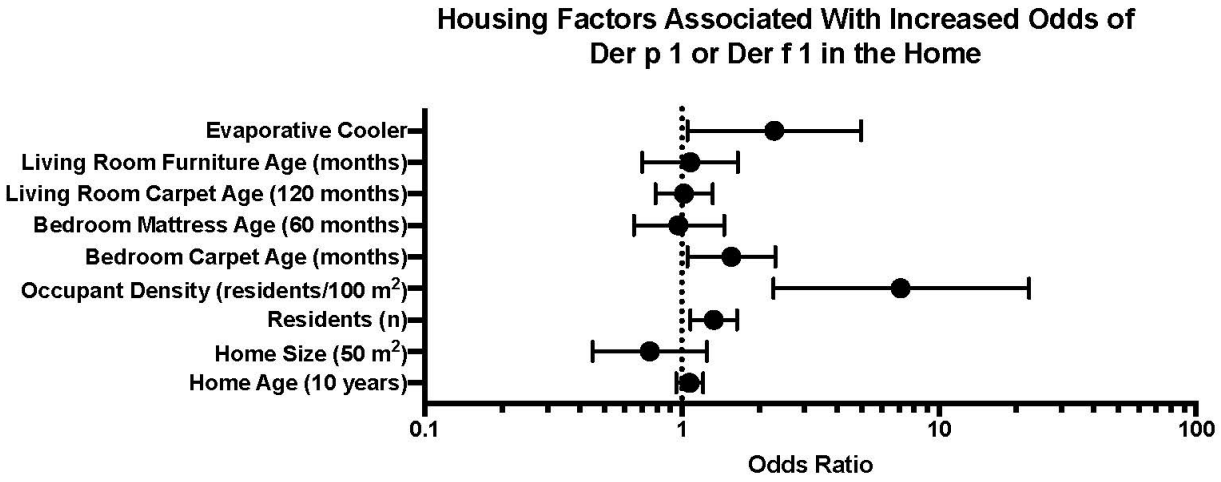

Figure 5-1: Housing Factors associated with increased odds of dust mite allergen in the home. Odds ratio for evaporative cooler vs. central air conditioning or none was calculated using large sample/asymptotic approximate odds ratio (i.e. not exact). All other characteristics are exact odds ratios.

5.5.3 Endotoxin concentration (EU/mg) and surface load (EU/m^2)

Endotoxin concentrations were higher in homes with evaporative coolers compared to homes with central air conditioning for all individual sample locations and all sample locations combined, but these associations were statistically significant for only upholstered living room furniture samples (GM = 8.05 vs. 2.85 EU/mg, $P < 0.01$) and all sample locations combined (GM = 3.60 vs. 1.29 EU/mg, $P = 0.03$) (Figure 2A, Supplemental Table 3). Results were qualitatively similar for endotoxin surface load (Figure 2B, Supplemental Table 3). Endotoxin concentration and surface load were significantly lower for bedroom mattress compared to bedroom carpet samples (Supplemental Table 4). The multiple Tobit regression model for endotoxin concentration selected style of home and sample location. After adjusting for style of home and sample location, homes with evaporative coolers still had significantly higher endotoxin concentrations than homes with central air conditioning ($P = 0.03$). The multiple Tobit regression model for endotoxin surface load selected home age, home size, style of home and sample

location. After adjusting for home age, home size, style of home and sample location, air conditioning type was no longer significantly associated with endotoxin surface load (P = 0.08).

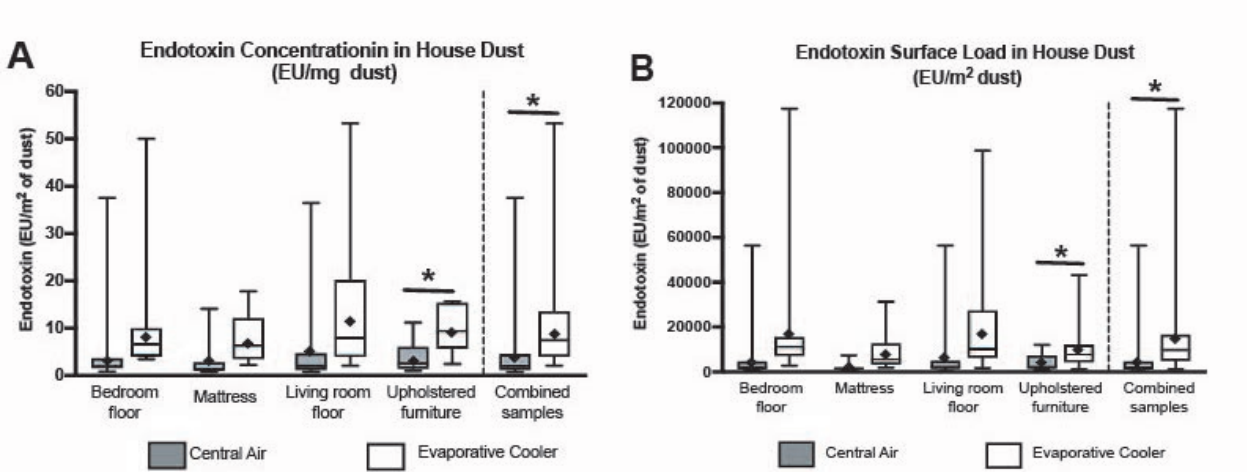

Figure 5-2: Endotoxin concentration and surface load in homes with central air conditioning or none and evaporative cooling. Endotoxin concentration (2A) and endotoxin surface load (2B) in homes with central air conditioning (n=28) and evaporative coolers (n=20) according to sampling location in the home (Living room floor, Upholstered furniture, Bedroom floor, Mattress). The concentration and surface load of all of the samples (Combined samples) is also shown for endotoxin. The box plots present minimum, quartile 1, median, quartile 3, maximum and arithmetic mean (♦) values. * P<0.05

5.5.4 β-(1→3)-D-glucan concentration (µg/mg) and surface load (µg/m^2)

β-(1→3)-D-glucan concentrations were significantly higher in homes with evaporative coolers compared to homes with central air conditioning for all individual sample locations and all sample locations combined (Figure 3A, Supplemental Table 5). Results were qualitatively similar for β-(1→3)-D-glucan surface load (Figure 3B, Supplemental Table 5). Home age, number of residents and bedroom carpet age were significantly associated with increased β-(1→3)-D-glucan concentration and surface load, whereas apartment versus two-story homes and living room furniture age were significantly associated with decreased β-(1→3)-D-glucan concentration and surface load (Supplemental Table 6). Stepwise variable selection for β-(1→3)-D-glucan concentration selected number of residents, bedroom mattress age and living room furniture age. After adjusting for number of residents, bedroom mattress age and living room

furniture age, homes with evaporative coolers still had significantly higher β-(1→3)-D-glucan concentrations than homes with central air conditioning ($P < 0.01$). Stepwise variable selection for β-(1→3)-D-glucan surface load selected number of residents and living room furniture age. After adjusting for number of residents and living room furniture age, homes with evaporative coolers still had significantly higher β-(1→3)-D-glucan surface loads than homes with central air conditioning ($P < 0.01$).

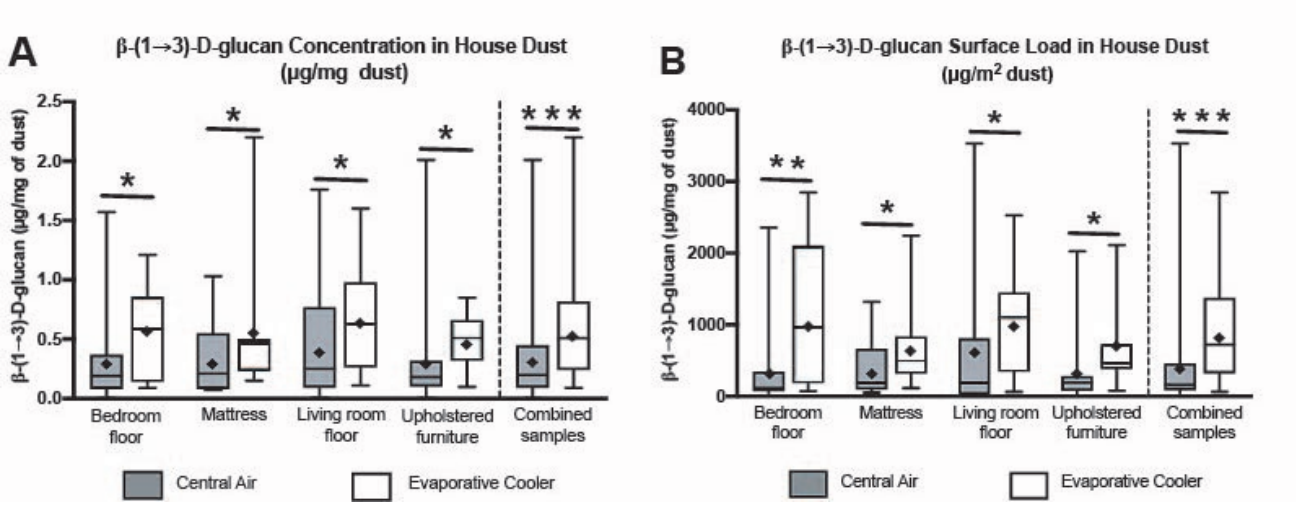

Figure 5-3: β-(1→3)-D-glucan concentration and surface load in homes with central air conditioning or none and evaporative cooling. β-(1→3)-D-glucan concentration (2A) and β-(1→3)-D-glucan surface load (2B) in homes with central air conditioning (n=28) and evaporative coolers (n=20) according to sampling location in the home (Living room floor, Upholstered furniture, Bedroom floor, Mattress). The concentration and surface load of all of the samples (Combined samples) is also shown for β-(1→3)-D-glucan. The box plots present minimum, quartile 1, median, quartile 3, maximum and arithmetic mean (♦) values. * P<0.05 **P<0.01 ***P<0.001Results for analyses of 72-hour mean RH and temperature data, Der f 1 and Der p 1 concentration, and unadjusted associations between 72-hour mean RH and temperature, Der f 1, Der p 1, and combined Der f 1 or Der p 1 concentration, endotoxin concentration and surface load, and β-(1→3)-D-glucan concentration and surface load are described in the Supporting Information (Supplemental Results, Indoor RH and Temperature, Der f 1 and Der p 1 allergen concentration, Spearman's rank correlation coefficients, Supplemental Tables 7-11).

5.6 Discussion

The prevalence of asthma and allergic sensitization in children has increased dramatically in recent decades, and the significant economic and quality of life impacts stemming from this has led to increased interest in understanding possible causes and prevention methods [132]. Human exposure to microbes and bioaerosols during different developmental windows and at different exposure levels can drive exacerbations, and paradoxically, can also play a protective role [133] in allergic diseases. Thus, improved understanding of environmental exposures, and the resultant effects, is paramount. Because children and adults spend on average between 60 – 80% of their time indoors at home, the home is a key microenvironment for exposure to bioaerosols. While previous studies have examined associations between house dust and indoor bioaerosols, only a few have examined the impact that residential cooling systems have on these levels. Our findings help clarify the role evaporative coolers play in indoor bioaerosol levels. In this study, we found significantly higher levels of combined Der p 1 or Der f 1, endotoxin, and β-(1→3)-D-glucan concentrations and surface loads in the dust of homes with evaporative cooling compared to those with central air conditioning. This study was performed during the summer months in low-income homes in a semi-arid climate (Utah County, Utah, USA) using four sample locations.

Prior studies from the Western U.S. and Australia report that children living in homes with evaporative coolers are more likely to be sensitized to HDM allergens [111], and homes with evaporative coolers are more likely to have clinically significant levels of Der p 1 and Der f 1 in settled dust [106, 109]. The prevailing theory is that humidity from evaporative coolers provides enough moisture to indoor air to allow HDMs to survive in homes in dry climates. Findings from our study only partially support this theory. Both the prevalence and levels of Der

p 1 and Der f 1 measured in our study homes are low compared to homes in more humid climates [134-136]. In fact, only two samples in our study were above the threshold concentration (≥ 2.0 ug/g dust) for sensitization [137]. In addition, no samples were above the 10 ug/g dust level that has been recommended as a threshold for the development of asthma symptoms in sensitized individuals [138, 139]. A prior study of middle-income homes in Utah, and a study of mixed-income homes in rural western Montana and northern Idaho, both reported low levels of mite allergens in approximately 20 - 25% of homes, independent of air conditioning type [110, 140]. However, when homes are sampled according to socioeconomic status, as in this study, a different pattern emerges. For instance, a prior study of low-income homes with evaporative coolers in Utah [141] reported similarly low levels of mite allergens, but at a much higher prevalence (68%) than found in middle-income homes in the same community [110]. Our findings in this study were similar, with 55% of evaporative cooler homes testing positive for Der p 1 or Der f 1 in at least one location. Additionally, RH alone does not appear to explain this result.

An alternate theory supported by our data is that humidity from evaporative coolers works in tandem with occupant density and other housing factors to create an indoor environment that supports low levels of HDM populations in some dry climates, such as the Rocky Mountain States in the U.S. Our results show that evaporative coolers, increased number of residents, and older carpets were significantly associated with increased HDM allergen levels, but the characteristic with the strongest association was higher occupant density. Higher occupant densities in crowded, low-income housing may significantly increase indoor moisture through exhalation, cooking, bathing, and transfer of perspiration from bodies to upholstered furniture and mattresses. Higher occupant densities may lead to more people sitting and/or

sleeping on mattresses and furniture, leading to more body moisture wicking into the fabric, and a higher concentration of shed skin cells, which provide a food source for HDMs. Older carpets may also serve as a reservoir for dead skin cells, which help support mite populations. The mean occupant density for homes in this study and the prior low-income study in Utah were 4.79 and 3.83 residents/100 m^2, respectively [141]. In contrast, occupant densities for middle-income homes in Utah were 1.72 residents/100 m^2 [110]. Thus, it appears that low RH in homes in dry climates, even when evaporative coolers are used, discourages dust mite growth unless there are compounding housing factors. Future studies on the relationship between evaporative coolers and mite allergens should consider housing factors and socioeconomic variables that may influence HDM growth and reproduction, particularly occupant density.

In this study, endotoxin concentrations were significantly higher in homes with evaporative coolers compared to homes with central air conditioning. Evaporative coolers had a 2.79-fold increase in endotoxin concentration levels (EU/mg), and a 3.49-fold increase in endotoxin surface load (EU/m^2) across the four sampling locations. Few studies have considered the influence that heating, ventilation, and air conditioning (HVAC) systems have on indoor endotoxin levels. Gereda et al. (2001), in a study of metropolitan homes in the Denver, CO area, found that central air conditioning was associated with lower endotoxin levels [105]. Johnston et al. (2017), in a study of middle-income homes in Utah, reported endotoxin levels three to six times higher in homes with evaporative coolers compared to homes with central air conditioners [107]. Similarly, Lemons et al. (2017) found that endotoxin levels were approximately three times greater in homes with evaporative coolers compared to homes with central air conditioners in the Reno, NV area [108]. Although endotoxin levels were relatively low in our study, the observed proportional differences in endotoxin levels between the two types of air conditioning

systems are consistent with Lemons et al. (2017) and Johnston et al. (2017), suggesting that evaporative coolers do tend to significantly increase residential endotoxin levels.

One plausible explanation for the higher levels of endotoxin found in homes with evaporative coolers is that Gram-negative bacteria grow in evaporative cooler sump water during summer months, and the evaporative cooler distributes these bacteria, or their cell wall components, throughout the home. Macher & Girman (1990) found that Gram-negative bacteria grew to concentrations up to 1.4×10^5 cfu/ml over the course of the summer, and that these species were also recovered from indoor, but not outdoor, air [112]. However, this study was limited to a single home during the course of one summer. In contrast, Lemons et al. (2017) found no difference in airborne bacterial species between evaporative vs. central air conditioner homes [108]. Residential bioaerosols are often found on particles with aerodynamic diameters ranging from 0.1 – 10 µm, many of which are larger and settle out of the air quickly after resuspension [142, 143]. Thus, many indoor bioaerosols may be underrepresented by stationary air samples. To better understand the influence evaporative coolers have on endotoxins and Gram-negative bacteria in the home, future research may consider comparing bacterial species from settled house dust in addition to air samples.

We used β-(1→3)-D-glucan as an omnibus measure of fungi in homes in this study and, to our knowledge, this is the first study to compare β-(1→3)-D-glucan levels among homes with evaporative and central air conditioning. β-(1→3)-D-glucan levels were significantly higher in evaporative cooling homes at all four sample locations. Evaporative coolers had a 2.64-fold increase in β-(1→3)-D-glucan concentration levels (µg/mg), and a 3.64-fold increase in β-(1→3)-D-glucan surface load (µg/m^2) across the four locations. Thus, of the three bioaerosols measured, β-(1→3)-D-glucan levels had the strongest and most consistent statistical increase in

the evaporative cooling homes when compared to central air conditioning. In general, our findings are consistent with two prior studies that measured indoor fungi in homes with evaporative coolers. Sneller & Pinnas (1987) found significantly higher levels, and greater diversity, of fungal species in homes with evaporative coolers compared with central air conditioners [26]. The most conclusive evidence to date is reported by Lemons et al. (2017), who found a higher prevalence of hydrophilic fungi in homes with evaporative coolers, including species in the order Pleosporales which are highly allergenic [108]. A likely explanation for our findings is that fungi grow in the sump water or cooling pads, and fungal spores are transported into the home during evaporative cooler operation. Lemons et al. found that species isolated from the sides of the water reservoir did not match with fungal species found in indoor air, and they suggest that the hydrophilic species found in indoor air originate from the cooling pads [108]. Future studies may clarify this issue by comparing fungal species found on evaporative cooler pads with those found in settled dust or air samples inside the home.

The role of residential exposure to mold in protecting from or exacerbating asthma and allergy is not fully understood [144]. Certain types of fungi have been shown to be associated with protection from asthma and may also play a key role in influencing the composition of the microbiota and immune system [96, 145]. Additional studies have identified no protective association between β-(1→3)-D-glucan exposure in household dust and health [146], while others have found it is associated with increased asthma prevalence in school aged children [147]. High levels of fungal exposure have been strongly implicated in the development and prevalence of asthma [148-150]. Whether or not fungal exposure is protective or harmful may depend upon the fungal species and the type and level of exposure. Fungal growth due to water damage in the home has been shown to be associated with increased levels of asthma [151] and

low amounts of fungal diversity in house dust have been associated with asthma development [152]. Similar correlations between increases in asthma and a decrease in bacterial diversity have also been reported [153]. These findings are supportive of an extension of the hygiene hypothesis called the "biodiversity hypothesis" which takes into consideration the decrease in biodiversity of the microbes in our living environment as risk factors for inflammatory diseases, in addition to the microbes in our food, water, and on domestic animals [154].

One critical issue that remains unresolved is how, when, and what type of microbial exposure is protective or harmful. Previous work has found protective effects of residential environmental exposure on the development of asthma and allergies. Children who have had high microbial exposures (increased numbers of siblings, grew up on a farm, frequent contact with farm animals) have been found to be at a reduced risk for asthma and allergies [116]. Exposure to coal or wood heating as children was also found to lower the risk for asthma, hay fever, and pollen sensitization [155]. In all of these cases, living in an environment as a child that is rich in microbial exposure, particularly lipopolysaccharide, was found to be protective [24, 144]. Findings from this and other studies suggest that evaporative coolers play a significant role in changing the microbiological and bioaerosol profile of homes, although the immunological health benefits or risks associated with these changes are not fully understood.

It is possible that early-life exposure to microbes and bioaerosols from evaporative coolers could confer protection against allergies and asthma, consistent with the hygiene hypothesis [113, 114]. Recent findings from a large pediatric cohort study in Colorado found no association between evaporative cooler use and dust mite or mold sensitization when comparing children living in homes with evaporative coolers vs. central air conditioners. Interestingly, they did report significantly lower prevalence of allergic rhinitis among children living in homes with

evaporative coolers [156]. Conversely, other studies show that children living in homes with evaporative coolers are more likely to test positive for sensitization to mold and HDM allergens [111], and are more likely to experience lower respiratory tract illness in infancy [157]. Evaporative coolers are often incentivized for energy savings in dry climates, but there is little data on potential health risks or benefits of their use, warranting a longitudinal health study. While our study does not directly address health outcomes, it is a relevant issue that needs to be addressed when considering whether or not to develop or keep policies that provide financial incentives to get or replace evaporative coolers.

Although selecting our study homes based on household income allowed us to control for socioeconomic factors, this study was limited by a relatively small sample size drawn from one community. Thus, our results may not be generalizable to homes in other locations. Due to logistical challenges and the fact that evaporative coolers are only used for a few months out of the year, we did not complete our sample collection until October, 2017. Homes in the final weeks of sample collection, which included several evaporative cooler homes, had likely stopped using their air conditioners for the year. This likely explained why we did not see a difference in RH levels between evaporative cooler and air conditioner homes.

In conclusion, we found significantly higher levels of combined Der p 1 or Der f 1, endotoxin, and β-(1→3)-D-glucans in low-income homes with evaporative coolers when compared to homes with central air conditioning. Based on this and other studies, it appears that evaporative coolers have a significant and potentially important impact on the microbiological and bioaerosol profile of homes in dry climates. There are several questions that remain unanswered regarding the health benefits or risks associated with evaporative coolers, which should be addressed by future studies.

5.6.1 Acknowledgements

We would like to thank the Woman, Infants, and Children (WIC) office at the Utah County Health Department (UCHD) for their support in recruiting participants for this study. We are also indebted to the gracious individuals who participated in this study for allowing us into their homes to collect our samples. This research was funded by the Ira and Mary Lou Fulton Gift Fund at Brigham Young University.

Table 5-1: Characteristics of low-income homes in Utah Country, Utah, Summer 2017

Characteristic	Homes, n	Missing, n	GM	GSD	Min	Max	Dust Samples, n (%)	Missing Dust Samples[†], n	p-value[‡]
Central air conditioning or none									
Total	28						86 (100)	26	
Home age, years	28		31.70	2.13	10.00	137.00			
Home size, m^2	28		96.22	1.50	46.45	241.55			
Style of home, n (%)									
Apartment	7 (25)						23 (27)	5	
Single story	2 (7)						7 (8)	1	
Two story	9 (32)						28 (33)	8	
Other[§]	10 (36)						28 (33)	12	
Residents, n	28		4.71[¶]	1.80[¶]	1.00	8.00			
Occupant density, residents/100 m^2	28		4.50	1.54	0.98	11.66			
Bedroom carpet age, months	26	2	91.62	4.07	1.00	924.00			
Bedroom mattress age, months	28		30.13	3.45	1.00	156.00			
Living room carpet age, months	25	3	67.43	4.37	1.00	960.00			
Living room furniture age, months	28		56.19	2.28	12.00	324.00			
Sample location, n (%)									
Bedroom carpet							26 (30)	2	
Bedroom mattress							16 (19)	12	

Characteristic	Homes, n	Missing, n	GM	GSD	Min	Max	Dust Samples, n (%)	Missing Dust Samples[†], n	p-value[‡]
Living room carpet							24 (28)	4	
Living room furniture							20 (23)	8	
Evaporative cooler									
Total	20						65 (100)	15	
Home age, years	19	1	51.53	1.43	37.00	112.00			0.002
Home size, m^2	19	1	86.72	1.40	41.81	140.00			0.39
Style of home, n (%)									
Apartment	5 (25)						17 (26)	3	
Single story	6 (30)						19 (29)	5	
Two story	4 (20)						15 (23)	1	
Other[§]	5 (25)						14 (22)	6	0.19[††]
Residents, n	20		4.90[¶]	1.92[¶]	2.00	11.00			0.75[‡‡]
Occupant density, residents/100 m^2	19	1	5.26	1.53	2.15	10.09			0.95
Bedroom carpet age, months	17	3	99.38	4.21	2.00	876.00			0.89
Bedroom mattress age, months	20		44.17	2.76	8.00	240.00			0.37
Living room carpet age, months	17	3	53.65	4.40	2.00	876.00			0.96
Living room furniture age, months	20		49.48	2.88	6.00	240.00			0.23
Sample location, n (%)									
Bedroom carpet							20 (31)		

Characteristic	Homes, n	Missing, n	GM	GSD	Min	Max	Dust Samples, n (%)	Missing Dust Samples[†], n	p-value[‡]
Bedroom mattress							16 (25)	4	
Living room carpet							19 (29)	1	
Living room furniture							10 (15)	10	
All homes									
Total	48						151 (100)	41	
Home age, years	47	1	38.58	1.94	10.00	137.00			
Home size, m^2	47	1	92.26	1.46	41.81	241.55			
Style of home, n (%)									
Apartment	12 (25)						40 (26)	8	
Single story	8 (17)						26 (17)	6	
Two story	13 (27)						43 (28)	9	
Other[§]	15 (31)						42 (28)	18	
Residents, n	48		4.79[¶]	1.83[¶]	1.00	11.00			
Occupant density, residents/100 m^2	47	1	4.79	1.54	0.98	11.66			
Bedroom carpet age, months	43	5	94.62	4.06	1.00	924.00			
Bedroom mattress age, months	48		35.33	3.18	1.00	240.00			
Living room carpet age, months	42	6	61.47	4.32	1.00	960.00			
Living room furniture age, months	48		53.29	2.51	6.00	324.00			
Sample location, n (%)									

Characteristic	Homes, n	Missing, n	GM	GSD	Min	Max	Dust Samples, n (%)	Missing Dust Samples†, n	p-value‡
Bedroom carpet							46 (30)	2	
Bedroom mattress							32 (21)	16	
Living room carpet							43 (28)	5	
Living room furniture							30 (20)	18	

Abbreviations: GM, geometric mean; GSD, geometric standard deviation; Min, minimum; Max, maximum.

† Although four dust samples were collected from each house (i.e., 192 total dust samples were collected), dust samples were designated "missing" if not enough dust could be collected to measure the analytes of interest (e.g., because the mattress, furniture, or carpet was newer or made out of leather).

‡ Estimated via t-tests of the natural logarithm transformed values.

§ Includes basement apartment (two homes, seven dust samples), condo (one home, three dust samples), duplex (four homes, nine dust samples), four plex (one home, three dust samples), four plex split level (one home, two dust samples), split entry (two homes, five dust samples), trailer (one home, three samples), tri-level split (one home, four samples), and not applicable (two homes, six dust samples).

¶ Arithmetic mean and arithmetic standard deviation.

†† Estimated via χ^2 tests.

‡‡ Estimated via t-tests of the original values

5.7 Supplemental methods

5.7.1 Indoor temperature and RH measurement

Indoor air temperature and relative humidity (RH) measurements were continuously logged every 5 minutes for approximately 72 hours during the sampling period. Collection was performed using Extech SD500 humidity/temperature dataloggers (Extech Instruments, Corp., Waltham, MA, USA) placed 0.91-1.83 m (3-6 ft) above the floor in a central living area within the home and distanced from cooling/heating vents. NIST-traceable calibration of temperature and humidity sensors was performed prior to data collection, and all instruments were found to be within the manufacturer's tolerances of 0.8°C (1.5°F) and 4% RH. A weather monitoring station located on the campus of Brigham Young University was used to measure outdoor air temperature and RH measurements during the sampling period.

5.7.2 Statistical techniques

Seventy-two-hour mean RH and temperature were normally distributed, so arithmetic means (AM), 95% confidence intervals (CI), minimums, and maximums were calculated. Linear regression models were used to calculate unadjusted AM differences, 95% CI, and p-values that estimated associations between air conditioning type or housing characteristics and 72-hour mean RH or temperature. Stepwise variable selection was used to develop linear regression models that included housing characteristics that were associated with 72-hour mean RH and temperature. Entry and exit significance levels were set at $\alpha = 0.15$. Linear regression models were then used to calculate associations between air conditioning type and 72-hour mean RH and temperature adjusting for housing characteristics that were identified via stepwise variable selection.

Spearman's rank correlation coefficients were used to estimate unadjusted associations between 72-hour mean RH and temperature, Der f 1, Der p 1, and combined Der f 1 or Der p 1 concentration, endotoxin concentration and surface load, and β-(1→3)-D-glucan concentration and surface load.

5.8 Supplemental results

5.8.1 Indoor RH and temperature

Seventy-two-hour RH was not statistically significantly different (P = 0.82) among homes with central air conditioning (AM = 43.91%) and homes with evaporative coolers (AM = 44.54%), but 72-hour mean temperature was significantly lower (P < 0.01) in homes with evaporative coolers (AM = 23.31°C) compared to homes with central air conditioning (AM = 24.56°C) (Supplemental Table 7). None of the housing characteristics were significantly associated with 72-hour mean RH or temperature (Supplemental Table 8). Stepwise variable selection for 72-hour mean RH did not select any housing characteristic. Stepwise variable selection for 72-hour mean temperature did not select any housing characteristic.

The average daily outdoor temperature and RH during the study period were 19.13℃ and 41.03% respectively.

5.8.2 Der f 1 and Der p 1 allergen concentration

Twenty-two (15%) dust samples were positive (i.e., above detection limits) for Der f 1 and 16 (11%) dust samples were positive for Der p 1 (Supplemental Table 9). Although not statistically significant, the odds of Der f 1 concentrations above the detection limit were higher in homes with evaporative coolers compared to homes with central air conditioning for all individual sample locations and all sample locations combined (Supplemental Table 9). Results were generally qualitatively similar for Der p 1 (Supplemental Table 9). Der f 1 concentration

was significantly inversely associated with home size, but significantly positively associated with occupant density (Supplemental Table 10). Number of residents and occupant density were significantly positively associated with Der p 1 concentration (Supplemental Table 10). Stepwise variable selection for Der f 1 selected home size. Adjusting the odds ratio for air conditioning type and Der f 1 for home size gave qualitatively similar results (OR = 2.06; 95% CI: 0.80, 5.32; P = 0.14). Stepwise variable selection for Der p 1 selected number of residents and bedroom mattress age. Adjusting the odds ratio for air conditioning type and Der p 1 for number of residents and bedroom mattress age gave qualitatively similar results (OR = 3.09; 95% CI: 0.85, 11.28; P = 0.09).

5.8.3 Spearman's rank correlation coefficients

Spearman's rank correlation coefficients generally indicated weak to moderate unadjusted associations between 72-hour mean RH and temperature, Der f 1, Der p 1, and combined Der f 1 or Der p 1 concentration, endotoxin concentration and surface load, and β-(1→3)-D-glucan concentration and surface load, although several of these associations were statistically significant (Supplemental Table 11).

Supplemental Table 1. House dust mite allergen (combined Der f 1 or Der p 1) concentration in low-income homes in Utah County, Utah, Summer 2017.

House Dust Mite Allergen Concentration	Negative[†,‡], n (%)	Positive[†,‡]					Unadjusted Exact OR (Exact 95% CI)
		n (%)	GM	GSD	Min	Max	
Combined Der f 1 or Der p 1, µg/g of dust							
All samples	117 (77)	34 (23)	0.15	3.15	0.04	2.50	
Central air conditioning[§]	72 (84)	14 (16)	0.09	2.03	0.04	0.43	Reference
Evaporative cooler	45 (69)	20 (31)	0.21	3.64	0.04	2.50	2.29 (1.05, 4.98)[¶]
Bedroom carpet							
Central air conditioning[§]	21 (81)	5 (19)	0.09	2.56	0.04	0.43	Reference
Evaporative cooler	14 (70)	6 (30)	0.35	3.78	0.06	2.50	1.80 (0.46, 7.06)[¶]
Bedroom mattress							
Central air conditioning[§]	14 (88)	2 (13)	0.10	2.58	0.05	0.19	Reference
Evaporative cooler	11 (69)	5 (31)	0.14	2.45	0.05	0.30	3.07 (0.40, 38.12)
Living room carpet							
Central air conditioning[§]	21 (88)	3 (13)	0.08	1.56	0.05	0.12	Reference
Evaporative cooler	12 (63)	7 (37)	0.19	4.40	0.04	2.08	3.95 (0.73, 28.14)
Living room furniture							
Central air conditioning[§]	16 (80)	4 (20)	0.11	2.04	0.05	0.26	Reference
Evaporative cooler	8 (80)	2 (20)	0.16	7.21	0.04	0.65	1.00 (0.08, 8.88)

Abbreviations: CI, confidence interval; Der f 1, *Dermatophagoides farinae*; Der p 1, *Dermatophagoides pteronyssinus*; GM, geometric mean; GSD, geometric standard deviation; Min, minimum; Max, maximum; OR, odds ratio.

† 41 dust samples did not have enough dust in which to measure dust mite allergen concentration.

‡ The detection limit was 0.04 μg/g of dust.

§ Includes 24 homes (76 dust samples) that had central air conditioning and four homes (10 dust samples) that had no air conditioning.

¶ Large sample/asymptotic approximate OR (large sample/asymptotic approximate 95% CI) (i.e., not exact).

Supplemental Table 2. Characteristics and house dust mite allergen (combined Der f 1 or Der p 1) concentration of low-income homes in Utah County, Utah, Summer 2017.

	House Dust Mite Allergen (Combined Der f 1 or Der p 1) Concentration[†]			
Characteristic	Negative[‡], n (%)	Positive[‡], n (%)	Missing, n	Unadjusted OR (95% CI)
Home age, 10 years			4	1.07 (0.95, 1.21)
Home size, 50 m^2			4	0.75 (0.45, 1.25)
Style of home, n (%)				
Apartment	30 (26)	10 (29)		1.46 (0.51, 4.17)
Single story	17 (15)	9 (26)		2.29 (0.65, 8.20)
Two story	35 (30)	8 (24)		Reference
Other[§]	35 (30)	7 (21)		0.88 (0.24, 3.11)
Residents, n				1.33 (1.08, 1.64)
Occupant density, residents/100 m^2[¶]			4	7.10 (2.27, 22.42)
Bedroom carpet age, months[¶]			16	1.56 (1.05, 2.31)
Bedroom mattress age, 60 months				0.97 (0.65, 1.46)
Living room carpet age, 120 months			18	1.02 (0.79, 1.32)
Living room furniture age, months[¶]				1.08 (0.70, 1.65)
Sample location, n (%)				
Bedroom carpet	35 (30)	11 (32)		Reference
Bedroom mattress	25 (21)	7 (21)		0.89 (0.30, 2.62)

Living room carpet	33 (28)	10 (29)	0.96 (0.36, 2.57)
Living room furniture	24 (21)	6 (18)	0.80 (0.26, 2.44)

Abbreviations: CI, confidence interval; Der f 1, *Dermatophagoides farinae*; Der p 1, *Dermatophagoides pteronyssinus*; OR, odds ratio.

† 41 dust samples did not have enough dust in which to measure dust mite allergen concentration.

‡ The detection limit was 0.04 μg/g of dust.

§ Includes basement apartment (two homes, seven dust samples), condo (one home, three dust samples), duplex (four homes, nine dust samples), four plex (one home, three dust samples), four plex split level (one home, two dust samples), split entry (two homes, five dust samples), trailer (one home, three samples), tri-level split (one home, four samples), and not applicable (two homes, six dust samples).

¶ Transformed by taking the natural logarithm of the original values.

Supplemental Table 3. House dust endotoxin concentration and surface load in low-income homes in low-income homes in Utah County, Utah, Summer 2017.

House Dust Endotoxin	Negative[†,‡], n (%)	Positive[†,‡]					p-value[§]
		n (%)	GM[§]	95% CI[§]	Min[¶]	Max[¶]	
Concentration: endotoxin units/mg of dust (EU/mg)							
All samples	9 (6)	138 (94)	2.01	1.26, 3.22	0.71	53.25	
Central air conditioning[††]	5 (6)	78 (94)	1.29	0.70, 2.38	0.71	37.56	
Evaporative cooler	4 (6)	60 (94)	3.60	1.79, 7.24	2.07	53.25	0.03
Bedroom carpet							
Central air conditioning[††]	1 (4)	25 (96)	1.62	0.64, 4.10	0.80	37.56	
Evaporative cooler	1 (5)	18 (95)	3.74	1.26, 11.09	3.45	50.01	0.25
Bedroom mattress							
Central air conditioning[††]	3 (19)	13 (81)	0.20	0.02, 1.88	0.71	14.08	
Evaporative cooler	2 (13)	14 (88)	1.34	0.15, 12.19	2.21	17.78	0.24
Living room carpet							
Central air conditioning[††]	1 (4)	23 (96)	1.74	0.61, 4.95	0.77	36.43	
Evaporative cooler	1 (5)	18 (95)	4.79	1.48, 15.51	2.07	53.25	0.21
Living room furniture							
Central air conditioning[††]	0 (0)	17 (100)	2.85	1.97, 4.10	1.01	11.18	
Evaporative cooler	0 (0)	10 (100)	8.05	5.00, 12.98	2.42	15.60	< 0.01

House Dust Endotoxin	Negative[†,‡], n (%)	Positive[†,‡]					p-value[§]
		n (%)	GM[§]	95% CI[§]	Min[¶]	Max[¶]	
Surface load: endotoxin units/m^2 (EU/m^2)							
All samples	9 (6)	138 (94)	2,210.29	1,358.45, 3,596.29	387.60	117,468.79	
Central air conditioning[††]	5 (6)	78 (94)	1,272.19	676.53, 2,392.33	387.60	56,524.41	
Evaporative cooler	4 (6)	60 (94)	4,546.82	2,215.28, 9,332.28	1,064.54	117,468.79	0.01
Bedroom carpet							
Central air conditioning[††]	1 (4)	25 (96)	1,662.45	640.52, 4,314.85	820.55	56,367.92	
Evaporative cooler	1 (5)	18 (95)	6,266.32	2,052.68, 19,129.47	2,770.03	117,468.79	0.08
Bedroom mattress							
Central air conditioning[††]	3 (19)	13 (81)	170.45	17.65, 1,646.03	409.12	7,317.81	
Evaporative cooler	2 (13)	14 (88)	1,320.20	139.11, 12,529.32	1,865.75	31,293.03	0.21
Living room carpet							
Central air conditioning[††]	1 (4)	23 (96)	1,866.83	652.65, 5,339.84	387.60	56,524.41	
Evaporative cooler	1 (5)	18 (95)	6,893.91	2,115.52, 22,465.44	1,671.51	98,739.80	0.11
Living room furniture							
Central air conditioning[††]	0 (0)	17 (100)	2,740.14	1,726.48, 4,348.92	758.73	12,103.91	
Evaporative cooler	0 (0)	10 (100)	6,975.90	3,819.77, 12,739.82	1,064.54	43,221.02	0.02

Abbreviations: CI, confidence interval; GM, geometric mean; Min, minimum; Max, maximum.

[†] 45 dust samples did not have enough dust in which to measure endotoxin concentration or surface load.

‡ The detection limit was 0.0001 endotoxin units/mg of dust (EU/mg) or 0.03 to 0.32 endotoxin units/m^2 (EU/m^2).

§ Estimated via Tobit regression models of the natural logarithm transformed values.

¶ Calculated from positive samples only.

†† Includes 24 homes (73 dust samples) that had central air conditioning and four homes (10 dust samples) that had no air conditioning.

Supplemental Table 4. Characteristics and house dust endotoxin concentration and surface load of low-income homes in Utah County, Utah, Summer 2017.

	House Dust Endotoxin[†]				
				Concentration	Surface Load
Characteristic	Negative[‡], n (%)	Positive[‡], n (%)	Missing, n	Unadjusted exp(β)[§] (95% CI[§])	Unadjusted exp(β)[§] (95% CI[§])
Home age, 10 years			4	1.05 (0.89, 1.23)	1.10 (0.93, 1.30)
Home size, 50 m^2			4	0.65 (0.37, 1.15)	0.67 (0.38, 1.21)
Style of home, n (%)					
Apartment	0 (0)	38 (28)		2.86 (0.81, 10.03)	2.27 (0.62, 8.38)
Single story	1 (11)	25 (18)		2.85 (0.70, 11.56)	3.22 (0.75, 13.78)
Two story	4 (44)	38 (28)		Reference	Reference
Other[¶]	4 (44)	37 (27)		1.13 (0.33, 3.88)	1.05 (0.29, 3.78)
Residents, n				1.07 (0.83, 1.38)	1.13 (0.87, 1.46)
Occupant density, residents/100 m^{2}[††]			4	2.46 (0.81, 7.51)	2.79 (0.88, 8.84)
Bedroom carpet age, months[††]			14	1.21 (0.86, 1.69)	1.24 (0.87, 1.75)
Bedroom mattress age, 60 months				1.08 (0.66, 1.78)	1.06 (0.64, 1.77)
Living room carpet age, 120 months			16	1.09 (0.80, 1.48)	1.07 (0.78, 1.47)
Living room furniture age, months[††]				0.88 (0.53, 1.46)	0.82 (0.48, 1.40)
Sample location, n (%)					
Bedroom carpet	2 (22)	43 (31)		Reference	Reference

Bedroom mattress	5 (56)	27 (20)	0.29 (0.07, 0.96)	0.19 (0.05, 0.72)
Living room carpet	2 (22)	41 (30)	1.18 (0.36, 3.86)	1.15 (0.34, 3.87)
Living room furniture	0 (0)	27 (20)	1.83 (0.47, 7.03)	1.34 (0.33, 5.39)

Abbreviations: CI, confidence interval.

† 45 dust samples did not have enough dust in which to measure endotoxin concentration or surface load.

‡ The detection limit was 0.0001 endotoxin units/mg of dust (EU/mg) or 0.03 to 0.32 endotoxin units/m^2 (EU/m^2).

§ Estimated via Tobit regression models of the natural logarithm transformed values. Exponentiated regression coefficient and 95% CI is the geometric mean house dust endotoxin concentration or surface load ratio for a specified change in the independent variable or exp(β) – 1 = percent change in geometric mean house dust endotoxin concentration or surface load for a specified change in the independent variable.

¶ Includes basement apartment (two homes, seven dust samples), condo (one home, two dust samples), duplex (four homes, nine dust samples), four plex (one home, three dust samples), four plex split level (one home, two dust samples), split entry (two homes, five dust samples), trailer (one home, three samples), tri-level split (one home, four samples), and not applicable (two homes, six dust samples).

†† Transformed by taking the natural logarithm of the original values.

Supplemental Table 5. House dust β-(1→3)-D-glucan concentration and surface load in low-income homes in Utah County, Utah, Summer 2017.

House Dust β-(1→3)-D-glucan	n (%)[†, ‡]	GM[§]	95% CI[§]	Min	Max	p-value[§]
Concentration: µg/mg of dust						
All samples	147 (100)	0.26	0.21, 0.32	0.0031	2.20	
Central air conditioning[¶]	85 (58)	0.17	0.13, 0.22	0.0031	2.01	
Evaporative cooler	62 (42)	0.45	0.33, 0.60	0.09	2.20	< 0.01
Bedroom carpet						
Central air conditioning[¶]	26 (18)	0.17	0.10, 0.28	0.0031	1.57	
Evaporative cooler	18 (12)	0.44	0.24, 0.79	0.09	1.21	0.02
Bedroom mattress						
Central air conditioning[¶]	16 (11)	0.22	0.14, 0.34	0.071	1.03	
Evaporative cooler	16 (11)	0.42	0.27, 0.66	0.15	2.20	0.04
Living room carpet						
Central air conditioning[¶]	23 (16)	0.17	0.093, 0.30	0.0066	1.76	
Evaporative cooler	18 (12)	0.50	0.26, 0.99	0.11	1.60	0.02
Living room furniture						
Central air conditioning[¶]	20 (14)	0.15	0.087, 0.27	0.0034	2.01	
Evaporative cooler	10 (7)	0.41	0.18, 0.92	0.099	0.85	0.05
Surface load: µg/m²						
All samples	147 (100)	284.13	221.09, 365.16	2.10	3531.92	

House Dust β-(1→3)-D-glucan	n (%)[†, ‡]	GM[§]	95% CI[§]	Min	Max	p-value[§]
Central air conditioning[¶]	85 (58)	164.69	121.88, 222.53	2.10	3531.92	
Evaporative cooler	62 (42)	600.14	421.87, 853.74	63.93	2844.91	< 0.01
Bedroom carpet						
Central air conditioning[¶]	26 (18)	151.40	84.82, 270.24	2.10	2357.25	
Evaporative cooler	18 (12)	655.29	326.60, 1314.77	73.16	2844.91	< 0.01
Bedroom mattress						
Central air conditioning[¶]	16 (11)	230.99	144.60, 369.01	51.77	1319.85	
Evaporative cooler	16 (11)	502.16	314.34, 802.20	115.36	2242.55	0.02
Living room carpet						
Central air conditioning[¶]	23 (16)	164.26	79.58, 339.03	2.51	3531.92	
Evaporative cooler	18 (12)	708.98	312.52, 1608.40	63.93	2527.37	0.01
Living room furniture						
Central air conditioning[¶]	20 (14)	140.59	75.52, 261.70	3.60	2022.89	
Evaporative cooler	10 (7)	504.78	209.63, 1215.50	79.39	2111.29	0.02

Abbreviations: CI, confidence interval; GM, geometric mean; Min, minimum; Max, maximum.

[†] 45 dust samples did not have enough dust in which to measure β-(1→3)-D-glucan concentration or surface load.

[‡] The detection limit was 0.0000625 μg/mg of dust or 0.02 to 0.20 μg/m^2.

[§] Estimated via linear regression models of the natural logarithm transformed values.

¶ Includes 24 homes (75 dust samples) that had central air conditioning and four homes (10 dust samples) that had no air conditioning.

Supplemental Table 6. Characteristics and house dust β-(1→3)-D-glucan concentration and surface load of low-income homes in Utah County, Utah, Summer 2017.

		House Dust β-(1→3)-D-glucan[†]		
			Concentration	Surface Load
Characteristic	n (%)[‡]	Missing, n	Unadjusted exp(β)[§] (95% CI[§])	Unadjusted exp(β)[§] (95% CI[§])
Home age, 10 years		4	1.08 (1.01, 1.16)	1.12 (1.03, 1.22)
Home size, 50 m^2		4	1.27 (0.99, 1.63)	1.24 (0.92, 1.67)
Style of home, n (%)				
Apartment	39 (27)		0.48 (0.28, 0.83)	0.41 (0.21, 0.77)
Single story	24 (16)		1.78 (0.96, 3.30)	1.89 (0.90, 3.96)
Two story	43 (29)		Reference	Reference
Other[¶]	41 (28)		0.91 (0.54, 1.54)	0.86 (0.46, 1.62)
Residents, n			1.24 (1.12, 1.38)	1.28 (1.12, 1.45)
Occupant density, residents/100 m^{2}[††]		4	1.41 (0.86, 2.32)	1.58 (0.87, 2.86)
Bedroom carpet age, months[††]		16	1.17 (1.01, 1.35)	1.18 (1.00, 1.41)
Bedroom mattress age, 60 months			1.15 (0.92, 1.43)	1.22 (0.94, 1.58)
Living room carpet age, 120 months		18	0.98 (0.86, 1.11)	0.94 (0.81, 1.10)
Living room furniture age, months[††]			0.76 (0.61, 0.96)	0.74 (0.56, 0.97)
Sample location, n (%)				
Bedroom carpet	44 (30)		Reference	Reference

Bedroom mattress	32 (22)	1.21 (0.67, 2.19)	1.24 (0.61, 2.51)
Living room carpet	41 (28)	1.09 (0.63, 1.89)	1.13 (0.58, 2.20)
Living room furniture	30 (20)	0.85 (0.47, 1.56)	0.78 (0.38, 1.61)

Abbreviations: CI, confidence interval.

† 45 dust samples did not have enough dust in which to measure β-(1→3)-D-glucan concentration or surface load.

‡ The detection limit was 0.0000625 μg/mg of dust or 0.02 to 0.20 μg/m^2.

§ Estimated via linear regression models of the natural logarithm transformed values. Exponentiated regression coefficient and 95% CI is the geometric mean house dust β-(1→3)-D-glucan concentration or surface load ratio for a specified change in the independent variable or exp(β) − 1 = percent change in geometric mean house dust β-(1→3)-D-glucan concentration or surface load for a specified change in the independent variable.

¶ Includes basement apartment (two homes, seven dust samples), condo (one home, three dust samples), duplex (four homes, nine dust samples), four plex (one home, three dust samples), four plex split level (one home, two dust samples), split entry (two homes, five dust samples), trailer (one home, two samples), tri-level split (one home, four samples), and not applicable (two homes, six dust samples).

†† Transformed by taking the natural logarithm of the original values.

Supplemental Table 7. House relative humidity and temperature in low-income homes in Utah County, Utah, Summer 2017.

House 72-hour Mean Weather	n (%)	AM[†]	95% CI[†]	Min	Max	p-value[†]
Relative humidity, %						
All samples	48 (100)	44.18	41.49, 46.86	25.39	71.58	
Central air conditioning[‡]	28 (58)	43.91	40.36, 47.47	27.11	71.58	
Evaporative cooler	20 (42)	44.54	40.34, 48.74	25.39	65.35	0.82
Temperature, °C						
All samples	48 (100)	24.04	23.56, 24.52	21.12	28.00	
Central air conditioning[‡]	28 (58)	24.56	23.97, 25.14	21.84	28.00	
Evaporative cooler	20 (42)	23.31	22.62, 24.00	21.12	26.37	< 0.01

Abbreviations: AM, arithmetic mean; CI, confidence interval; Min, minimum; Max, maximum.

[†] Estimated via linear regression models of the original values.

[‡] Includes 24 homes that had central air conditioning and four homes that had no air conditioning.

Supplemental Table 8. Characteristics and house relative humidity and temperature of low-income homes in Utah County, Utah, Summer 2017.

	House 72-hour Mean Weather			
			Relative Humidity	Temperature
Characteristic	n (%)	Missing, n	Unadjusted β[†] (95% CI[†])	Unadjusted β[†] (95% CI[†])
Home age, 10 years		1	0.11 (-0.83, 1.04)	-0.01 (-0.18, 0.16)
Home size, 50 m^2		1	-1.94 (-5.20, 1.31)	0.06 (-0.54, 0.67)
Style of home, n (%)				
Apartment	12 (25)		2.11 (-5.43, 9.65)	0.20 (-1.16, 1.55)
Single story	8 (17)		-0.39 (-8.85, 8.07)	-0.50 (-2.02, 1.02)
Two story	13 (27)		Reference	Reference
Other[‡]	15 (31)		4.29 (-2.85, 11.43)	0.18 (-1.11, 1.46)
Residents, n			0.04 (-1.46, 1.54)	<0.01 (-0.26, 0.27)
Occupant density, residents/100 $m^{2§}$		1	2.94 (-3.22, 9.09)	0.23 (-0.91, 1.37)
Bedroom carpet age, months[§]		5	-1.60 (-3.60, 0.41)	0.13 (-0.25, 0.51)
Bedroom mattress age, 60 months			-0.87 (-3.88, 2.14)	-0.23 (-0.76, 0.31)
Living room carpet age, 120 months		6	-1.07 (-2.78, 0.64)	0.16 (-0.15, 0.47)
Living room furniture age, months[§]			1.05 (-1.91, 4.01)	-0.16 (-0.69, 0.37)

Abbreviations: CI, confidence interval.

[†] Estimated via linear regression models of the original values.

[‡] Includes basement apartment (two homes), condo (one home), duplex (four homes), four plex (one home), four plex split level (one home), split entry (two homes), trailer (one home), tri-level split (one home), and not applicable (two homes).

§ Transformed by taking the natural logarithm of the original values.

Supplemental Table 9. House dust mite allergen (Der f 1 and Der p 1) concentration in low-income homes in Utah County, Utah, Summer 2017.

House Dust Mite Allergen Concentration	Negative[†,‡], n (%)	Positive[†,‡]					Unadjusted Exact OR (Exact 95% CI)
		n (%)	GM	GSD	Min	Max	
Der f 1, µg/g of dust							
All samples	129 (85)	22 (15)	0.16	3.61	0.04	2.50	
Central air conditioning[§]	77 (90)	9 (10)	0.11	2.09	0.04	0.43	Reference
Evaporative cooler	52 (80)	13 (20)	0.20	4.63	0.04	2.50	2.14 (0.85, 5.37)[¶]
Bedroom carpet							
Central air conditioning[§]	22 (85)	4 (15)	0.11	2.64	0.04	0.43	Reference
Evaporative cooler	15 (75)	5 (25)	0.43	4.29	0.06	2.50	1.81 (0.33, 10.74)
Bedroom mattress							
Central air conditioning[§]	15 (94)	1 (6)	0.12	N/A	0.12	0.12	Reference
Evaporative cooler	13 (81)	3 (19)	0.09	2.90	0.04	0.30	3.34 (0.23, 193.60)
Living room carpet							
Central air conditioning[§]	21 (88)	3 (13)	0.08	1.56	0.05	0.12	Reference
Evaporative cooler	15 (79)	4 (21)	0.22	6.15	0.05	2.08	1.84 (0.27, 14.46)
Living room furniture							
Central air conditioning[§]	19 (95)	1 (5)	0.26	N/A	0.26	0.26	Reference
Evaporative cooler	9 (90)	1 (10)	0.04	N/A	0.04	0.04	2.06 (0.02, 174.28)

House Dust Mite Allergen Concentration	Negative[†,‡], n (%)	Positive[†,‡]					Unadjusted Exact OR (Exact 95% CI)
		n (%)	GM	GSD	Min	Max	
Der p 1, µg/g of dust							
All samples	135 (89)	16 (11)	0.13	2.60	0.04	0.65	
Central air conditioning[§]	80 (93)	6 (7)	0.08	2.03	0.04	0.27	Reference
Evaporative cooler	55 (85)	10 (15)	0.17	2.75	0.04	0.65	2.42 (0.83, 7.06)[¶]
Bedroom carpet							
Central air conditioning[§]	25 (96)	1 (4)	0.04	N/A	0.04	0.04	Reference
Evaporative cooler	18 (90)	2 (10)	0.15	1.67	0.11	0.22	2.72 (0.13, 170.31)
Bedroom mattress							
Central air conditioning[§]	14 (88)	2 (13)	0.12	3.24	0.05	0.27	Reference
Evaporative cooler	13 (81)	3 (19)	0.16	2.32	0.06	0.28	1.59 (0.16, 21.95)
Living room carpet							
Central air conditioning[§]	24 (100)	0 (0)	N/A	N/A	N/A	N/A	Reference
Evaporative cooler	15 (79)	4 (21)	0.13	3.82	0.04	0.61	7.74 (1.24, ∞)[††]
Living room furniture							
Central air conditioning[§]	17 (85)	3 (15)	0.08	1.62	0.05	0.13	Reference

House Dust Mite Allergen Concentration	Negative[†,‡], n (%)	Positive[†,‡]					Unadjusted Exact OR (Exact 95% CI)
		n (%)	GM	GSD	Min	Max	
Evaporative cooler	9 (90)	1 (10)	0.65	N/A	0.65	0.65	0.64 (0.01, 9.38)

Abbreviations: CI, confidence interval; Der f 1, *Dermatophagoides farinae*; Der p 1, *Dermatophagoides pteronyssinus*; GM, geometric mean; GSD, geometric standard deviation; Min, minimum; Max, maximum; N/A, not applicable; OR, odds ratio.

[†] 41 dust samples did not have enough dust in which to measure dust mite allergen concentration.

[‡] The detection limit was 0.04 µg/g of dust.

[§] Includes 24 homes (76 dust samples) that had central air conditioning and four homes (10 dust samples) that had no air conditioning.

[¶] Large sample/asymptotic approximate OR (large sample/asymptotic approximate 95% CI) (i.e., not exact).

[††] Median unbiased estimate.

Supplemental Table 10. Characteristics and house dust mite allergen (Der f 1 and Der p 1) concentration of low-income homes in Utah County, Utah, Summer 2017.

Characteristic	House Dust Mite Allergen Concentration[†]			
	Negative[‡], n (%)	Positive[‡], n (%)	Missing, n	Unadjusted OR (95% CI)
Der f 1				
Home age, 10 years			4	0.98 (0.84, 1.15)
Home size, 50 m^2			4	0.30 (0.12, 0.74)
Style of home, n (%)				
Apartment	31 (24)	9 (41)		3.81 (0.86, 23.71)[§]
Single story	22 (17)	4 (18)		2.39 (0.37, 17.83)[§]
Two story	40 (31)	3 (14)		Reference
Other[¶]	36 (28)	6 (27)		2.20 (0.43, 14.60)[§]
Residents, n				0.90 (0.69, 1.17)
Occupant density, residents/100 m^2[††]			4	4.47 (1.28, 15.59)
Bedroom carpet age, months[††]			16	1.36 (0.86, 2.16)
Bedroom mattress age, 60 months				1.17 (0.75, 1.82)
Living room carpet age, 120 months			18	1.11 (0.84, 1.47)
Living room furniture age, months[††]				0.79 (0.49, 1.28)
Sample location, n (%)				
Bedroom carpet	37 (29)	9 (41)		Reference

Characteristic	House Dust Mite Allergen Concentration[†]			
	Negative[‡], n (%)	Positive[‡], n (%)	Missing, n	Unadjusted OR (95% CI)
Bedroom mattress	28 (22)	4 (18)		0.59 (0.12, 2.39)[§]
Living room carpet	36 (28)	7 (32)		0.80 (0.23, 2.72)[§]
Living room furniture	28 (22)	2 (9)		0.30 (0.03, 1.60)[§]
Der p 1				
Home age, 10 years			4	1.14 (0.97, 1.33)
Home size, 50 m^2			4	1.49 (0.88, 2.52)
Style of home, n (%)				
Apartment	38 (28)	2 (13)		0.33 (0.03, 1.99)[§]
Single story	19 (14)	7 (44)		2.24 (0.56, 9.36)[§]
Two story	37 (27)	6 (38)		Reference
Other[¶]	41 (30)	1 (6)		0.15 (<0.01, 1.35)[§]
Residents, n				2.03 (1.45, 2.86)
Occupant density, residents/100 m^{2}[††]			4	6.45 (1.50, 27.79)
Bedroom carpet age, months[††]			16	1.39 (0.88, 2.19)
Bedroom mattress age, 60 months				0.49 (0.21. 1.14)
Living room carpet age, 120 months			18	0.80 (0.49, 1.31)
Living room furniture age, months[††]				1.21 (0.67, 2.20)
Sample location, n (%)				

Characteristic	House Dust Mite Allergen Concentration[†]			
	Negative[‡], n (%)	Positive[‡], n (%)	Missing, n	Unadjusted OR (95% CI)
Bedroom carpet	43 (32)	3 (19)		Reference
Bedroom mattress	27 (20)	5 (31)		2.62 (0.47, 18.25)[§]
Living room carpet	39 (29)	4 (25)		1.46 (0.23, 10.63)[§]
Living room furniture	26 (19)	4 (25)		2.18 (0.34, 16.09)[§]

Abbreviations: CI, confidence interval; Der f 1, *Dermatophagoides farinae*; Der p 1, *Dermatophagoides pteronyssinus*; OR, odds ratio.

[†] 41 dust samples did not have enough dust in which to measure dust mite allergen concentration.

[‡] The detection limit was 0.04 µg/g of dust.

[§] Exact OR (exact 95% CI) (i.e., not large sample/asymptotic approximate).

[¶] Includes basement apartment (two homes, seven dust samples), condo (one home, three dust samples), duplex (four homes, nine dust samples), four plex (one home, three dust samples), four plex split level (one home, two dust samples), split entry (two homes, five dust samples), trailer (one home, three samples), tri-level split (one home, four samples), and not applicable (two homes, six dust samples).

[††] Transformed by taking the natural logarithm of the original values.

Supplemental Table 11. Spearman's rank correlation coefficients (p-values) for associations between house relative humidity, temperature, and dust mite allergen, endotoxin, and β-(1→3)-D-glucan concentration and surface load of low-income homes in Utah County, Utah, Summer 2017.

	Weather or House Dust Analyte								
Weather or House Dust Analyte	72-hour mean relative humidity	72-hour mean temperature	Der f 1 concentration[†]	Der p 1 concentration[†]	Der f 1 or p 1 concentration[†]	Endotoxin concentration[‡]	Endotoxin surface load[‡]	β-(1→3)-D-glucan concentration[§]	β-(1→3)-D-glucan surface load[§]
72-hour mean relative humidity	1.00								
72-hour mean temperature	-0.04 (0.66)	1.00							
Der f 1 concentration	0.19 (0.02)[¶]	0.05 (0.53)[¶]	1.00						
Der p 1 concentration	0.09 (0.27)[¶]	-0.20 (0.02)[¶]	0.10 (0.21)[¶]	1.00					
Der f 1 or p 1 concentration	0.20 (0.02)[¶]	-0.07 (0.39)[¶]	0.77 (< 0.01)[¶]	0.64 (< 0.01)[¶]	1.00				
Endotoxin concentration	0.02 (0.86)[††]	-0.18 (0.04)[††]	0.09 (0.28)[¶,††]	0.17 (0.04)[¶,††]	0.18 (0.03)[¶,††]	1.00			
Endotoxin surface load	-0.03 (0.71)[††]	-0.20 (0.02)[††]	0.05 (0.58)[¶,††]	0.17 (0.04)[¶,††]	0.16 (0.05)[¶,††]	0.90 (< 0.01)[††]	1.00		
β-(1→3)-D-glucan concentration	-0.39 (< 0.01)	-0.32 (< 0.01)	-0.15 (0.07)[¶]	0.22 (0.01)[¶]	0.02 (0.80)[¶]	0.27 (< 0.01)[††]	0.23 (< 0.01)[††]	1.00	
β-(1→3)-D-glucan surface load	-0.33 (< 0.01)	-0.35 (< 0.01)	-0.11 (0.17)[¶]	0.22 (0.01)[¶]	0.05 (0.59)[¶]	0.30 (< 0.01)[††]	0.30 (< 0.01)[††]	0.93 (< 0.01)[††]	1.00

Abbreviations: Der f 1, *Dermatophagoides farinae*; Der p 1, *Dermatophagoides pteronyssinus*.

[†] 41 dust samples did not have enough dust in which to measure dust mite allergen concentration.

[‡] 45 dust samples did not have enough dust in which to measure endotoxin concentration or surface load.

[§] 45 dust samples did not have enough dust in which to measure β-(1→3)-D-glucan concentration or surface load.

¶ Association with house dust mite allergen concentration above the detection limit compared to below the detection limit.

†† Calculated from positive endotoxin concentration or surface load samples only.

CHAPTER 6: CONCLUSIONS AND FUTURE DIRECTIONS

This thesis describes efforts to understand the immune system and its response to disease from different perspectives. Concluding remarks and future directions will be addressed individually.

6.1 Flow cytometry education

This research project aims to describe a flow cytometry course for others who may want to implement a similar program. This paper is the first full semester course described in the literature. Flow cytometry is a versatile, high throughput technique that may be underutilized at many research universities. Increasing the availability of flow cytometry education could increase research productivity and discoveries. The course focuses on conceptual understanding, technical skills and analytical abilities, all of which we believe are important for students in their use of flow cytometry.

Because of the descriptive aim of the paper, the survey instrument and other course design elements weren't as rigorous as they might have been. Future directions certainly would include replicating the same survey in multiple class groups. Furthermore, students in this current study were only asked to self-evaluate their abilities, and the results should be compared and corroborated with actual skills assessments in future studies.

6.2 CAR T cell metabolism

CAR T cells are an exciting development in cancer treatment, because they use a patient's own immune system to treat the cancer. Results have been effective in leukemia and other fluid cancers, but solid tumors present a problem. Immune cells have a difficult time competing for resources with rapidly growing cancer cells. Various co-receptors have been used in CAR T cells in hopes of making them stronger and more specific. This project looked at CAR T cells with

two different second generation co-receptors, and the third generation CAR, to better understand their metabolic usage.

As noted above, this is currently a work in progress. Creating CAR T cells in the amounts and stability needed for the testing has required extra optimization that has not been completed. Finishing that testing and validating the results is the first future direction. The constructs are working to produce virus but transducing activated T cells has not yet been done very successfully. Sorting may be useful to increase purity. Then, after noting the differences, other tests can be used. Mitochondrial mass seems to be crucial for memory cells, so measuring mitochondrial mass in these various CAR T cells would be a natural next step. Even further, a metabolomics assay could identify which materials are being used, and elucidate important pathways for CAR T cells.

6.3 CD5 T cell metabolism

Co-receptors can have a large effect on T cell activation, either boosting a signal, or dampening it. CD5 is a negative co-receptor that prevents T cells from over activating, most commonly known for its role in thymic development. However, CD5 is also known to modulate T cell activity throughout the life of a cell, and there is evidence that CD5 expression levels can change calcium activation. This suggested that CD5 could play a role in the metabolism of T cell activation, perhaps mediating the metabolic switch. CD5 KO T cells had significantly higher mitochondrial respiration and glycolysis as compared to WT T cells, indicating that CD5 generally dampens the metabolism of T cells. This is useful knowledge when considering immunotherapies such as checkpoint blockades, which target negative co-receptors to allow immune cells to work unhindered.

One major next step for this project is attempting to block CD5 in wild type cells with antibodies and measuring cytotoxicity, cytokine productions, and other measures of immune effectiveness. This assay would provide evidence parallel to checkpoint inhibitors. It would also allow the phenotypes to be more directly linked to CD5, as opposed to linked genetic problems.

Creating CD5 KO CAR T cells, or CD5 blocked CAR T cells would also be an important next step in understanding the viability of CD5 as a potential target in immunotherapy. This could combine the techniques and knowledge from the previous project with this new discovery to study the synergy of the two approaches.

6.4 Evaporative cooling and bioaerosols

This project looked to understand the unique environment created by evaporative cooling in a home, as compared in central air. We hypothesized that evaporative cooling would create a hospitable environment for potential allergens and asthma triggers. Dust mite levels, bacterial endotoxin and fungal β-(1→3)-D-glucans were quantified, along with extensive characterization of the homes where dust samples were collected. Low-income homes with evaporative cooling did have significantly higher levels of bioaerosols (dust mites, endotoxins, and β-(1→3)-D-glucans). Fungal levels specifically (β-(1→3)-D-glucan) had the most significant increase in homes with evaporative cooling. The immunological and health consequences of increased bioaerosols levels are relatively unknown, with conflicting data about protective exposure or aggravating triggers at different windows of time. Understanding this home environment, where children and adults spend a significant percentage of their time, can be helpful in understanding and preventing important developing health conditions such as asthma.

In the future, this project could benefit from a larger and more diverse sample size. These results may not be generalizable because of the relatively homogenous population chosen. A

rigorous study of the dust in homes would also include a comparison of the same homes using central air and using evaporative cooling before and after they switch cooling types. This type of study could also be extended to other common areas for children, like school, childcare, community centers, churches, and more.

APPENDIX A: SUPPLEMENTAL PUBLICATIONS

7.1 Supplemental Figure 1. ASM genome announcement

AMERICAN SOCIETY FOR MICROBIOLOGY | Microbiology Resource Announcements

GENOME SEQUENCES

Genome Sequences of Nine *Erwinia amylovora* Bacteriophages

Ruchira Sharma,[a] Jordan A. Berg,[a] Nolan J. Beatty,[a] Minsey C. Choi,[a] Ashlin E. Cowger,[a] Brooke J. R. Cozzens,[a] Steven G. Duncan,[a] Christopher P. Fajardo,[a] Hannah P. Ferguson,[a] Trevon Galbraith,[a] Jacob A. Herring,[a] Taalin R. Hoj,[a] Jill L. Durrant,[a] Jonathan R. Hyde,[a] Garrett L. Jensen,[a] Si Yang Ke,[a] Shalee Killpack,[a] Jared L. Kruger,[a] Eliza E. K. Lawrence,[a] Ifeanyichukwu O. Nwosu,[a] Tsz Ching Tam,[a] Daniel W. Thompson,[a] Josie A. Tueller,[a] Megan E. H. Ward,[a] Charles J. Webb,[a]† Madison E. Wood,[a] Edward L. Yeates,[a] David A. Baltrus,[b] Donald P. Breakwell,[a] Sandra Hope,[a] Julianne H. Grose[a]

[a]Microbiology and Molecular Biology Department, Brigham Young University, Provo, Utah, USA
[b]School of Plant Sciences, The University of Arizona, Tempe, Arizona, USA

ABSTRACT *Erwinia amylovora* is a plant pathogen belonging to the *Enterobacteriaceae* family, a family containing many plant and animal pathogens. Herein, we announce nine genome sequences of *E. amylovora* bacteriophages isolated from infected apple trees along the Wasatch Front in Utah.

At an estimated total number of 10^{31}, phages are by far the most abundant biological entity on the planet (1–7). They dramatically influence the evolution of bacteria by their ability to infect and kill their hosts and to transfer genetic material. *Erwinia amylovora* is a rod-shaped facultative anaerobic member of the *Enterobacteriaceae* bacterial family, which includes many well-characterized Gram-negative plant and animal pathogens, such as *Salmonella* spp., *Escherichia coli*, and *Klebsiella* spp. As the causative agent of fire blight, *Erwinia amylovora* infects members of the Rosaceae plant family, causing diseased areas to appear burnt (8–10). The isolation and characterization of phages that infect *E. amylovora* may aid in our understanding of these bacteria and provide potential treatment for this devastating agricultural disease. Herein, we announce the genome sequences of nine *E. amylovora* bacteriophages, vB_EamM_Asesino, vB_EamM_Alexandra, vB_EamM_Bosolaphorus, vB_EamM_Desertfox, vB_EamM_MadMel, vB_EamM_Mortimer, vB_EamP_Pavtok, vB_EamM_SunLIRen, and vB_EamM_Wellington.

Phages were isolated from apple trees along the Wasatch Front in Utah that appeared to harbor fire blight infection. Phages were plaque purified through a minimum of three passages after amplification via enrichment culture (11). All nine phages reported in this announcement infect the *Erwinia amylovora* ATCC 29780 strain, as indicated by plaque assays, and their characteristics are summarized in Table 1. Genomic DNA was extracted (Phage DNA isolation kit; Norgen Biotek), a library was made using the Illumina TruSeq DNA Nano kit, and sample genomes were sequenced by Illumina HiSeq 2500 sequencing (250-bp paired end) and assembled with Geneious (12) version 8.1 using *de novo* assembly with medium-low sensitivity and various percentages of data. All phages circularized upon assembly and were annotated using DNA Master (http://cobamide2.bio.pitt.edu/computer.htm), giving preference for calls that gave full coding potential coverage.

The nine phages were grouped into five distinct clusters by genomic dot plot and average nucleotide identity analyses, as previously described (11), with the first three groups containing jumbo *Myoviridae*. The first jumbo group included four myoviruses, vB_EamM_Bosolaphorus, vB_EamM_Desertfox, vB_EamM_MadMel, and vB_EamM_Mortimer, which are similar to previously published *Erwinia* phage Ea35-70 (13), as well as other phages we have isolated (14). The second group included two jumbo myoviruses, vB_EamM_Asesino and vB_EamM_Wellington, with similarity to the well-characterized *Salmonella* SPN3US phage (15) and related phages. The third is a single

Received 18 August 2018 **Accepted** 12 September 2018 **Published** 11 October 2018

Citation Sharma R, Berg JA, Beatty NJ, Choi MC, Cowger AE, Cozzens BJR, Duncan SG, Fajardo CP, Ferguson HP, Galbraith T, Herring JA, Hoj TR, Durrant JL, Hyde JR, Jensen GL, Ke SY, Killpack S, Kruger JL, Lawrence EEK, Nwosu IO, Tam TC, Thompson DW, Tueller JA, Ward MEH, Webb CJ, Wood ME, Yeates EL, Baltrus DA, Breakwell DP, Hope S, Grose JH. 2018. Genome sequences of nine *Erwinia amylovora* bacteriophages. Microbiol Resour Announc 7:e00944-18. https://doi.org/10.1128/MRA.00944-18.

Editor J. Cameron Thrash, Louisiana State University

Address correspondence to Julianne H. Grose, grosejulianne@gmail.com.

† Deceased. Charles J. Webb did not see or approve the final version of this paper.

TABLE 1 Properties of nine *Erwinia amylovora* bacteriophage genomes

Name	GenBank accession no.	SRA accession no.	Total no. of reads	No. of reads used	Assembly fold coverage (range [mean])	Length (bp)	No. of ORFs[a]	No. of tRNAs	G+C content (%)
vB_EamP_Pavtok	MH426726	SRX4597602	1,301,332	386,192	492–2,086 (1,069)	61,401	62	0	36.9
vB_EamM_SunLIRen	MH426725	SRX4597606	1,301,332	386,192	8,249–42,422 (13,566)	84,559	141	22	36.3
vB_EamM_Wellington	MH426724	SRX4597603	626,048	372,488	133–514 (329.7)	244,950	295	8	50.3
vB_EamM_Asesino	KX397364	SRX4597609	2,222,038	1,022,382	512–1,378 (1,037.7)	246,290	289	12	51.2
vB_EamM_Alexandra	MH248138	SRX4597608	381,540	200,005	63–516 (166.3)	266,532	349	0	49.8
vB_EamM_Bosolaphorus	MG655267	SRX4597604	778,168	326,344	83–555 (248.4)	272,228	321	1	49.4
vB_EamM_Desertfox	MG655268	SRX4597605	1,930,470	1,138,933	115–612 (352.9)	272,458	320	0	49.6
vB_EamM_Mortimer	MG655270	SRX4616109	2,581,160	287,396	47–207 (129.4)	273,914	325	1	49.5
vB_EamM_MadMel	MG655269	SRX4597607	1,604,720	1,443,568	567–1,577 (1,213.9)	275,000	321	0	49.4

[a]ORFs, open reading frames based on current annotation.

jumbo myovirus, EamM_Alexandra, which has similarity to previously published *Erwinia* phages EamM_Yoloswag (14) and EamM_Y3 (16). Podovirus vB_EamP_Pavtok and myovirus vB_EamM_SunLIRen are similar to *Erwinia* phages PEp14 and phiEa21-4 (17), respectively. The three jumbo myovirus groups package DNA by headful packaging (14) based on homology to phage phiKZ terminase (18), and their bp 1 was chosen by alignment to their phage family. PhageTerm (19) was used to determine the packaging strategy of SunLIRen and Pavtok. SunLIRen appeared to have headful packaging, and its bp 1 was assigned based on homology alignment to *Erwinia* phage phiEa21-4, while the packaging strategy of Pavtok is unknown, and its bp 1 was assigned due to homology to PEp14.

Data availability. The GenBank and SRA accession numbers for the nine *Erwinia* bacteriophages are listed in Table 1.

ACKNOWLEDGMENTS

We thank the Howard Hughes Medical Institute Science Education Alliance–Phage Hunters Advancing Genomics and Evolutionary Science (SEA-PHAGES) for phage analysis training. In addition, we thank Ed Wilcox (BYU DNA Sequencing Center) and Michael Standing (BYU Microscopy Lab).

This work was graciously funded by a USDA grant (to D.A.B., University of Arizona) and the Department of Microbiology and Molecular Biology and the College of Life Sciences at Brigham Young University, as well as a private donor.

REFERENCES

1. Bergh O, Børsheim KY, Bratbak G, Heldal M. 1989. High abundance of viruses found in aquatic environments. Nature 340:467–468. https://doi.org/10.1038/340467a0.
2. Wommack KE, Colwell RR. 2000. Virioplankton: viruses in aquatic ecosystems. Microbiol Mol Biol Rev 64:69–114. https://doi.org/10.1128/MMBR.64.1.69-114.2000.
3. Brüssow H, Hendrix RW. 2002. Phage genomics: small is beautiful. Cell 108:13–16. https://doi.org/10.1016/S0092-8674(01)00637-7.
4. Wilhelm SW, Jeffrey WH, Suttle CA, Mitchell DL. 2002. Estimation of biologically damaging UV levels in marine surface waters with DNA and viral dosimeters. Photochem Photobiol 76:268–273.
5. Hendrix RW. 2003. Bacteriophage genomics. Curr Opin Microbiol 6:506–511. https://doi.org/10.1016/j.mib.2003.09.004.
6. Hambly E, Suttle CA. 2005. The viriosphere, diversity, and genetic exchange within phage communities. Curr Opin Microbiol 8:444–450. https://doi.org/10.1016/j.mib.2005.06.005.
7. Suttle CA. 2005. Viruses in the sea. Nature 437:356–361. https://doi.org/10.1038/nature04160.
8. Khan MA, Zhao Y, Korban SS. 2012. Molecular mechanisms of pathogenesis and resistance to the bacterial pathogen *Erwinia amylovora*, causal agent of fire blight disease in rosaceae. Plant Mol Biol Rep 30:247–260. https://doi.org/10.1007/s11105-011-0334-1.
9. Schroth M, Thomson S, Hildebrand D, Moller W. 1974. Epidemiology and control of fire blight. Annu Rev Phytopathol 12:389–412. https://doi.org/10.1146/annurev.py.12.090174.002133.
10. Thomson SV. 2000. Epidemiology of fire blight 2, p 9–36. *In* Vanneste J (ed), Fire blight: the disease and its causative agent, *Erwinia amylovora*. CABI Publishing, Wallingford, United Kingdom.
11. Arens DK, Brady TS, Carter JL, Pape JA, Robinson DM, Russell KA, Staley LA, Stettler JM, Tateoka OB, Townsend MH, Whitley KV, Wienclaw TM, Williamson TL, Johnson SM, Grose JH. 2018. Characterization of two related *Erwinia* myoviruses that are distant relatives of the PhiKZ-like jumbo phages. PLoS One 13:e0200202. https://doi.org/10.1371/journal.pone.0200202.
12. Kearse M, Moir R, Wilson A, Stones-Havas S, Cheung M, Sturrock S, Buxton S, Cooper A, Markowitz S, Duran C, Thierer T, Ashton B, Meintjes P, Drummond A. 2012. Geneious Basic: an integrated and extendable desktop software platform for the organization and analysis of sequence data. Bioinformatics 28:1647–1649. https://doi.org/10.1093/bioinformatics/bts199.
13. Yagubi AI, Castle AJ, Kropinski AM, Banks TW, Svircev AM. 2014. Complete genome sequence of Erwinia *amylovora bacteriophage* vB_EamM_Ea35-70. Genome Announc 2:e00413-14. https://doi.org/10.1128/genomeA.00413-14.
14. Esplin IND, Berg JA, Sharma R, Allen RC, Arens DK, Ashcroft CR, Bairett SR, Beatty NJ, Bickmore M, Bloomfield TJ, Brady TS, Bybee RN, Carter JL, Choi MC, Duncan S, Fajardo CP, Foy BB, Fuhriman DA, Gibby PD, Grossarth SE, Harbaugh K, Harris N, Hilton JA, Hurst E, Hyde JR, Ingersoll K, Jacobson CM, James BD, Jarvis TM, Jaen-Anieves D, Jensen GL, Knabe BK, Kruger JL, Merrill BD, Pape JA, Payne Anderson AM, Payne DE, Peck MD, Pollock SV, Putnam MJ, Ransom EK, Ririe DB, Robinson DM, Rogers SL, Russell KA, Schoenhals JE, Shurtleff CA, Simister AR, Smith HG, Stephenson MB, et al. 2017. Genome sequences of 19 novel *Erwinia amylovora* bacteriophages. Genome Announc 5:e00931-17. https://doi.org/10.1128/genomeA.00931-17.
15. Lee JH, Shin H, Kim H, Ryu S. 2011. Complete genome sequence of *Salmonella* bacteriophage SPN3US. J Virol 85:13470–13471. https://doi.org/10.1128/JVI.06344-11.
16. Buttimer C, Born Y, Lucid A, Loessner MJ, Fieseler L, Coffey A. 2018. *Erwinia amylovora* phage vB_EamM_Y3 represents another lineage of hairy *Myoviridae*. Res Microbiol 30062–30067. https://doi.org/10.1016/j.resmic.2018.04.006.
17. Lehman SM, Kropinski AM, Castle AJ, Svircev AM. 2009. Complete genome of the broad-host-range *Erwinia amylovora* phage phiEa21-4 and its relationship to *Salmonella* phage Felix O1. Appl Environ Microbiol 75:2139–2147. https://doi.org/10.1128/AEM.02352-08.
18. Mesyanzhinov VV, Robben J, Grymonprez B, Kostyuchenko VA, Bourkaltseva MV, Sykilinda NN, Krylov VN, Volckaert G. 2002. The genome of bacteriophage phiKZ of *Pseudomonas aeruginosa*. J Mol Biol 317:1–19. https://doi.org/10.1006/jmbi.2001.5396.
19. Garneau JR, Depardieu F, Fortier L-C, Bikard D, Monot M. 2017. PhageTerm: a fast and user-friendly software to determine bacteriophage termini and packaging mode using randomly fragmented NGS data. Sci Rep 7:8292. https://doi.org/10.1038/s41598-017-07910-5.

7.2 Supplementary Figure 2. Flavonoid metabolities

Available online at www.sciencedirect.com
ScienceDirect
Journal of Nutritional Biochemistry 62 (2018) 95–107
Journal of Nutritional Biochemistry

Common gut microbial metabolites of dietary flavonoids exert potent protective activities in β-cells and skeletal muscle cells☆

Benjamin F. Bitner[a,1], Jason D. Ray[a,2], Kyle B. Kener[a], Jacob A. Herring[a,b], Josie A. Tueller[b], Deborah K. Johnson[b], Claudia M. Tellez Freitas[b], Dane W. Fausnacht[c], Mitchell E. Allen[c], Alexander H. Thomson[c], K. Scott Weber[b], Ryan P. McMillan[c,d], Matthew W. Hulver[c,d], David A. Brown[c,d,e], Jeffery S. Tessem[a], Andrew P. Neilson[f,*]

[a]Department of Nutrition, Dietetics and Food Science, Brigham Young University, S243 ESC, Provo, UT 84602
[b]Department of Microbiology and Molecular Biology, Brigham Young University, 3137 LSB, Provo, UT 84602
[c]Department of Human Nutrition, Foods and Exercise, Virginia Tech, 1981 Kraft Dr., Blacksburg, VA 24060
[d]Metabolic Phenotyping Core Facility, Virginia Tech, 1981 Kraft Dr., Blacksburg, VA 24060
[e]Virginia Tech Center for Drug Discovery, 800 West Campus Dr. Room 3111, Blacksburg, VA 24061
[f]Department of Food Science and Technology, Virginia Tech, 1981 Kraft Dr., Blacksburg, VA 24060

Received 18 May 2018; received in revised form 20 August 2018; accepted 11 September 2018

Abstract

Flavonoids are dietary compounds with potential anti-diabetes activities. Many flavonoids have poor bioavailability and thus low circulating concentrations. Unabsorbed flavonoids are metabolized by the gut microbiota to smaller metabolites, which are more bioavailable than their precursors. The activities of these metabolites may be partly responsible for associations between flavonoids and health. However, these activities remain poorly understood. We investigated bioactivities of flavonoid microbial metabolites [hippuric acid (HA), homovanillic acid (HVA), and 5-phenylvaleric acid (5PVA)] in primary skeletal muscle and β-cells compared to a native flavonoid [(−)-epicatechin, EC]. In muscle, EC was the most potent stimulator of glucose oxidation, while 5PVA and HA simulated glucose metabolism at 25 μM, and all compounds preserved mitochondrial function after insult. However, EC and the metabolites did not uncouple mitochonndrial respiration, with the exception of 5PVA at10 μM. In β-cells, all metabolites more potently enhanced glucose-stimulated insulin secretion (GSIS) compared to EC. Unlike EC, the metabolites appear to enhance GSIS without enhancing β-cell mitochondrial respiration or increasing expression of mitochondrial electron transport chain components, and with varying effects on β-cell insulin content. The present results demonstrate the activities of flavonoid microbial metabolites for preservation of β-cell function and glucose utilization. Additionally, our data suggest that metabolites and native compounds may act by distinct mechanisms, suggesting complementary and synergistic activities in vivo which warrant further investigation. This raises the intriguing prospect that bioavailability of native dietary flavonoids may not be as critical of a limiting factor to bioactivity as previously thought.

Keywords: Hippuric acid; Homovanillic acid; 5-Phenylvaleric acid; (−)-Epicatechin; Insulin; Respiration

1. Introduction

Incidence rates of type-2 diabetes and obesity are rising worldwide. In addition to traditional medical interventions, complementary lifestyle strategies such as diet and exercise are needed to blunt this epidemic. Flavonoids from cocoa, fruit, tea and other sources have been identified as dietary bioactive compounds with potential anti-obesity and anti-diabetes activities. Many of these flavonoids, such as quercetin [1] and procyanidins [2], have poor oral bioavailability and thus low circulating concentrations. Non-extractable/bound flavonoids (from cocoa, *etc.*) and oxidized flavonoids, such as theaflavins and thearubigins from oolong and black teas, have extremely limited oral bioavailability [3,4] and vanishing low circulating concentrations. As an extreme example, consumption of 700 mg theaflavins (equivalent to~30 cups of black tea), produced maximal blood concentrations of only 1 μg/L (~1.8 nM) in humans [3]. Therefore,

* Grants, sponsors, and funding sources: Funding for this work was provided, in part, by the Virginia Agricultural Experiment Station and the Hatch Program of the National Institute of Food and Agriculture, U.S. Department of Agriculture (APN and DAB), American Diabetes Association (1-JF-05-24 to MWH), the National Institutes of Health-NIDDK (2RO1 DK-078765), R01 HL123647 to DAB), BYU mentoring environment grant (JST), BYU ORCA Grant (BFB), American Diabetes Association (1-17-IBS-101 to JST), and a grant from the Diabetes Action Research and Education Foundation (Grant #461 to JST).
* Corresponding author at: 1981 Kraft Dr. Rm 1013, Blacksburg, VA 24060. Tel.: +1 540 231 8391; fax: +1 540 231 9293.
E-mail address: andrewn@vt.edu (A.P. Neilson).
[1] Current affiliation: UC Irvine School of Medicine, Irvine, CA.
[2] Current affiliation: Yale University, New Haven, CT.

https://doi.org/10.1016/j.jnutbio.2018.09.004
0955-2863/

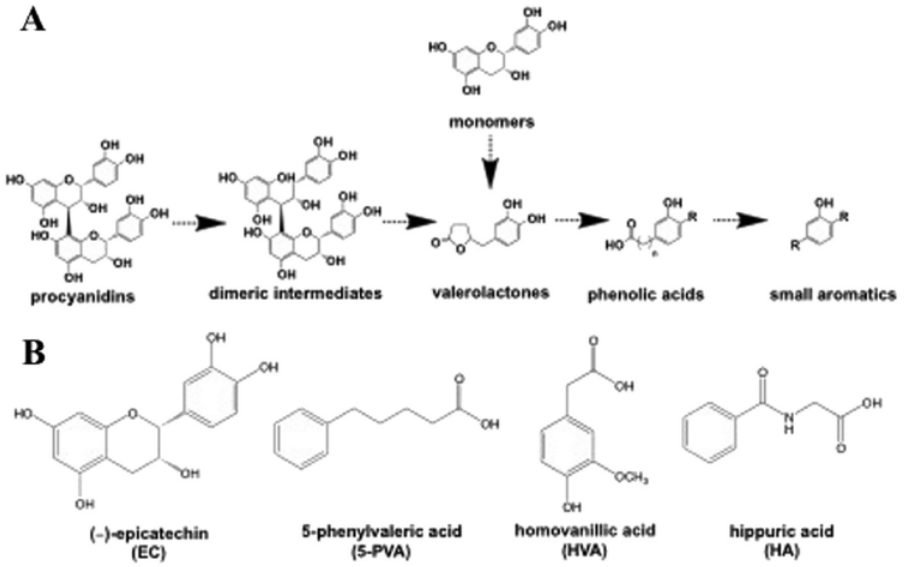

Fig. 1. (A) Schematic showing representative sequential metabolism of representative flavonoids [a dimeric procyanidin, and (−)-epicatechin monomer] by the gut microbiota. (B) Structures of (−)-epicatechin and the three representative flavonoid microbial metabolites employed in this present study.

circulating concentrations of the native species may represent a very small fraction of the ingested dose, whereas the majority reaches the colon unabsorbed. Unabsorbed flavonoids are extensively metabolized by the gut microbiota to a series of smaller metabolites such as valerolactones, phenylalkyl acids, and smaller aromatics (Fig. 1A) [4–9]. While some metabolites are unique to individual flavonoid compounds or subclasses, dozens of metabolites are common to most flavonoids [10,11]. These metabolites are comparatively more bioavailable than their native flavonoid precursors, and in many cases represent the predominant circulating forms following flavonoid consumption [10]. For example, a recent study of pharmacokinetics following consumption of grape pomace demonstrated that anthocyanins and procyanidins were not detected in blood and catechins and their phase-II conjugates exhibited maximum blood levels of 7–136 nM (with only 1 compound reaching at least 100 nM), while microbial metabolites exhibited maximum blood levels of 3–1170 nM (with 8 compounds reaching at least 100 nM) [12]. In an extreme example, consumption of 6 cups of green or black tea resulted in circulating metabolite levels in the mM range (hippuric acid, HA, reached 2.3 mM) [13]. This highlights the comparative importance of these metabolites as potential bioactives in circulation following the consumption of flavonoids.

Even flavonoids with comparatively high bioavailability (monomeric catechins, etc.) are only present in the bloodstream at nM to very low μM levels following consumption of typical doses in foods and supplements [14,15]. These doses are generally lower than the range of concentrations typically used to study mechanisms in cell culture models (1–100 μM, or sometimes higher). Despite poor bioavailability and low circulating concentrations, many of these compounds (and foods rich in them) appear to effectively prevent or ameliorate metabolic syndrome even at low dietary doses in animals [16] and humans [17]. Dietary efficacy, despite poor bioavailability and/or low circulating concentrations of the native forms, suggests three mechanisms by which ingested flavonoids exert their activities: (1) native flavonoids primarily exert their activities in the gut lumen (inhibition of digestive enzymes, alteration of microbiome composition and function, *etc.*) [18,19] and/or epithelium (improving barrier function, immune development, etc.) [20] where they are at highest concentrations (μM-mM range), (2) native flavonoids primarily exert their activity in peripheral tissues even at the very low (pM-low μM range) circulating levels achieved, or (3) microbial metabolites of flavonoids generated by commensal microbiota in the lower gut exert activities locally in the gut and systemically [21,22].

Considering the relatively high concentrations of microbial metabolites documented in plasma compared to the native compounds, it is plausible that these metabolites may be responsible, at least in part, for observed associations between dietary flavonoids and health outcomes. While all of the three possible scenarios identified above likely occur simultaneously, the potential anti-diabetic and anti-obesity activities of microbial metabolites formed from unabsorbed flavonoids remain poorly understood.

Recent provocative evidence has strengthened the argument that native flavonoids may exert their effects independent of systemic bioavailability: either directly on the microbiota, or by formation of bioavailable microbial metabolites that then act in peripheral tissues [23]. *In vitro*, 3-(3-hydroxyphenyl)propionoic acid (a microbial metabolite common to many flavonoids) prevented loss of insulin-stimulated nitric oxide synthesis and activity under high glucose concentrations in human aortic endothelial cells [24]. In human skeletal muscle myotubes, various microbial metabolites stimulated glucose and oleic acid uptake [25]. Recent studies demonstrated that phenylacetic and phenylpropionic acid have protective activities in pancreatic β-cells and islets [26,27] and protect hepatocytes from acetaminophen injury [28]. Two recent studies demonstrated that valerolactones inhibited monocyte adhesion to endothelial cells [29]. A key animal study demonstrated that administration of antibiotics (depletion of gut microbiota and their associated metabolites) abolished the ability of procyanidin-rich grape seed extract to prevent inflammation, insulin resistance, hyperglycemia and weight gain in a high-fat feeding mouse model [30]. Furthermore, antibiotic

administration reversed the ability of blackcurrant anthocyanins to ameliorate diet-induced obesity in mice [31]. Finally, digestion and microbial metabolism of berry flavonoids did not diminish their protective activities against colon cancer [32]. While the in vivo studies did not measure metabolite production, they strongly suggest that these effects are mediated by the microbiota and/or their metabolites produced from the native dietary flavonoids. Perhaps the most well-known microbial metabolites, the phenylalkyl acids (phenylacetic, phenyl propionic, and phenylvaleric acids) have not been well studied, and the phenylvaleric acids have not been studied at all to our knowledge. Some compounds that are microbial metabolites have been studied, but only because they also exist as native compounds in foods, such as the cinnamic acids and small aromatics such as vanillic acid. These compounds have been shown to possess anti-diabetic and anti-obesity activities in β-cell, skeletal muscle, hepatocyte and adipose models (see Supplementary Information). Finally, some microbial metabolites of flavonoids have been shown to possess enhanced anti-tumor and anti-platelet aggregation activities compared to the native forms [33].

Despite these promising findings, relatively little work has been done to characterize the effects of these metabolites in cell or animal models, in comparison to the exhaustive body of literature on the bioactivities of native flavonoids. The majority of research that does exist on these metabolites has focused on their formation, but not their activities nor mechanisms of action. Our objectives were therefore to 1) investigate the anti-diabetic activities of microbial flavonoid metabolites (including a poorly-studied class, phenylvaleric acids) in β-cells and primary skeletal muscle cells, 2) compare these activities to those of a control native flavonoid, and 3) suggest potential mechanisms by which these activities may occur. Our findings demonstrate that these metabolites possess potent bioactivities, and may contribute to the observed peripheral tissue effects of dietary flavonoids.

2. Materials and methods

2.1. Materials

Three representative metabolites representative of three distinct classes of metabolites common to a variety of dietary flavonoids were selected for investigation: hippuric acid (HA, 98%), homovanillic acid (HVA), and 5-phenylvaleric acid (5PVA, 99%) were obtained from Sigma (St. Louis, MO). A native flavanol, (−)-epicatechin (EC, Sigma), was used as a positive control; note that the three selected metabolites can be obtained by metabolism of EC and related compounds [9]. Structures of these compounds are shown in Fig. 1B. All compounds were tested over a range of 0–100 μM (depending upon the specific assay) in water or DMSO, with equal final concentrations of DMSO in cell media for all treatments. Generally, doses of 5–25 μM were employed, which are easily obtainable in circulation for metabolites but which represent the extreme upper end of what is attainable for native flavonoids [13,34]. Microbial metabolites, similar to those of native flavonoids, exhibit pharmacokinetic curves that depend on a variety of factors and circulating concentrations necessarily fluctuate over time based on consumption frequency. The levels employed herein are attainable following flavonoid consumption but are not continuously present, similar to those of native dietary flavonoids. Furthermore, while compounds and doses were uniform across experiments, differences in some aspects (treatment times, *etc.*) were necessary due to the use of established, robust experimental protocols for each model system.

2.2. Skeletal muscle experiments

Skeletal muscle metabolism experiments were conducted per previously published methods [35,36], with modifications. Primary human muscle cells were cultured for measuring palmitate and glucose oxidation. Cultures of primary human muscle cells were obtained from a singler subject who provided written informed consent under an approved protocol by Virginia Polytechnic Institute and State University Institutional Review Board (approval #11–770). The subject was a healthy Caucasian male, age 22 years, with a BMI of 23.6 and 20.9% body fat.

2.2.1. Skeletal muscle substrate metabolism

Cells were grown in low glucose DMEM supplemented with 10% fetal bovine serum and SkGM SingleQuots (Lonza, Walkersville, MD, USA). Upon reaching ~80% confluence in standard 12-well plates, cells were differentiated for 7 days in 2% horse serum. All experiments were performed on day 7 of differentiation following overnight serum deprivation. The compounds tested were treated for 24 h prior to assessment of substrate metabolism. Fatty acid oxidation was assessed by measuring and summing $^{14}CO_2$ production (complete) and ^{14}C-labeled acid-soluble metabolites (incomplete) from the oxidation of [1-^{14}C] palmitic acid (American Radiolabeled Chemicals, St. Louis, MO, USA). Briefly, cells were incubated in media containing radiolabeled substrate along with the compound at 5 or 10 μM, or vehicle only (0 μM, 0.1% DMSO) for 3 h at 37 °C, 5% CO_2. Following incubation media was removed and acidified with 45% perchloric acid to elute gaseous $^{14}CO_2$. $^{14}CO_2$ was trapped in 1 M NaOH over the course of 1 h. The NaOH was then placed in a liquid scintillation counter and counted. Data were expressed as means±S.E.M. and is normalized to total protein content. Glucose oxidation was assessed by measuring $^{14}CO_2$ production from the oxidation of [U-^{14}C] glucose (American Radiolabeled Chemicals, St. Louis, MO, USA) in a manner similar to fatty acid oxidation expect for the substitution of glucose in place of palmitic acid. Compounds were tested at 10 and 25 μM.

2.2.2. Skeletal muscle cell respiration

Oxygen consumption rate (OCR) was measured with our established protocols [37] using a XF96 Seahorse Extracellular Flux Analyzer (Agilent Technologies, Santa Clara, CA, USA). C2C12 myoblast studies are commonly used by our groups as a fast and practical model to screen for compound efficacy. Because differentiating cells into myotubes takes 7 days continuously in the SeaHorse plate, we utilized the myoblasts as a more feasible approach. Cultured C2C12 muscle cells were seeded at a density of 1.5×10^4 per well in supplemented DMEM media [4.5 g/L D-Glucose, L-Glutamine, and 110 mg/L Sodium Pyruvate supplemented with 10% Fetal Bovine Serum (FBS) and 1% Penicillin Streptomycin (PSA)] on a Seahorse XF96 Cell Culture Microplate. Cells were then incubated overnight at 37 °C in 5% CO_2 to allow for adherence. Following adherence, cells were pretreated for 4 h with 10% FBS/1% PSA DMEM containing the test compounds (5 and 10 μM) or vehicle only (≤0.1% DMSO). After the 4-h pretreatment, 500 μM H_2O_2 was added to injure the cells, and the microplate was subsequently incubated for an additional 4 h. Following incubation, the cells were washed with supplemented XF media (XF base media plus 1 mM pyruvate, 2 mM glutamine, 10 mM glucose) twice before adding a final volume of 180 μL per well. A XF Cell Mitochondrial Stress Test was completed to assess the bioenergetic status of the cells by injecting ATP synthase inhibitor oligomycin (1 μg/mL), inner membrane uncoupler fluorocarbonyl cyanide (FCCP, 2 μM), and complex III inhibitor antimycin A (2 μM). Oxygen consumption rate data were normalized by subtracting non-mitochondrial rates of respiration (after antimycin A), and are expressed as pmol O_2 per minute per 1.5×10^4 cells. Mitochondrial coupling efficiency was calculated by taking the ATP-dependent respiration (baseline-oligomycin) and dividing by the basal rates for internal normalization.

2.3. β-Cell experiments

β-cell metabolism experiments were conducted per previously published methods, with modifications [38,39].

2.3.1. INS-1832/13 β-cell culture

Cell culture was performed per our established protocols [40–44]. The INS-1 derived 832/13 rat β-cell line was maintained in complete RPMI 1640 medium with L-glutamine and 11.2 mM glucose supplemented with 50 U/ml penicillin, 50 μg/ml streptomycin, 10 mM HEPES, 10% fetal bovine serum, and INS-1 supplement, as previously described. For all glucose-stimulated insulin secretion and respiration assays using the 832/13 β-cells, cells were plated at 0 h, treated with test compounds at 24 h, and harvested at 48 h. Stock solutions of test compounds were made at 100 mM, and diluted in media for assays at final concentrations of 0–100 μM (0.1% DMSO in all treatments).

2.3.2. Glucose-stimulated insulin secretion

Glucose-stimulated insulin secretion (GSIS) was performed as previously described [40]. Briefly, INS-1832/13 β-cells were plated and grown to confluency in standard 24-well plates. Upon reaching confluency, cells were cultured with test compounds at 0–100 μM in complete media for 24 h. Following the 24 h treatment, cells were washed with PBS and preincubated in secretion assay buffer (SAB) for 1.5 h (114 mM NaCl, 4.7 mM KCl, 1.2 mM KH_2PO_4 1.16 mM $MgSO_4$, 20 mM HEPES, 2.5 mM $CaCl_2$, 0.2% BSA, pH 7.2) containing 2.5 mM glucose. GSIS was performed by incubating quadruplicate replicate wells of cells previously cultured with test compounds in SAB containing 2.5 mM glucose for 1 h (basal), followed by 1 h in SAB with 16.7 mM glucose (glucose stimulation), followed by collection of the respective buffers, as previously described. For total insulin content, β-cells stimulated with 16.7 mM glucose for 1 h were lysed in RIPA buffer with protease inhibitors (Life Technologies). Secreted insulin and total insulin was measured in SAB using a rat insulin RIA kit (MP Biomedicals), and normalized to total cellular protein concentration (determined by BCA assay), as previously described.

2.3.3. INS-1832/13 β-cell oxygen consumption rate

Oxygen consumption rate (OCR) was measured using an XFp Extracellular Flux Analyzer (Agilent Technologies). INS-1832/13 β-cells were seeded at 2.0×10^4 cells/well in complete 832/13 RPMI 1640 medium (L-glutamine, 11.2 mM glucose supplemented,

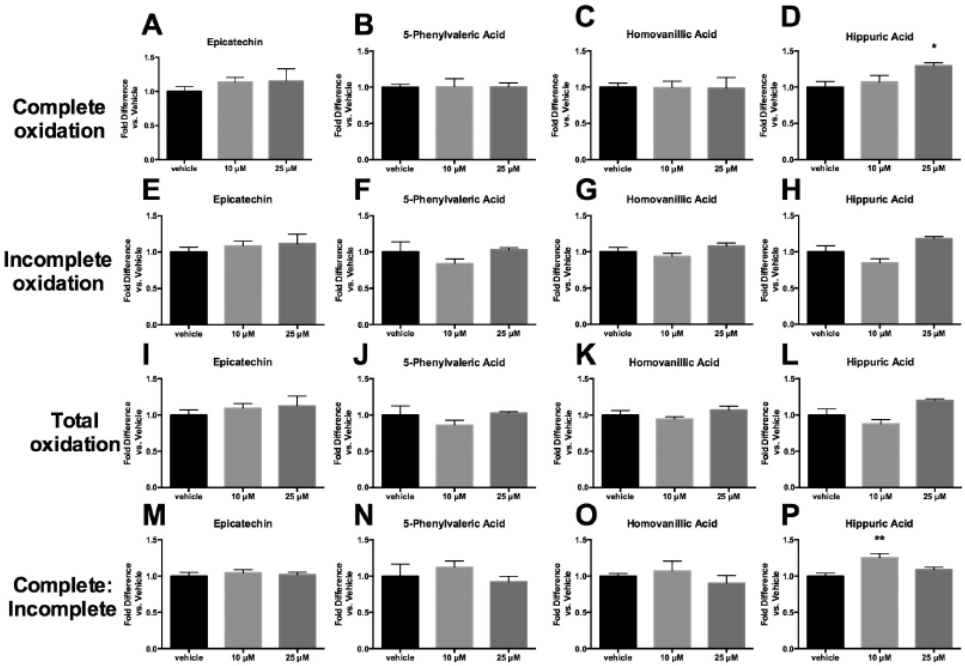

Fig. 2. Fatty acid oxidation in primary human skeletal muscle cells treated with either hippuric acid, homovanillic acid, 5-phenylvaleric acid, or epicatechin. Complete oxidation represents evolution of $^{14}CO_2$ from ^{14}C-labeled palmitate. Incomplete oxidation represents production of ^{14}C-labeled acid-soluble metabolites (ASMs) from ^{14}C-labeled palmitate. Total oxidation represents the sum of complete and incomplete oxidation. Values represent mean±S.E.M. from n=4 replicates, normalized to vehicle (vehicle expressed as 1). Data were analyzed by one-way ANOVA. If a significant treatment effect was detected, Dunnett's post hoc test was performed within each compound to compare each dose to the vehicle control. Significance vs. vehicle control is indicated by: *$P \le 0.05$, **$P \le 0.01$.

50 U/ml penicillin, 50 µg/ml streptomycin, 10 mM HEPES, 10% fetal bovine serum, and INS-1 supplement) on a Seahorse XFp Cell Culture Microplate. Cells were incubated overnight and then treated with test compounds at 10 µM, 5 µM or 0 µM in complete RPMI 1640 media. Following 24 h of culture with the compounds, cells were incubated in 2.5 mM glucose SAB for 3 h. Following incubation, buffer was exchanged for 180 µL fresh pre-warmed 2.5 mM glucose SAB per well. A XF Cell Mitochondrial Stress Test was completed to assess the bioenergetic status of the cells by injecting glucose (16.7 mM, in order to examine respiration under glucose stimulation), oligomycin (4 µM), FCCP (2.5 µM), and antimycin A with rotenone (2.5 µM). Residual oxygen consumption was determined following inhibition of complex III with the addition of rotenone and antimycin A. This state of residual oxygen consumption served as a baseline correction for all of the other states. All data were normalized to protein content of each well, determined by BCA assay.

2.3.4. Western blotting

832/13 beta cells were plated in standard 6-welll plates, grown to confluency, and cultured overnight in media containing each test compound at 10 µM or vehicle control (0.1%DMSO in both). Cells were washed in PBS and harvested in RIPA buffer followed by sonication. Protein concentration was quantified by BCA, and 30 µg was run per sample. Western blotting and transfer was performed as previously described [38,40,41]. Blot were probed using the Anti Rt/Ms. Total OxPhos Complex Kit (1:250, Life Technologies, Carlsbad, CA) which contains a cocktail of antibodies for the electron transport chain (ETC) components ATP5A (Complex V), UQCR2 (Complex III), MTCO1 (Complex IV), SDHB (Complex II) and NDUFB8 (Complex I). Blot was imaged in the linear range using a LI-COR Odyssey CLx (LI-COR Biotechnology, Lincoln, NE). Blotting was performed on triplicate samples.

2.4. Statistics

All results are expressed as mean±S.E.M. For activity assays, data were analyzed by 1- or 2-way ANOVA as appropriate. For 2-way ANOVAs, if a significant main effect of treatment compound dose was detected, Dunnett's post hoc test was performed within the high-glucose treatments to compare each dose to the vehicle (0 µM) control. For one-way ANOVAs, if a significant treatment effect was detected, Dunnett's post hoc test was performed within each compound to compare each dose to the vehicle controls. Significance was defined *a priori* as $P<.05$. Statistical analyses were performed on Prism v6.0f (GraphPad, La Jolla, CA).

3. Results and discussion

3.1. Skeletal muscle

3.1.1. Skeletal muscle metabolism

The ability of EC (+ control, native flavonoid) and three representative metabolites (HA, HVA and 5PVA) to influence fatty acid or glucose uptake and metabolism was examined in primary human skeletal muscle cells. As shown in Fig. 2, these compounds exhibited minimal ability to alter fatty acid oxidation. The only statistically significant findings were that HA was able to increase complete fatty acid oxidation at 25 µM (Fig. 2D) and increase the ratio of complete:incomplete oxidation at 10 µM (Fig. 2P). While these results suggest that HA has more potent activities than EC, overall the enhancement of fatty acid oxidation does not seem to be a significant mechanism of action for these metabolites. These results suggest that, despite a reported finding that metabolites increased oleic acid uptake in human skeletal muscle myotubes [25], alteration of fatty acid oxidation in skeletal muscle may not be a primary mechanism by which flavonoid microbial metabolites exert anti-diabetic and anti-obesity activities.

Glucose oxidation results (Fig. 3) were more promising than fatty acid oxidation. EC appeared to be the most potent stimulator of glucose utilization, increasing activity at both 10 and 25 µM (Fig. 3A).

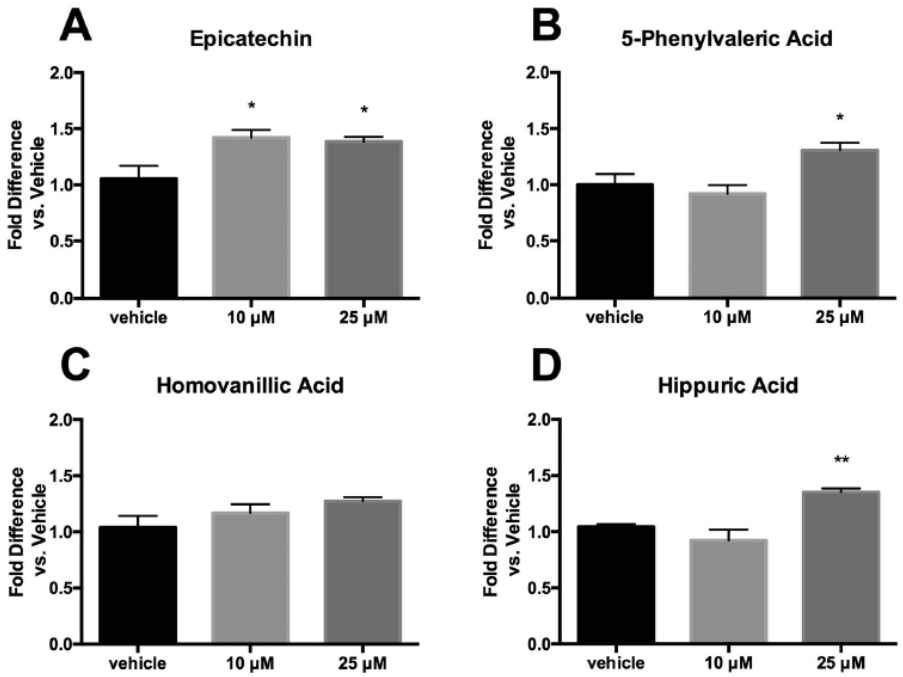

Fig. 3. Glucose oxidation in primary human skeletal muscle cells treated with either hippuric acid, homovanillic acid, 5-phenylvaleric acid, or epicatechin. Oxidation represents evolution of $^{14}CO_2$ from ^{14}C-labeled glucose. Values represent mean±S.E.M. from $n=4$ replicates, normalized to vehicle (vehicle expressed as 1). Data were analyzed by one-way ANOVA. If a significant treatment effect was detected, Dunnett's post hoc test was performed within each compound to compare each dose to the vehicle control. Significance vs. vehicle control is indicated by: $^{*}P \le 0.05$, $^{**}P \le 0.01$, $^{***}P \le 0.001$, $^{****}P \le 0.0001$.

While HVA had no apparent activity, both 5PVA and HA were able to simulate glucose metabolism at 25 μM (Fig. 3B-D). While the EC activity at lower concentrations suggests that it is more potent than the metabolites on an equal concentration basis, it is important to keep in mind that the metabolites tend to exist in circulation at higher levels than the native forms. Thus, the observed increase in glucose oxidation for 5PVA and HA, combined with previous reports that microbial metabolites stimulate glucose uptake [25], suggest promise for the ability of these metabolites to exert significant benefits on blood glucose levels in vivo.

3.1.2. Skeletal muscle cell respiration

The effects of EC and the three metabolites on respiration in normal, uninjured C2C12 cells are shown in Fig. 4. We utilized a peroxide stress paradigm since heightened mitochondrial ROS burdens are observed in skeletal muscle from humans and animal models of diabetes, often before the onset of overt systemic hyperglycemia [45]. Respiration curves for controls and each dose, including basal, leak (oligomycin) and maximal (FCCP) respiration, are shown in Fig. 4A and B. None of the compounds tested significantly enhanced basal respiration (Fig. 4C), ATP-dependent respiration (Fig. 4E), maximal respiration (Fig. 4F), or respiratory reserve (the difference between basal and maximal respiration, which reflects reserve bioenergetic capacity available to the cell, Fig. 4G) compared to the control at either 5 or 10 μM compared to vehicle control. Coupling efficiency was not influenced by any of the compounds at any concentration, with the exception of 5PVA at 10 μM (Fig. 4H). HA and 5PVA both modestly enhanced 'leak' respiration at 10 μM (Fig. 4D), suggesting either slight mitochondrial injury (potentially due to minor pro-oxidant effects at these higher doses) or mitochondrial uncoupling. The data in uninjured cells generally suggest that EC and the metabolites do not alter skeletal muscle respiration under normal conditions at low doses, and indicate that do not appear to acutely uncouple mitochondria or partially inhibit the respiratory chain (both of which have been postulated as a strategy to treat obesity/diabetes for decades) with the possible exception of HA and 5PVA at high doses [46,47].

The effects of EC and the metabolites on C2C12 cells exposed to peroxide challenge (*i.e.* injured) are presented in Fig. 5. Peroxide treatment induced mitochondrial injury as assessed by increased 'leak' respiration (respiration after oligomycin roughly doubled) (Fig. 5D) and lower rates of maximal respiration (FCCP), ATP-dependent respiration (Fig. 5E), respiratory reserve capacity (Fig. 5G), and coupling efficiency (Fig. 5H) for H_2O_2 treated cells (red bars) compared to control (blue bars). While there were some differences in basal respiration, this can be due to slight respiratory uncoupling due to the injury and should be interpreted with caution. Each of the compounds studied significantly protected against peroxide-mediated injury at 5 μM, reflected by reduced leak respiration, and preserved maximal respiration respiratory reserve and/or coupling efficiency at the same level as the uninjured control despite peroxide challenge (Fig. 5D-H). As observed for uninjured cells, one metabolite actually worsened cell injury as measured by leak respiration, although in this case it was 10 μM HVA (as opposed to HA and PVA in uninjured cells), again suggesting either cellular injury or uncoupling. Interestingly, while HA and 5PVA increased leak

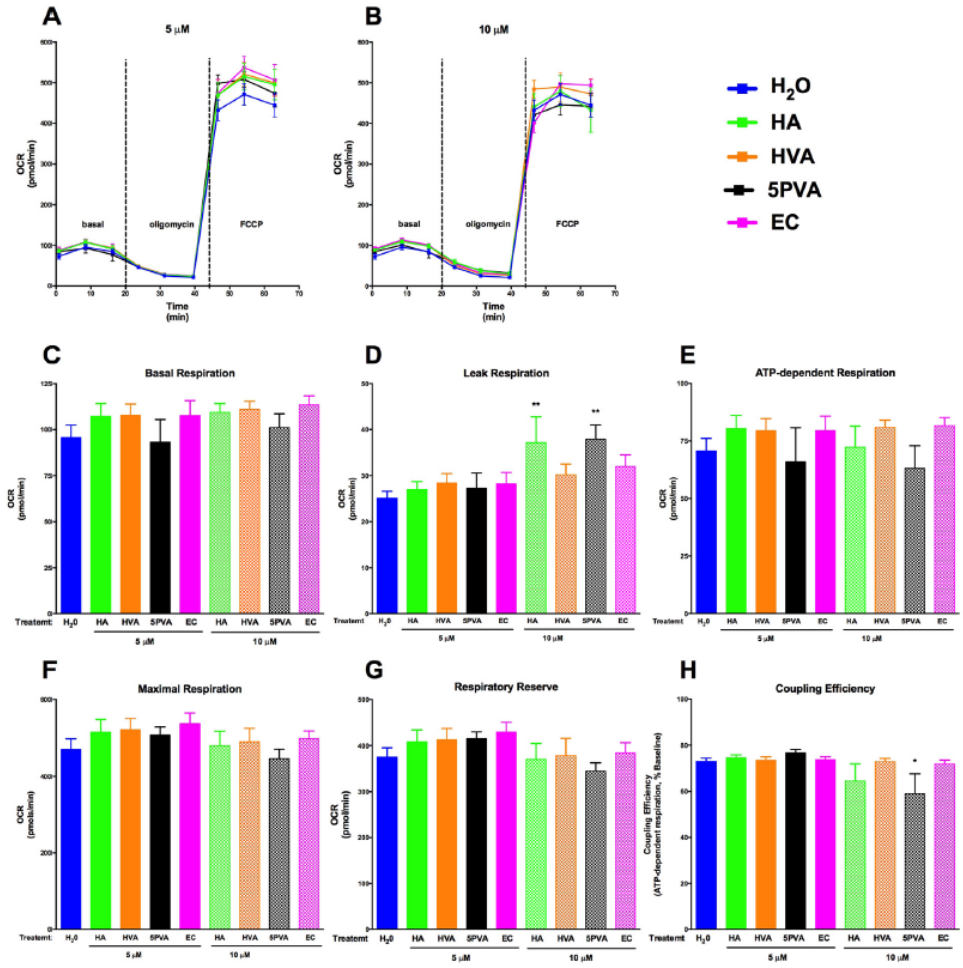

Fig. 4. Corrected mitochondrial respiration data for C2C12 cells cultured acutely (4 h) in the presence of hippuric acid (HA), homovanillic acid (HVA), 5-phenylvaleric acid (5PVA), or epicatechin (EC): oxygen consumption rate (OCR) curves for treatments at 5 μM (**A**) and 10 μM (**B**), basal respiration (**C**), leak respiration (after oligomycin, **D**), ATP-dependent respiration (**E**), maximal respiration (after FCCP, **F**) respiratory reserve (maximal − basal, **G**), and coupling efficiency (ATP-dependent respiration/basal respiration, **H**). Oxygen consumption rate data were normalized by subtracting non-mitochondrial rates of respiration (after antimycin A, not shown), and are expressed as pmol O_2 per minute per 1.5×10^4 cells. Values represent mean±S.E.M. from $n=8$ replicates. Data were analyzed by one-way ANOVA. If a significant treatment effect was detected, Dunnett's post hoc test was performed within each compound to compare each dose to the vehicle control (H_2O). Significance vs. vehicle control is indicated by: $^*P \le 0.05$, $^{**}P \le 0.01$, $^{***}P \le 0.001$, $^{****}P \le 0.0001$.

respiration in the absence of H_2O_2, there was only a slight additional increase in leak respiration with H_2O_2 treatment. These data indicate that HA and 5PVA may have pro-oxidant effects similar to H_2O_2, but that these metabolites did not exacerbate leak respiration when combined with H_2O_2 stress. Future studies that further examine the effects of HA and 5PVA will advance our understanding of these compounds on mitochondrial bioenergetics. The 10 μM dose was generally ineffective for all compounds except HA, which partly preserved respiratory reserve (Fig. 5E). These results suggest that EC and the flavonoid microbial metabolites preserve skeletal mitochondrial function after oxidative insult, notably at lower micromolar concentrations.

3.2. β-Cells

3.2.1. β-Cell glucose-stimulated insulin secretion

In addition to substrate utilization in skeletal muscle, β-cell function is a critical target at all stages of diabetes development. We sought to examine the impact of EC and representative flavonoid metabolites on GSIS in a β-cell model (Fig. 6). We have previously demonstrated that the epicatechin-rich fraction from cocoa enhances β-cell GSIS at 25 μg/ml [38]. In the present experiment, EC was able to enhance GSIS in INS-1832/13 β-cells but only at 100 μM (Fig. 6A), which is not physiologically relevant, suggesting minimal relevance for activity in vivo. Interestingly, all three microbial metabolites

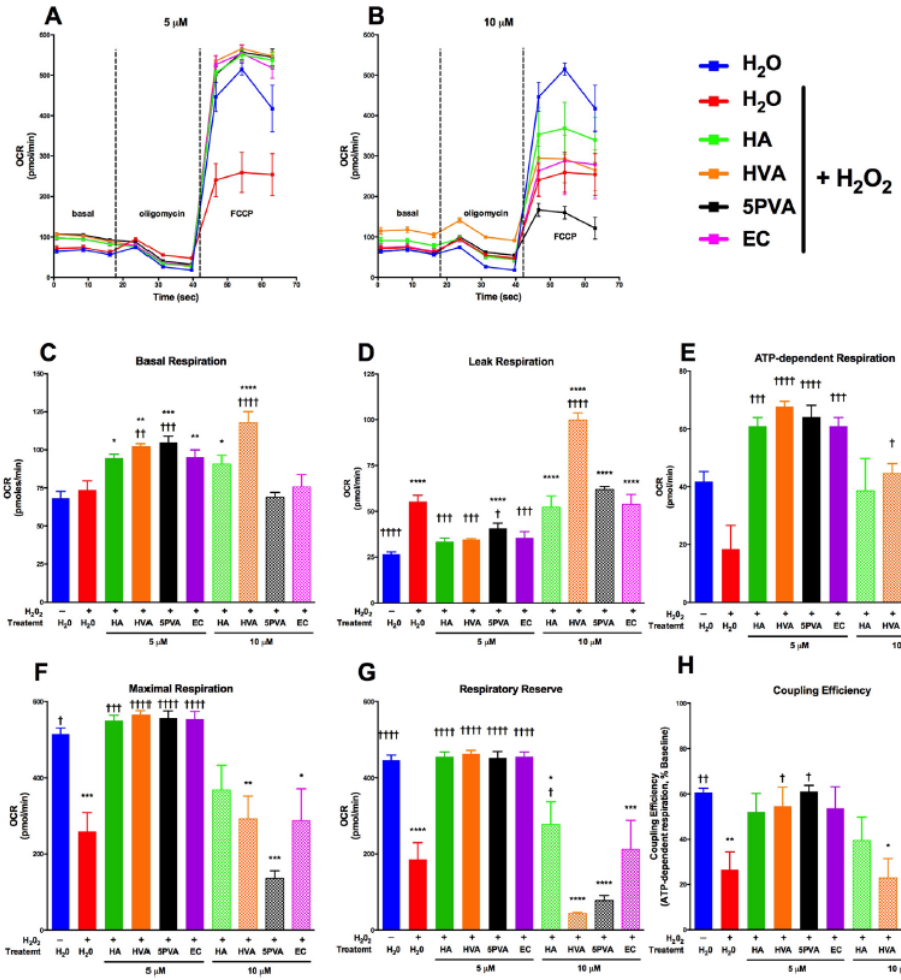

Fig. 5. Corrected mitochondrial respiration data for H_2O_2-injured C2C12 cells cultured acutely (4 h) in the presence of hippuric acid (HA), homovanillic acid (HVA), 5-phenylvaleric acid (5PVA), or epicatechin (EC): oxygen consumption rate (OCR) curves for treatments at 5 μM (**A**) and 10 μM (**B**), basal respiration (**C**), leak respiration (after oligomycin, **D**), ATP-dependent respiration (**E**), maximal respiration (after FCCP, **F**) respiratory reserve (maximal − basal, **G**), and coupling efficiency (ATP-dependent respiration/basal respiration, **H**). Oxygen consumption rate data were normalized by subtracting non-mitochondrial rates of respiration (after antimycin A, not shown), and are expressed as pmol O_2 per minute per 1.5×10^4 cells. Values represent mean±S.E.M. from $n=8$ replicates. Data were analyzed by one-way ANOVA. If a significant treatment effect was detected, Dunnett's post hoc test was performed within each compound to compare each dose to the vehicle control (H_2O) as well as injury control ($H_2O + H_2O_2$). Significance vs. vehicle control is indicated by: $^*P\leq0.05$, $^{**}P\leq0.01$, $^{***}P\leq0.001$, $^{****}P\leq0.0001$; significance vs. injury control is indicated by: $\dagger P \leq 0.05$, $\dagger\dagger P \leq 0.01$, $\dagger\dagger\dagger P \leq 0.001$, $\dagger\dagger\dagger\dagger\dagger P \leq 0.0001$.

demonstrated significant induction of GSIS at concentrations from 5–100 μM (Fig. 6B-D) except HA, which induced GSIS at 5–50 μM but not 100 μM). These data demonstrate that the metabolites increase GSIS at much lower (and physiologically relevant) concentrations compared to EC, suggesting that the metabolites are more potent stimulators of GSIS than native EC. This fact, combined with the greater bioavailability of microbial metabolites than the parent compound, point towards the potential contribution of microbial metabolites to the observed effects of dietary flavanoids.

To further investigate the effects of these compounds on INS-1832/13 β-cells, we examined the cellular insulin content under stimulatory conditions (16.7 mM glucose) to determine if treatment impacted insulin expression (Fig. 7). An increase in insulin content, concomitant with an increase in insulin secretion would indicate greater insulin expression, while a decrease in insulin content with no change in insulin secretion would indicate an impediment in insulin production. EC exhibited small increases in insulin content (Fig. 7A), but the effect was inconsistent across doses. Interestingly, increases in insulin content were vastly different across the metabolites (Fig. 7B-D), despite similarities observed in GSIS. 5PVA and HVA stimulated greater insulin content, particularly at lower doses. HA exhibited a slight increase in insulin content at 50 μM. These results are intriguing, as they suggest distinct mechanism at play that impinges on β-cell insulin secretion. The results for EC are consistent with our previous

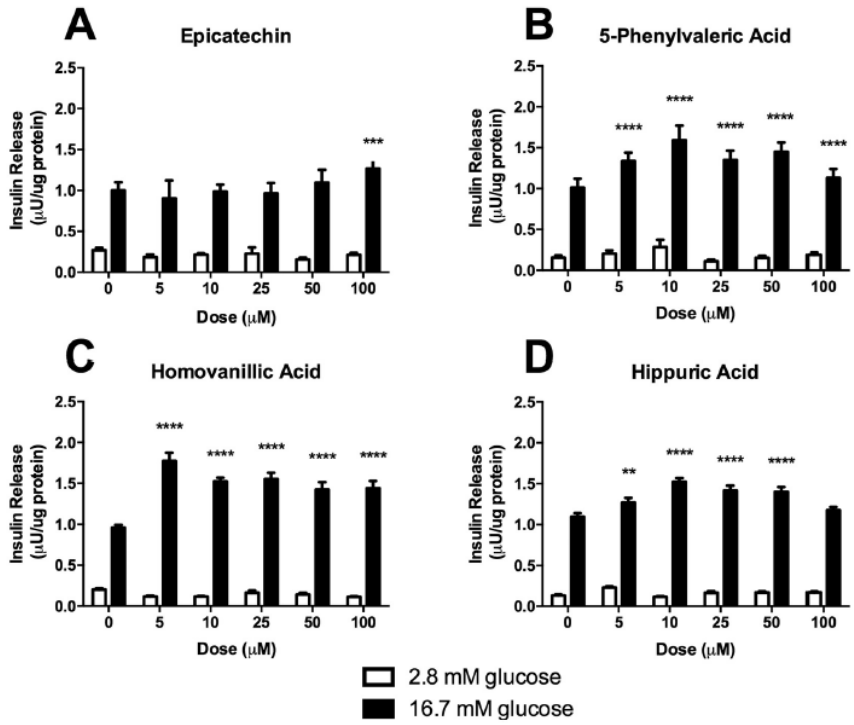

Fig. 6. Glucose-stimulated insulin secretion in INS-1 derived 832/13 rat β-cells treated with either hippuric acid, homovanillic acid, 5-phenylvaleric acid, or epicatechin. Values represent mean±S.E.M. from $n=6$ replicates. Data were analyzed by 2-way ANOVA. If a significant main effect of treatment compound dose was detected, Dunnett's post hoc test was performed within the high-glucose treatments to compare each dose to the untreated (0 μM) control. Significance vs. untreated control is indicated by: $^{*}P \le 0.05$, $^{**}P \le 0.01$, $^{***}P \le 0.001$, $^{****}P \le 0.0001$.

results demonstrating increased insulin secretion at high doses, without concurrent increase in insulin content [38]. For 5PVA and HVA we observed increased GSIS and increased cellular insulin content. The increased insulin content could be due to greater insulin gene expression, enhanced insulin processing, or improved insulin stability. As has been previously shown, increased cellular insulin content can be sufficient to enhance GSIS [48]. Therefore, the enhanced insulin secretion from β-cells treated with these metabolites, particularly at lower doses, may be due to an increased insulin load, rather than modulation of the β-cell glucose sensing machinery. The GSIS observed by HA occurs with minimal changes to insulin content. The data suggest that flavonoid microbial metabolites may exert significant effects on β-cell function by increasing both β-cell insulin production and insulin secretion. These distinct mechanisms suggest complementary and synergistic activities of various metabolites present simultaneously following flavonoid consumption, and thus warrant further investigation in vitro and in vivo.

3.2.2. β-Cell respiration

Given our previous data demonstrating enhanced β-cell mitochondrial respiration due to exposure to EC from cocoa [38,39], we sought to define the effect of culture in the presence of EC and microbial metabolites on β-cell mitochondrial respiration under basal conditions (low glucose) and glucose stimulation (Fig. 8). Basal respiration rate was significantly increased by 10 μM EC, and appeared to be somewhat reduced (albeit not statistically significantly) by 5 and 10 μM HA (Fig. 8C). The same results were also observed under glucose stimulation and maximal respiration (although the level of glucose induced respiration is surprisingly less than what has been observed in other studies) (Fig. 8D-E). None of the compounds tested significantly affected respiratory reserve (Fig. 8F). It is important to note that the low means and comparatively high S.E.M.'s for respiratory reserve in this case are indicative of the fact that these cells were essentially already operating near maximal respiration in the basal state (Fig. 8A-B, F). Note that uncoupling and ATP-dependent respiration were not plotted individually from these data due to differences in the question being asked between the β-cells (do these compounds enhance respiration as a means to improve β-cell function?) vs. the skeletal muscle cells (do these compounds enhance respiration *via* uncoupling as a means to improve energy expenditure, and do they protect from injury?). The finding that EC enhances respiration is consistent with our previous data [38,39]. Coupled with the GSIS data (Fig. 6), these respiration data suggest several novel findings. First, EC does not enhance GSIS except at extremely high doses despite enhancing β-cell respiration at lower doses. Second, HA enhances GSIS despite inhibition of β-cell respiration (although these reductions were not statistically significant, this trend appears to be of practical significance as suggested by Fig. 8C-E). Third, HVA and 5PVA enhance GSIS despite not affecting β-cell respiration. Thus, these data demonstrate that while each of the epicatechin metabolites enhances GSIS; their individual mechanisms do not all increase insulin release through modulating mitochondrial respiration. Therefore, the mechanisms by which these compounds exert their effects are likely distinct and thus warrant further investigation.

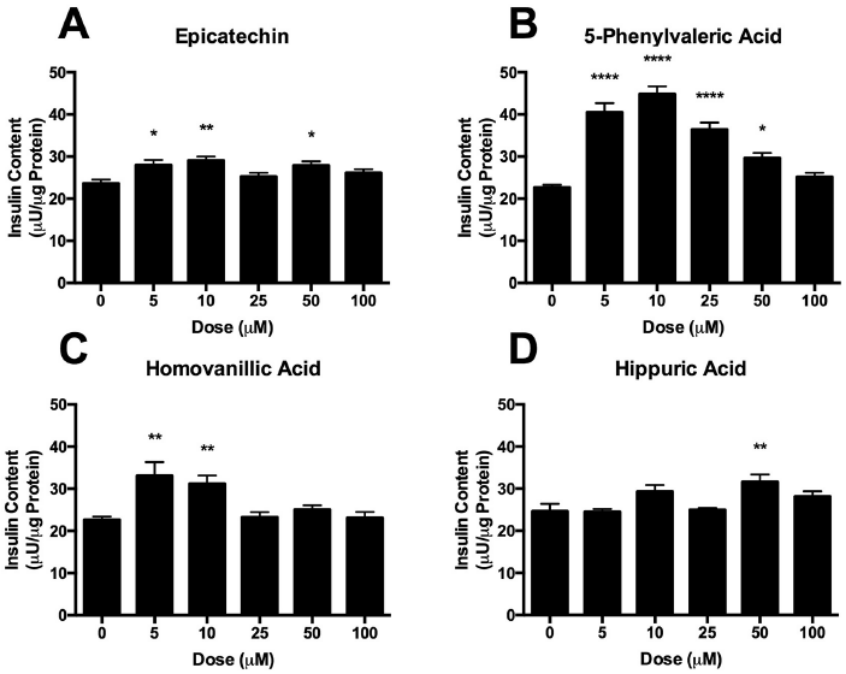

Fig. 7. Total insulin content of INS-1 derived 832/13 rat β-cells cultured in 16.7 mM glucose treated with either hippuric acid, homovanillic acid, 5-phenylvaleric acid, or epicatechin. Values represent mean±S.E.M. from $n=6$ replicates. Data were analyzed by one-way ANOVA. If a significant treatment effect was detected, Dunnett's post hoc test was performed to compare each dose to the untreated (0 μM) control. Significance vs. untreated control is indicated by: *$P \le 0.05$, **$P \le 0.01$, ***$P \le 0.001$, ****$P \le 0.0001$.

3.2.3. Expression of ETC components

To validate the changes that we observed in β-cell respiration after treatment with EC or the gut metabolites, we measured protein levels of select ETC components (Fig. 9). Similar to what was observed in our mitochondrial respiration studies, only treatment with EC changed protein levels of ETC components. These data validate our previous findings that while the metabolites do enhance glucose stimulated insulin secretion, it appears to be through extra mitochondrial modifications.

3.3. Discussion

The premise of this study was to explore the possibility that the unique activities of microbial flavonoid metabolites on peripheral tissues may contribute to the observed bioactivities of native dietary flavonoids. In other words, can dietary flavonoids exert significant bioactivities despite poor bioavailability, or is bioavailability of the native dietary species at peripheral target tissues indeed the primary limiting factor for bioactivity in vivo? Our central hypothesis, spanning this study and others in progress, is that the systemic, peripheral tissue activities of microbial metabolites may account for a significant portion of observed bioactivity following dietary flavonoid exposure in vivo.

The present results demonstrate the potent activities of flavonoid microbial metabolites, particularly for preservation of β-cell function, enhancement of skeletal muscle glucose utilization and protection of skeletal muscle respiratory function from oxidative injury, Therefore, these data suggest that further investigation of the anti-diabetic activities of flavonoid microbial metabolites is warranted. Additionally, our data suggest that metabolites and native compounds may act by distinct mechanisms, suggesting complementary and synergistic activities in vivo. Specifically, our data demonstrate that the gut metabolites enhance β-cell glucose stimulated insulin secretion more effectively than EC. Furthermore, unlike EC, these metabolites appear to do this without enhancing mitochondrial respiration or increasing expression of mitochondrial electron transport chain components, and with varying effects on β-cell insulin content. Insulin secretion is dependent on ATP production in the β-cell due to glycolysis, TCA cycle and the *ETC*. In addition, the increases in ATP closes K^+ channels which cause membrane depolarization and opening of Ca^{2+} channels which allow Ca^{2+} influx. The modulation of these two channels is an area of future interest in determining how the metabolites enhance glucose stimulated insulin secretion. In skeletal muscle, these compounds appear to enhance glucose utilization, but do not appear to enhance respiration under normal conditions. Therefore, mitochondrial uncoupling does not appear to be a mechanism by which these compounds can prevent obesity and glucose intolerance, with the exception of HA and 5PVA at high doses. However, they do appear to significantly protect respiratory function against oxidative injury. The objective of these respiration experiments was to evaluate the impacts of the selected compounds on overall respiration. Future mechanistic experiments, including use of ETC complex inhibitors as well as comparing intact cells, permeabilized cells and isolated mitochondria, will be useful to elucidate the specific mechanisms by which the microbial metabolites exert these effects on respiration. Future work will also provide new insight that address some of the current study

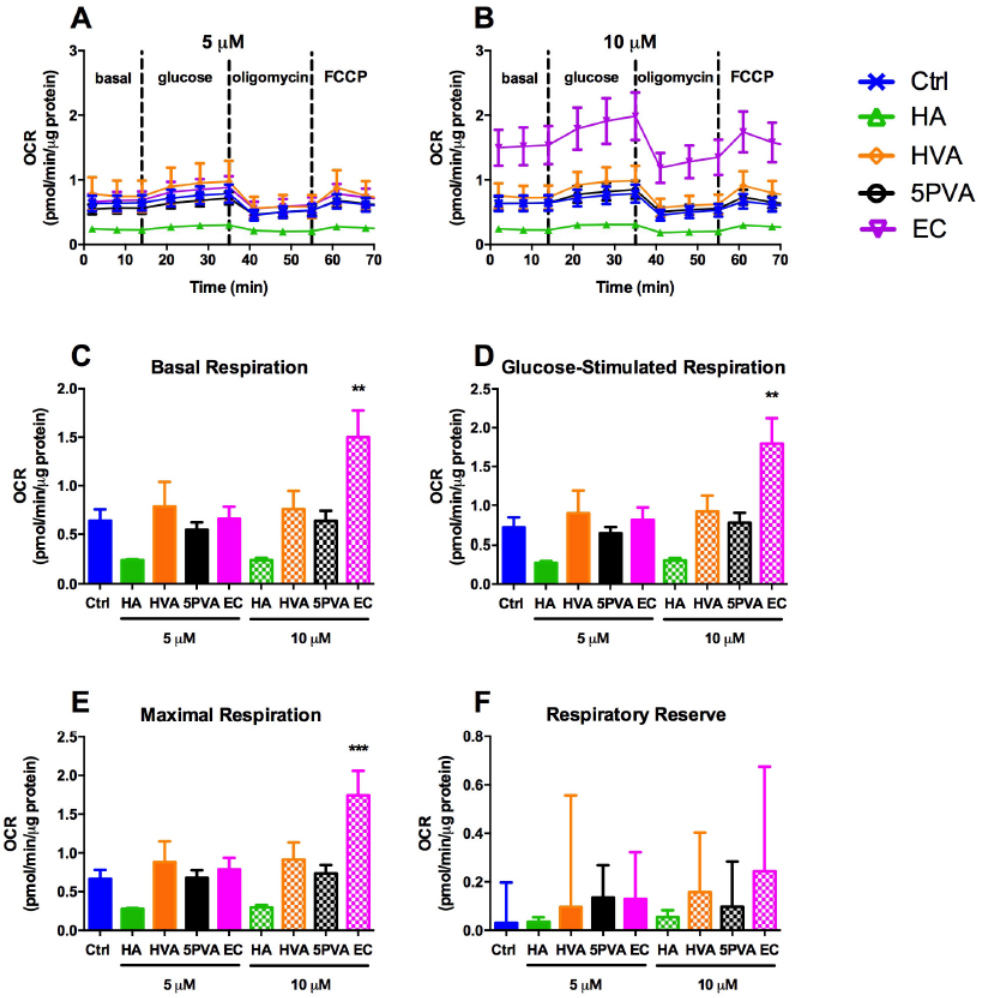

Fig. 8. Corrected mitochondrial respiration measured after culturing INS-1832/13 β-cells for 24 h in the presence of 0, 5 or 10 μM hippuric acid (HA), homovanillic acid (HVA), 5-phenylvaleric acid (5PVA), or epicatechin (EC): (**A**) 0 (Ctrl) and 5 μM, (**B**) 0 (Ctrl) and 10 μM, (**C**) Basal respiration (2 min), (**D**) glucose-stimulated respiration (21 min), (**E**) maximal respiration (61 min) and (**F**) respiratory reserve (maximal − basal). Oxygen consumption rate data were normalized by subtracting non-mitochondrial rates of respiration (after antimycin A, not shown), and are expressed as pmol O_2 per minute, normalizer per μg protein. Values represent mean±S.E.M. from $n=5$ replicates. Significance vs. untreated control is indicated by: $^{*}P \le 0.05$, $^{**}P \le 0.01$, $^{***}P \le 0.001$, $^{****}P \le 0.0001$.

limitations, such as examining compound efficacy in differentiated muscle myotubes from mouse and human (to compliment myoblast studies that were conducted herein).

The results presented here make significant additions to the small, yet growing, body of published data indicating that flavonoid microbial metabolites likely account for a significant fraction of many observed bioactivities of dietary flavonoids, particularly those with poor oral bioavailability of the native forms. These data help to explain epidemiological and experimental data suggesting that some dietary flavonoids (and potentially other classes of compounds, such as curcuminoids)possess potent bioactivities despite poor oral bioavailability. These results also suggest that the metabolites may be equally important to, if not more important than (in some cases), the native forms for in vitro mechanistic studies in cell culture models that attempt to recapitulate effects in peripheral tissues (hepatic, adipose, pancreatic, skeletal muscle, endothelial and other cell models). This is particularly true at compound doses in the mid to high μM range, which are commonly used for bioactives in cell culture but which are much more likely to be obtained by the microbial metabolites than the native dietary forms.

Moving forward, there is a need to further identify the most active individual metabolites (or metabolite profiles) that confer systemic benefits, to understand the characteristics of the microbiome that facilitate generation of these profiles, and to understand how inter-individual variability in microbial metabolism affects subsequent metabolite profiles and bioactivities [49]. This knowledge will be

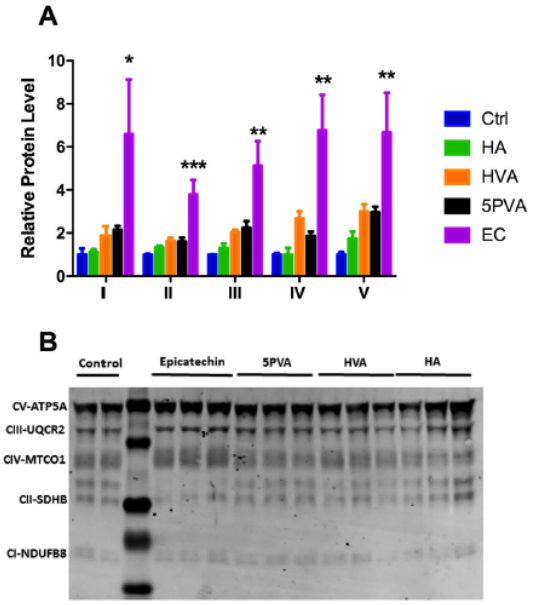

Fig. 9. (A) Expression levels of electron transport chain components ATP5A (Complex V), UQCR2 (Complex III), MTCO1 (Complex IV), SDHB (Complex II) and NDUFB8 (Complex I) as quantified by Western blotting. Values are presented as mean±S.E.M. from n=3 replicates per condition. Data were analyzed by one-way ANOVA. If a significant treatment effect was detected, Dunnett's post hoc test was performed to compare each dose to the untreated (0 μM) control. Significance vs. untreated control is indicated by: $^{*}P \le 0.05$, $^{**}P \le 0.01$, $^{***}P \le 0.001$, $^{****}P \le 0.0001$. (B) Representative Western blot.

critical for development of strategies to fully exploit the potential health benefits of dietary flavonoids. While initial studies have used antibiotics to eliminate the effect of the microbiome and microbiome-derived metabolites [30,31], germ-free and other gnotobiotic models will be instrumental in elucidation of the role of the microbiome in mediating the beneficial effects of poorly-bioavailable flavonoids. Furthermore, large-scale screening of several dozen (if not libraries of several hundred) microbial metabolites in peripheral tissue cell culture models will need to be performed in order to understand the tissue-specific mechanisms by which these compounds exert their activities. This will require advances in commercial availability of some metabolites, specifically the valerolactones, which to our knowledge are not currently available. It will also be important to conduct full dose-dependence studies of these metabolites. Furthermore, in vitro anaerobic fecal fermentations of flavonoids, with assessment of the bioactivity before and after fermentation in vitro and in vivo (*via* i.p. administration of filter-sterilized supernatants) will be useful to identify broad effects of microbial transformation.

It is important to note that we did not study valerolactones, which are among the early microbial metabolites of flavonoids. These compounds are present in high concentrations in circulation following flavonoid intake, and represent important compounds that may possess significant bioactivities. We did not study these compounds due to the lack of commercial availability, which is a significant obstacle for understanding their activities. Due to the provocative data in the present work, future work is needed to generate, isolate, and elucidate the activity of valerolactones. Two possible approaches include isolation from in vivo or ex vivo fecal fermentation mixtures, as well as synthetic approaches. These will need to be performed in order to complete our understanding of the potential bioactivities of flavonoid microbial metabolites.

It is also important to note that these microbial metabolites exist in circulation in the unconjugated forms studied, as well as Phase-II conjugates (sulfate, *O*-methyl and glucuronide forms) produced in enterocytes and hepatocytes following their absorption [50]. While the present work focused on the unconjugated forms, future work needs to be performed to elucidate the bioactivities of the conjugated forms. Such transformations can be performed using enterocytes, hepatocytes, liver microsomes, or isolated conjugating enzymes. Such studies will further advance the overall objective of the present work which is to understand the bioactivities of the actual circulating profile of compounds (unconjugated and phase-II conjugates of both native dietary flavonoids and their microbial metabolites) as opposed to just the native, unconjugated forms (*i.e.* the majority of existing studies).

4. Conclusion

In summary, our data demonstrate that flavonoid microbial metabolites stimulate β-cell function, as well as glucose utilization and mitochondrial respiration in skeletal muscle. These data support the hypothesis that dietary flavonoids may exert significant activity despite poor bioavailability *via* their microbial metabolites. This raises the intriguing prospect that bioavailability of native flavonoids may not be as critical of a limiting factor to bioactivity as previously thought. If, in fact, bioavailability of native flavonoids is not as crucial as currently thought, this would represent a paradigm shift in the thinking regarding how to exploit the activities of flavonoids in the diet. While development of strategies to enhance bioavailability of native compounds should not be discontinued, exploration of strategies that do not require bioavailability should receive extensive consideration as a parallel complementary approach to solving the same problem. Our overall logic for the proposed experiments moving forward is that we are quickly approaching an asymptote (diminishing novel returns) in terms of what we can learn from further studies focusing on the activities of native flavonoids. New approaches are now needed to answer the complex questions remaining.

Acknowledgement

Funding for this work was provided, in part, by the Virginia Agricultural Experiment Station and the Hatch Program of the National Institute of Food and Agriculture, U.S. Department of Agriculture (APN and DAB), American Diabetes Association (1-JF-05-24 to MWH), the National Institutes of Health-NIDDK (2RO1 DK-078765), R01 HL123647 to DAB), BYU mentoring environment grant (JST), BYU ORCA Grant (BFB), American Diabetes Association (1–17-IBS-101 to JST), and a grant from the Diabetes Action Research and Education Foundation (Grant #461 to JST).

Appendix A. Supplementary data

Supplementary data to this article can be found online at https://doi.org/10.1016/j.jnutbio.2018.09.004.

References

[1] Guo Y, Bruno RS. Endogenous and exogenous mediators of quercetin bioavailability. J Nutr Biochem 2015;26:201–10. https://doi.org/10.1016/j.jnutbio.2014.10.008.

[2] Wiese Stefanie, Esatbeyoglu Tuba, Winterhalter Peter, Kruse Hans-Peter, Winkler Stephanie, Bub Achim, et al. Comparative biokinetics and metabolism of pure monomeric, dimeric, and polymeric flavan-3-ols: a randomized cross-over study in humans. Mol Nutr Food Res 2015;59:610–21. https://doi.org/10.1002/mnfr.201400422.

[3] Mulder TPJ, van Platerink CJ, Wijnand Schuyl PJ, van Amelsvoort JMM. Analysis of theaflavins in biological fluids using liquid chromatography–electrospray mass spectrometry. J Chromatogr B Biomed Sci Appl 2001;760:271–9. https://doi.org/10.1016/S0378-4347(01)00285-7.
[4] González-Sarrías A, Espín JC, Tomás-Barberán FA. Non-extractable polyphenols produce gut microbiota metabolites that persist in circulation and show anti-inflammatory and free radical-scavenging effects. Trends Food Sci Technol 2017;69:281–8. https://doi.org/10.1016/j.tifs.2017.07.010.
[5] Ulaszewska MM, Trost K, Stanstrup J, Tuohy KM, Franceschi P, Chong MF-F, et al. Urinary metabolomic profiling to identify biomarkers of a flavonoid-rich and flavonoid-poor fruits and vegetables diet in adults: the FLAVURS trial. Metabolomics 2016;12:32. https://doi.org/10.1007/s11306-015-0935-z.
[6] Mulder TP, Rietveld AG, van Amelsvoort JM. Consumption of both black tea and green tea results in an increase in the excretion of hippuric acid into urine. Am J Clin Nutr 2005;81:256S–60S.
[7] Pereira-Caro G, Moreno-Rojas JM, Brindani N, Del Rio D, Lean MEJ, Hara Y, et al. Bioavailability of black tea Theaflavins: absorption, metabolism, and colonic catabolism. J Agric Food Chem 2017;65:5365–74. https://doi.org/10.1021/acs.jafc.7b01707.
[8] Chen H, Hayek S, Guzman JR, Gillitt ND, Ibrahim SA, Jobin C, et al. The microbiota is essential for the generation of black tea Theaflavins-derived metabolites. PLoS One 2012;7:e51001. https://doi.org/10.1371/journal.pone.0051001.
[9] Goodrich KM, Smithson AT, Ickes AK, Neilson AP. Pan-colonic pharmacokinetics of catechins and procyanidins in male Sprague–Dawley rats. J Nutr Biochem 2015;26:1007–14.
[10] Lin W, Wang W, Yang H, Wang D, Ling W. Influence of intestinal microbiota on the catabolism of flavonoids in mice. J Food Sci 2018;263:111–7. https://doi.org/10.1111/1750-3841.13544.
[11] Serra A, Macià A, Romero M-P, Reguant J, Ortega N, Motilva M-J. Metabolic pathways of the colonic metabolism of flavonoids (flavonols, flavones and flavanones) and phenolic acids. Food Chem 2012;130:383–93. https://doi.org/10.1016/j.foodchem.2011.07.055.
[12] Castello F, Costabile G, Bresciani L, Tassotti M, Naviglio D, Luongo D, et al. Bioavailability and pharmacokinetic profile of grape pomace phenolic compounds in humans. Arch Biochem Biophys 2018;646:1–9. https://doi.org/10.1016/j.abb.2018.03.021.
[13] Henning Susanne M, Wang Piwen, Abgaryan Narine, Vicinanza Roberto, de Oliveira Daniela Moura, Zhang Yanjun, et al. Phenolic acid concentrations in plasma and urine from men consuming green or black tea and potential chemopreventive properties for colon cancer. Mol Nutr Food Res 2013;57:483–93. https://doi.org/10.1002/mnfr.201200646.
[14] Scholl C, Lepper A, Lehr T, Hanke N, Schneider KL, Brockmöller J, et al. Population nutrikinetics of green tea extract. PLoS One 2018;13:e0193074. https://doi.org/10.1371/journal.pone.0193074.
[15] Clifford MN, Hooft VD, Jj J, Crozier A. Human studies on the absorption, distribution, metabolism, and excretion of tea polyphenols. Am J Clin Nutr 2013;98:1619S–30S. https://doi.org/10.3945/ajcn.113.058958.
[16] Kawser Hossain M, Abdal Dayem A, Han J, Yin Y, Kim K, Kumar Saha S, et al. Molecular mechanisms of the anti-obesity and anti-diabetic properties of flavonoids. Int J Mol Sci 2016;17:569. https://doi.org/10.3390/ijms17040569.
[17] Amiot MJ, Riva C, Vinet A. Effects of dietary polyphenols on metabolic syndrome features in humans: a systematic review. Obes Rev 2016;17:573–86. https://doi.org/10.1111/obr.12409.
[18] Gu Y, Hurst WJ, Stuart DA, Lambert JD. Inhibition of key digestive enzymes by cocoa extracts and Procyanidins. J Agric Food Chem 2011;59:5305–11. https://doi.org/10.1021/jf200180n.
[19] Ryan CM, Khoo W, Ye L, Lambert JD, O'Keefe SF, Neilson AP. Loss of native flavanols during fermentation and roasting does not necessarily reduce digestive enzyme-inhibiting bioactivities of cocoa. J Agric Food Chem 2016;64:3616–25. https://doi.org/10.1021/acs.jafc.6b01725.
[20] Bitzer ZT, Glisan SL, Dorenkott MR, Goodrich KM, Ye L, O'Keefe SF, et al. Cocoa procyanidins with different degrees of polymerization possess distinct activities in models of colonic inflammation. J Nutr Biochem 2015. https://doi.org/10.1016/j.jnutbio.2015.02.007.
[21] Masumoto S, Terao A, Yamamoto Y, Mukai T, Miura T, Shoji T. Non-absorbable apple procyanidins prevent obesity associated with gut microbial and metabolomic changes. Sci Rep 2016;6:31208. https://doi.org/10.1038/srep31208.
[22] Dorenkott MR, Griffin LE, Goodrich KM, Thompson-Witrick KA, Fundaro G, Ye L, et al. Oligomeric cocoa procyanidins possess enhanced bioactivity compared to monomeric and polymeric cocoa procyanidins for preventing the development of obesity, insulin resistance, and impaired glucose tolerance during high-fat feeding. J Agric Food Chem 2014;62:2216–27.
[23] Larrosa M, Luceri C, Vivoli E, Pagliuca C, Lodovici M, Moneti G, et al. Polyphenol metabolites from colonic microbiota exert anti-inflammatory activity on different inflammation models. Mol Nutr Food Res 2009;53:1044–54. https://doi.org/10.1002/mnfr.200800446.
[24] Qian Y, Babu PVA, Symons JD, Jalili T. Metabolites of flavonoid compounds preserve indices of endothelial cell nitric oxide bioavailability under glucotoxic conditions. Nutr Diabetes 2017;7:e286. https://doi.org/10.1038/nutd.2017.34.
[25] Ho GTT, Kase ET, Wangensteen H, Barsett H. Phenolic elderberry extracts, anthocyanins, Procyanidins, and metabolites influence glucose and fatty acid uptake in human skeletal muscle cells. J Agric Food Chem 2017;65:2677–85. https://doi.org/10.1021/acs.jafc.6b05582.
[26] Carrasco-Pozo C, Gotteland M, Castillo RL, Chen C. 3,4-dihydroxyphenylacetic acid, a microbiota-derived metabolite of quercetin, protects against pancreatic β-cells dysfunction induced by high cholesterol. Exp Cell Res 2015;334:270–82. https://doi.org/10.1016/j.yexcr.2015.03.021.
[27] Fernández-Millán E, Ramos S, Alvarez C, Bravo L, Goya L, Martín MÁ. Microbial phenolic metabolites improve glucose-stimulated insulin secretion and protect pancreatic beta cells against tert-butyl hydroperoxide-induced toxicity via ERKs and PKC pathways. Food Chem Toxicol 2014;66:245–53. https://doi.org/10.1016/j.fct.2014.01.044.
[28] Xue H, Xie W, Jiang Z, Wang M, Wang J, Zhao H, et al. 3,4-Dihydroxyphenylacetic acid, a microbiota-derived metabolite of quercetin, attenuates acetaminophen (APAP)-induced liver injury through activation of Nrf-2. Xenobiotica 2016;46:931–9. https://doi.org/10.3109/00498254.2016.1140847.
[29] Lee CC, Kim JH, Kim JS, Oh YS, Han SM, Park JHY, et al. 5-(3′,4′-Dihydroxyphenyl-γ-valerolactone), a major microbial metabolite of Proanthocyanidin, attenuates THP-1 monocyte-endothelial adhesion. Int J Mol Sci 2017;18:1363. https://doi.org/10.3390/ijms18071363.
[30] Liu Wen, Zhao Shaoqian, Wang Jiqiu, Shi Juan, Sun Yingkai, Wang Weiqing, et al. Grape seed proanthocyanidin extract ameliorates inflammation and adiposity by modulating gut microbiota in high-fat diet mice. Mol Nutr Food Res 2017;61:1601082. https://doi.org/10.1002/mnfr.201601082.
[31] Esposito D, Damsud T, Wilson M, Grace MH, Strauch R, Li X, et al. Black currant anthocyanins attenuate weight gain and improve glucose metabolism in diet-induced obese mice with intact, but not disrupted, gut microbiome. J Agric Food Chem 2015;63:6172–80. https://doi.org/10.1021/acs.jafc.5b00963.
[32] Brown EM, McDougall GJ, Stewart D, Pereira-Caro G, González-Barrio R, Allsopp P, et al. Persistence of anticancer activity in berry extracts after simulated gastrointestinal digestion and colonic fermentation. PLoS One 2012;7:e49740. https://doi.org/10.1371/journal.pone.0049740.
[33] Kim D-H, Jung E-A, Sohng I-S, Han J-A, Kim T-H, Han MJ. Intestinal bacterial metabolism of flavonoids and its relation to some biological activities. Arch Pharm Res 1998;21:17–23. https://doi.org/10.1007/BF03216747.
[34] van der Pijl PC, Foltz M, Glube ND, Peters S, Duchateau G. Pharmacokinetics of black tea-derived phenolic acids in plasma. J Funct Foods 2015;17:667–75. https://doi.org/10.1016/j.jff.2015.06.020.
[35] Frisard MI, McMillan RP, Marchand J, Wahlberg KA, Wu Y, Voelker KA, et al. Toll-like receptor 4 modulates skeletal muscle substrate metabolism. Am J Physiol Endocrinol Metab 2010;298:E988–98. https://doi.org/10.1152/ajpendo.00307.2009.
[36] Anderson AS, Roberts PC, Frisard MI, McMillan RP, Brown TJ, Lawless MH, et al. Metabolic changes during ovarian cancer progression as targets for sphingosine treatment. Exp Cell Res 2013;319:1431–42. https://doi.org/10.1016/j.yexcr.2013.02.017.
[37] Dai W, Cheung E, Alleman RJ, Perry JB, Allen ME, Brown DA, et al. Cardioprotective effects of mitochondria-targeted peptide SBT-20 in two different models of rat ischemia/reperfusion. Cardiovasc Drugs Ther 2016;30:559–66. https://doi.org/10.1007/s10557-016-6695-9.
[38] Rowley TJ, Bitner BF, Ray JD, Lathen DR, Smithson AT, Dallon BW, et al. Monomeric cocoa catechins enhance β-cell function by increasing mitochondrial respiration. J Nutr Biochem 2017;49:30–41. https://doi.org/10.1016/j.jnutbio.2017.07.015.
[39] Kener KB, Munk DJ, Hancock CR, Tessem JS. High-resolution respirometry to measure mitochondrial function of intact Beta cells in the presence of natural compounds. J Vis Exp 2018. https://doi.org/10.3791/57053.
[40] Hobson A, Draney C, Stratford A, Becker TC, Lu D, Arlotto M, et al. Aurora kinase A is critical for the Nkx6.1 mediated β-cell proliferation pathway. Islets 2015;7:e1027854. https://doi.org/10.1080/19382014.2015.1027854.
[41] Tessem JS, Moss LG, Chao LC, Arlotto M, Lu D, Jensen MV, et al. Nkx6.1 regulates islet β-cell proliferation via Nr4a1 and Nr4a3 nuclear receptors. Proc Natl Acad Sci 2014;111:5242–7. https://doi.org/10.1073/pnas.1320953111.
[42] Draney C, Hobson AE, Grover SG, Jack BO, Tessem JS. Cdk5r1 overexpression induces primary β-cell proliferation. J Diabetes Res 2016. https://doi.org/10.1155/2016/6375804.
[43] Reynolds MS, Hancock CR, Ray JD, Kener KB, Draney C, Garland K, et al. β-Cell deletion of Nr4a1 and Nr4a3 nuclear receptors impedes mitochondrial respiration and insulin secretion. Am J Physiol Endocrinol Metab 2016;311:E186–201. https://doi.org/10.1152/ajpendo.00022.2016.
[44] Ray Jason D, Kener Kyle B, Bitner Benjamin F, Wright Brent J, Ballard Matthew S, Barrett Emily J, et al. Nkx6.1-mediated insulin secretion and β-cell proliferation is dependent on upregulation of c-Fos. FEBS Lett 2016;590:1791–803. https://doi.org/10.1002/1873-3468.12208.
[45] Anderson EJ, Lustig ME, Boyle KE, Woodlief TL, Kane DA, Lin C-T, et al. Mitochondrial H2O2 emission and cellular redox state link excess fat intake to insulin resistance in both rodents and humans. J Clin Invest 2009;119:573–81. https://doi.org/10.1172/JCI37048.
[46] Owen MR, Doran E, Halestrap AP. Evidence that metformin exerts its anti-diabetic effects through inhibition of complex 1 of the mitochondrial respiratory chain. Biochem J 2000;348(Pt 3):607–14.
[47] Childress ES, Alexopoulos SJ, Hoehn KL, Santos WL. Small molecule mitochondrial Uncouplers and their therapeutic potential. J Med Chem 2017. https://doi.org/10.1021/acs.jmedchem.7b01182.
[48] García-Ocaña A, Vasavada RC, Cebrian A, Reddy V, Takane KK, López-Talavera J-C, et al. Transgenic overexpression of hepatocyte growth factor in the β-cell

markedly improves islet function and islet transplant outcomes in mice. Diabetes 2001;50:2752–62. https://doi.org/10.2337/diabetes.50.12.2752.
[49] Bolca S, Van de Wiele T, Possemiers S. Gut metabotypes govern health effects of dietary polyphenols. Curr Opin Biotechnol 2013;24:220–5. https://doi.org/10.1016/j.copbio.2012.09.009.
[50] Feliciano RP, Mills CE, Istas G, Heiss C, Rodriguez-Mateos A. Absorption, metabolism and excretion of cranberry (poly)phenols in humans: a dose response study and assessment of inter-individual variability. Nutrients 2017;9. https://doi.org/10.3390/nu9030268.

APPENDIX B: PUBLICATIONS AND PRESENTATIONS

8.1 Publications

Bitner, B. F., Ray, J. D., Kener, K. B., Herring, J. A., **Tueller, J. A.,** Johnson, D. K., . . . Neilson, A. P. (2018). "Common gut microbial metabolites of dietary flavonoids exert potent protective activities in β-cells and skeletal muscle cells." *Journal of Nutritional Biochemistry.* doi://doi.org/10.1016/j.jnutbio.2018.09.004

Sharma, R., Berg, J. A., Beatty, N. J., Choi, M. C., Cowger, A. E., Cozzens, B.…**Tueller, J.A.** … Grose, J. H. (2018). "Genome Sequences of Nine Erwinia amylovora Bacteriophages." *Microbiology resource announcements*, 7(14), e00944-18. doi:10.1128/MRA.00944-18

8.1.1 Publications under review

Johnston, J.D., Cowger, A.E., Graul, R.J, Nash, R., **Tueller, J.A.**, Hendrickson, N., Robinson, D.R., Beard, J.D., Weber, K.S. "Associations between evaporative cooling and dust mite allergens, endotoxins, and β-(1→3)-D-glucans in house dust: A study of low-income homes." Indoor Air. Submitted June 2019

Tueller, J.A., Whitley, K.W., Weber, K.S. "A full semester flow cytometry course increase student confidence." Biochemistry and Molecular Biology Education. Submitted May 2019.

8.2 Presentations

Poster Presentation. "A full semester flow cytometry course." American Society of Microbiology Intermountain Branch Meeting, Provo, UT, 13 April 2019.

Panel Participant. "How to be the Best TA Possible." College of Physical and Mathematical Sciences Conference, Provo, UT, 31 August 2018.

Oral Presentation, "Personal microbiome analysis enhances student engagement in introductory and senior level life sciences courses," American Society of Microbiology Tri-branch Meeting, Durango, CO, 6 April 2018.

Oral & Poster Presentation. "Generation and metabolic characterization of TK-1 specific 2nd and 3rd generation CAR vectors," Autumn Immunology Conference, Chicago, IL, 17 November 2017.

Poster Presentation. "Generation and metabolic characterization of TK-1 specific 2nd and 3rd generation CAR vectors" Utah Conference for Undergraduate Research, Orem, UT, 17 February 2017.

8.3 Honors and awards

Simmons Center for Cancer Research Summer Grant 2019

Garth L. Lee Science Teaching Award 2018

Teaching Enhancement Grant 2018

Authored grant to improve flow cytometry course at BYU, $7000 awarded

Phi Kappa Phi Graduate Studies Award 2018

REFERENCES

1. Punt, J., et al., *Kuby Immunology*. 8 ed. 2019: Macmillan.
2. Haron, J., *Flow Cytometry and Cell Sorting: A Practical Guide*. Vol. 3. 2013.
3. Stoyan, T., et al., *Teaching Basic Immunology Using Flow Cytometry.* The FASEB Journal, Across Societies, 2008. **22**(1).
4. Phillips, T.L. and K.K. Fu, *Quantification of combind radiation therapy and chemotherapy effects on critical normal tissues.* Cancer, 1976. **37**: p. 1186-1200.
5. Couzin-Frankel, J., *Cancer Immunotherapy: Breakthrough of the year.* Science, 2013. **342**(6165): p. 1432-1433.
6. Gilham, D.E., et al., *CAR-T cells and solid tumors: tuning T cells to challenge an inveterate foe.* Trends Mol Med, 2012. **18**(7): p. 377-84.
7. Maude, S.L., et al., *Chimeric antigen receptor T cells for sustained remissions in leukemia.* N Engl J Med, 2014. **371**(16): p. 1507-17.
8. Grupp, S.A., et al., *Chimeric antigen receptor-modified T cells for acute lymphoid leukemia.* N Engl J Med, 2013. **368**(16): p. 1509-1518.
9. Porter, D.L., et al., *Chimeric antigen receptor-modified T cells in chronic lymphoid leukemia.* N Engl J Med, 2011. **365**(8): p. 725-33.
10. Irving, M., et al., *Engineering Chimeric Antigen Receptor T-Cells for Racing in Solid Tumors: Don't Forget the Fuel.* Front Immunol, 2017. **8**: p. 267.
11. Chang, C.H., et al., *Metabolic Competition in the Tumor Microenvironment Is a Driver of Cancer Progression.* Cell, 2015. **162**(6): p. 1229-41.
12. Pearce, E.L. and E.J. Pearce, *Metabolic pathways in immune cell activation and quiescence.* Immunity, 2013. **38**(4): p. 633-43.
13. Sukumar, M., R. Roychoudhuri, and N.P. Restifo, *Nutrient Competition: A New Axis of Tumor Immunosuppression.* Cell, 2015. **162**(6): p. 1206-8.
14. Ruella, M., et al., *Overcoming the Immunosuppressive Tumor Microenvironment of Hodgkin Lymphoma Using Chimeric Antigen Receptor T Cells.* Cancer Discov, 2017. **7**(10): p. 1154-1167.
15. Leach, D.R., M.F. Krummel, and J.P. Allison, *Enhancement of Antitumor Immunity by CTLA-4 Blockade.* Science, 1996. **271**: p. 1734-1736.
16. Pardoll, D.M., *The blockade of immune checkpoints in cancer immunotherapy.* Nat Rev Cancer, 2012. **12**(4): p. 252-64.
17. Le, D.T., et al., *PD-1 Blockade in Tumors with Mismatch-Repair Deficiency.* N Engl J Med, 2015. **372**(26): p. 2509-20.
18. Tumeh, P.C., et al., *PD-1 blockade induces responses by inhibiting adaptive immune resistance.* Nature, 2014. **515**(7528): p. 568-71.
19. Parry, R.V., et al., *CTLA-4 and PD-1 receptors inhibit T-cell activation by distinct mechanisms.* Mol Cell Biol, 2005. **25**(21): p. 9543-53.
20. Watanabe, N., et al., *BTLA is a lymphocyte inhibitory receptor with similarities to CTLA-4 and PD-1.* Nat Immunol, 2003. **4**(7).
21. Weber, K.S., et al., *Distinct CD4+ helper T cells involved in primary and secondary responses to infection.* Proc Natl Acad Sci U S A, 2012. **109**(24): p. 9511-6.
22. Pena-Rossi, C., et al., *Negative Regulation of CD4 Lineage Development and Responses by CD5.* The Journal of Immunology, 1999(163): p. 6494-6501.
23. Freitas, C.M.T., D.K. Johnson, and K.S. Weber, *T Cell Calcium Signaling Regulation by the Co-Receptor CD5.* Int J Mol Sci, 2018. **19**(5).

24. Braun-Fahrlander, C., et al., *Environmental exposure to endotoxin and its relation to asthma in school-age children.* N Engl J Med, 2002. **347**(12): p. 869-77.
25. Litonjua, A.A., et al., *Race, socioeconomic factors, and area of residence are associated with asthma prevalence.* Pediatric Pulmonology, 1999. **28**(6): p. 394-401.
26. Sneller, M.R. and J.L. Pinnas, *Comparison of Airborne Fungi in Evaporative Cooled and Air-Conditioned Homes.* Annals of Allergy, 1987. **59**(4): p. 317-320.
27. Watt, J., *Evaporative air conditioning handbook*. 2012: Springer Science & Business Media.
28. Shapiro, H., *Practical Flow Cytometry*. 1985, Wiley Online.
29. Shapiro, H., *Practical Flow Cytometry : A Guide*. Vol. 4th edition. 2003, Hoboken, NJ.: Wiley.
30. Adan, A., et al., *Flow cytometry: basic principles and applications.* Crit Rev Biotechnol, 2017. **37**(2): p. 163-176.
31. Givans, A., *Flow Cytometry: An Introduction.* Methods in Molecular Biology, 2017. **699**.
32. Fleisher, T. and J.B. Oliveira, *Flow Cytometry*, in *Clinical Immunology (Principles and Practices)*. 2018, Elsevier.
33. Lee, J.A., et al., *MIFlowCyt: The minimum information about a flow cytometry experiment.* Cytometry Part A, 2008. **73A**(10): p. 926-930.
34. Weber, L.M. and M.D. Robinson, *Comparison of clustering methods for high-dimensional single-cell flow and mass cytometry data.* Cytometry Part A, 2016. **89**(12): p. 1084-1096.
35. Ugalmugale, S. and R. Swain, *Biotechnology Market Size By Application (Biopharmacy, Bioservices, Bioagriculture, Bioindustrial, Bioinformatics), By Technology (Fermentation, Tissue Engineering and Regeneration, PCR Technology, Nanobiotechnology, Chromatography, DNA Sequencing, Cell Based Assay), Industry Analysis Report, Regional Outlook (U.S., Canada, Germany, UK, France, Italy, Spain, Russia, China, Japan, India, South Korea, Brazil, Mexico, Argentina, Saudi Arabia, South Africa, UAE), Application Potential, Competitive Market Share & Forecast, 2018 – 2024*, in *Global Market Insights*. 2019, Global Market Insights: Delaware.
36. Fuller, K., et al., *An active, collaborative approach to learning skills in flow cytometry.* Adv Physiol Educ, 2016. **40**(2): p. 176-85.
37. Boothby, J.T., et al., *Teaching Phagocytosis Using Flow Cytometry.* Microbiology Education, 2004. **5**.
38. Forget, N., et al., *Teaching the microbial growth curve concept using microalgal cultures and flow cytometry.* Journal of Biological Education, 2010. **44**(4).
39. Ott, L.E. and S. Carson, *Immunological tools: engaging students in the use and analysis of flow cytometry and enzyme-linked immunosorbent assay (ELISA).* Biochem Mol Biol Educ, 2014. **42**(5): p. 382-97.
40. Lewis, J.R., et al., *Biotechnology apprenticeship for secondary-level students: teaching advanced cell culture techniques for research.* Cell Biol Educ, 2002. **1**(1): p. 26-42.
41. American Association for the Advancement of Science. *Vision and Change in Undergraduate Biology Education: a Call to Action*. 2016 [cited 2019 1 May 2019].
42. Handelsman, J., et al., *Scientific Teaching.* Science, 2004. **304**(April 2004): p. 521-522.
43. Rice, J.W., S.M. Thomas, and P. O'Toole, *Tertiary science education in the 21st century.* Australian Learning & Teaching Council, 2009.

44. Weber, K.S., J.L. Jensen, and S.M. Johnson, *Anticipation of Personal Genomics Data Enhances Interest and Learning Environment in Genomics and Molecular Biology Undergraduate Courses.* PLoS One, 2015. **10**(8): p. e0133486.
45. Salari, K., et al., *Evidence that personal genome testing enhances student learning in a course on genomics and personalized medicine.* PLoS One, 2013. **8**(7): p. e68853.
46. Meisel, S.F., et al., *Explaining, not just predicting, drives interest in personal genomics.* Genome Med, 2015. **7**(1): p. 74.
47. Bupp, M.G., *Flow Cytometry in Undergraduate Education [webinar]*. 2014.
48. Singer, S.R., N.R. Nielsen, and H.A. Schweingruber, *Biology education research: lessons and future directions.* CBE life sciences education, 2013. **12**(2): p. 129-132.
49. Wood, W.B., *Innovations in Teaching Undergraduate Biology and Why We Need Them.* Annual Review of Cell and Developmental Biology, 2009. **25**(1): p. 93-112.
50. Hoskins, S.G., D. Lopatto, and L.M. Stevens, *The C.R.E.A.T.E. Approach to Primary Literature Shifts Undergraduates' Self-Assessed Ability to Read and Analyze Journal Articles, Attitudes about Science, and Epistemological Beliefs.* CBE Life Sci Educ, 2011. **10**(Winter 2011): p. 368-378.
51. White, H.B., et al., *What Skills Should Students of Undergraduate Biochemistry and Molecular Biology Programs Have Upon Graduation?* Biochem Mol Biol Educ, 2013.
52. Rosenberg, S.A., M.E. Dudley, and N.P. Restifo, *Cancer immunotherapy.* N Engl J Med, 2008. **359**(10): p. 1072.
53. Rosenberg, S.A., J.C. Yang, and N.P. Restifo, *Cancer immunotherapy: moving beyond current vaccines.* Nat Med, 2004. **10**(9): p. 909-15.
54. Muranski, P. and N.P. Restifo, *Adoptive immunotherapy of cancer using CD4(+) T cells.* Curr Opin Immunol, 2009. **21**(2): p. 200-8.
55. Barrett, D.M., et al., *Chimeric antigen receptor therapy for cancer.* Annu Rev Med, 2014. **65**: p. 333-47.
56. Overwijk, W.W. and N.P. Restifo, *Autoimmunity and the immunotherapy of cancer: targeting the "self" to destroy the "other".* Crit Rev Immunol, 2000. **20**(6): p. 433-50.
57. Zhao, Y., et al., *Multiple injections of electroporated autologous T cells expressing a chimeric antigen receptor mediate regression of human disseminated tumor.* Cancer Res, 2010. **70**(22): p. 9053-61.
58. Gattinoni, L., Y. Ji, and N.P. Restifo, *Wnt/beta-catenin signaling in T-cell immunity and cancer immunotherapy.* Clin Cancer Res, 2010. **16**(19): p. 4695-701.
59. Gubser, P.M., et al., *Rapid effector function of memory CD8+ T cells requires an immediate-early glycolytic switch.* Nat Immunol, 2013. **14**(10): p. 1064-72.
60. Klein Geltink, R.I., et al., *Mitochondrial Priming by CD28.* Cell, 2017. **171**(2): p. 385-397 e11.
61. Menk, A.V., et al., *4-1BB costimulation induces T cell mitochondrial function and biogenesis enabling cancer immunotherapeutic responses.* J Exp Med, 2018. **215**(4): p. 1091-1100.
62. Gattinoni, L., et al., *Adoptive immunotherapy for cancer: building on success.* Nat Rev Immunol, 2006. **6**(5): p. 383-93.
63. Abate-Daga, D. and M.L. Davila, *CAR models: next-generation CAR modifications for enhanced T-cell function.* Mol Ther Oncolytics, 2016. **3**: p. 16014.

64. Zhong, X.S., et al., *Chimeric antigen receptors combining 4-1BB and CD28 signaling domains augment PI3kinase/AKT/Bcl-XL activation and CD8+ T cell-mediated tumor eradication.* Mol Ther, 2010. **18**(2): p. 413-20.
65. Ritchie, D.S., et al., *Persistence and efficacy of second generation CAR T cell against the LeY antigen in acute myeloid leukemia.* Mol Ther, 2013. **21**(11): p. 2122-9.
66. Gill, S., et al., *Preclinical targeting of human acute myeloid leukemia and myeloablation using chimeric antigen receptor-modified T cells.* Blood, 2014. **123**(15): p. 2343-54.
67. Gill, S. and C.H. June, *Going viral: chimeric antigen receptor T-cell therapy for hematological malignancies.* Immunol Rev, 2015. **263**(1): p. 68-89.
68. Porter, D.L., et al., *Chimeric antigen receptor T cells persist and induce sustained remissions in relapsed refractory chronic lymphocytic leukemia.* Sci Transl Med, 2015. **7**(303): p. 303ra139.
69. Ruella, M. and C.H. June, *Chimeric Antigen Receptor T cells for B Cell Neoplasms: Choose the Right CAR for You.* Curr Hematol Malig Rep, 2016. **11**(5): p. 368-84.
70. Moon, E.K., et al., *Multifactorial T-cell hypofunction that is reversible can limit the efficacy of chimeric antigen receptor-transduced human T cells in solid tumors.* Clin Cancer Res, 2014. **20**(16): p. 4262-73.
71. Zhao, Z., et al., *Structural Design of Engineered Costimulation Determines Tumor Rejection Kinetics and Persistence of CAR T Cells.* Cancer Cell, 2015. **28**(4): p. 415-428.
72. Vander Heiden, M.G., L.C. Cantley, and C.B. Thompson, *Understanding the Warburg Effect: The Metabolic Requirements of Cell Proliferation.* Science, 2009. **324**(5930): p. 1029-1033.
73. Ho, P.C., et al., *Phosphoenolpyruvate Is a Metabolic Checkpoint of Anti-tumor T Cell Responses.* Cell, 2015. **162**(6): p. 1217-28.
74. O'Neill, L.A., R.J. Kishton, and J. Rathmell, *A guide to immunometabolism for immunologists.* Nat Rev Immunol, 2016. **16**(9): p. 553-65.
75. Scharping, N.E., et al., *The Tumor Microenvironment Represses T Cell Mitochondrial Biogenesis to Drive Intratumoral T Cell Metabolic Insufficiency and Dysfunction.* Immunity, 2016. **45**(2): p. 374-88.
76. Chong, E.A., et al., *PD-1 blockade modulates chimeric antigen receptor (CAR)-modified T cells: refueling the CAR.* Blood, 2017. **129**(8): p. 1039-1041.
77. Kawalekar, O.U., et al., *Distinct Signaling of Coreceptors Regulates Specific Metabolism Pathways and Impacts Memory Development in CAR T Cells.* Immunity, 2016. **44**(2): p. 380-90.
78. Luengo, A., D.Y. Gui, and M.G. Vander Heiden, *Targeting Metabolism for Cancer Therapy.* Cell Chem Biol, 2017. **24**(9): p. 1161-1180.
79. Buck, M.D., et al., *Metabolic Instruction of Immunity.* Cell, 2017. **169**(4): p. 570-586.
80. Sugiura, A. and J.C. Rathmell, *Metabolic Barriers to T Cell Function in Tumors.* J Immunol, 2018. **200**(2): p. 400-407.
81. Lee, J., M. Sadelain, and R. Brentjens, *Retroviral transduction of murine primary T lymphocytes.* Methods Mol Biol, 2009. **506**: p. 83-96.
82. Kochenderfer, J.N., et al., *Adoptive transfer of syngeneic T cells transduced with a chimeric antigen receptor that recognizes murine CD19 can eradicate lymphoma and normal B cells.* Blood, 2010. **116**(19): p. 3875-86.

83. Posey, A.D., Jr., et al., *Engineered CAR T Cells Targeting the Cancer-Associated Tn-Glycoform of the Membrane Mucin MUC1 Control Adenocarcinoma.* Immunity, 2016. **44**(6): p. 1444-54.
84. Sadelain, M., I. Riviere, and S. Riddell, *Therapeutic T cell engineering.* Nature, 2017. **545**(7655): p. 423-431.
85. Topalian, S.L., C.G. Drake, and D.M. Pardoll, *Immune checkpoint blockade: a common denominator approach to cancer therapy.* Cancer Cell, 2015. **27**(4): p. 450-61.
86. Suzanne L. Topalian, M.D., F. Stephen Hodi, M.D., Julie R. Brahmer, M.D., Scott N. Gettinger, M.D., David C. Smith, M.D., David F. McDermott, M.D., John D. Powderly, M.D., Richard D. Carvajal, M.D., Jeffrey A. Sosman, M.D., Michael B. Atkins, M.D., Philip D. Leming, M.D., David R. Spigel, M.D.,, M.D. Scott J. Antonia, Ph.D., Leora Horn, M.D., Charles G. Drake, M.D., Ph.D., Drew M. Pardoll, M.D., Ph.D., Lieping Chen, M.D., Ph.D., William H. Sharfman, M.D., Robert A. Anders, M.D., Ph.D., Janis M. Taube, M.D.,, and M.S. Tracee L. McMiller, Haiying Xu, B.A., Alan J. Korman, Ph.D., Maria Jure-Kunkel, Ph.D., Shruti Agrawal, Ph.D., Daniel McDonald, M.B.A., Georgia D. Kollia, Ph.D., Ashok Gupta, M.D., Ph.D., Jon M. Wigginton, M.D., and Mario Sznol, M.D., *Safety Immunity of checkpoint blockade.* N Engl J Med, 2012.
87. Ribas, A. and J.D. Wolchok, *Cancer immunotherapy using checkpoint blockade.* Science, 2018. **351**.
88. TeSlaa, T. and M.A. Teitell, *Techniques to monitor glycolysis.* Methods Enzymol, 2014. **542**: p. 91-114.
89. Gopalakrishnan, V., et al., *Gut microbiome modulates response to anti–PD-1 immunotherapy in melanoma patients.* Science, 2018. **359**: p. 97-103.
90. Berger, A., *Science commentary: Th1 and Th2 responses: what are they?* British Medical Journal, 2000. **321**(7258): p. 424-424.
91. Schuijs, M.J., et al., *ALLERGY Farm dust and endotoxin protect against allergy through A20 induction in lung epithelial cells.* Science, 2015. **349**(6252): p. 1106-1110.
92. Renz, H., et al., *An exposome perspective: Early-life events and immune development in a changing world.* Journal of Allergy and Clinical Immunology, 2017. **140**(1): p. 24-40.
93. Cohen Hubal, E.A., et al., *Children's exposure assessment: a review of factors influencing Children's exposure, and the data available to characterize and assess that exposure.* Environ Health Perspect, 2000. **108**(6): p. 475-86.
94. Spalt, E.W., et al., *Time-location patterns of a diverse population of older adults: the Multi-Ethnic Study of Atherosclerosis and Air Pollution (MESA Air).* J Expo Sci Environ Epidemiol, 2016. **26**(4): p. 436.
95. Klepeis, N.E., et al., *The National Human Activity Pattern Survey (NHAPS): a resource for assessing exposure to environmental pollutants.* J Expo Anal Environ Epidemiol, 2001. **11**(3): p. 231-52.
96. Schram, D., et al., *Bacterial and fungal components in house dust of farm children, Rudolf Steiner School children and reference children - the PARSIFAL Study.* Allergy, 2005. **60**(5): p. 611-618.
97. Thorne, P.S., et al., *Predictors of Endotoxin Levels in US Housing.* Environmental Health Perspectives, 2009. **117**(5): p. 763-771.
98. Gehring, U., et al., *Levels and predictors of endotoxin in mattress dust samples from East and West German homes.* Indoor Air, 2004. **14**(4): p. 284-292.

99. Giovannangelo, M., et al., *Determinants of house dust endotoxin in three European countries - the AIRALLERG study.* Indoor Air, 2007. **17**(1): p. 70-79.
100. Chen, C.M., et al., *Geographical variation and the determinants of domestic endotoxin levels in mattress dust in Europe.* Indoor Air, 2012. **22**(1): p. 24-32.
101. Casas, L., et al., *Endotoxin, extracellular polysaccharides, and (1-3)-glucan concentrations in dust and their determinants in four European birth cohorts: results from the HITEA project.* Indoor Air, 2013. **23**(3): p. 208-218.
102. Holst, G., et al., *Determinants of house dust, endotoxin, and beta-(1 -> 3)-D-glucan in homes of Danish children.* Indoor Air, 2015. **25**(3): p. 245-259.
103. Wickens, K., et al., *Determinants of endotoxin levels in carpets in New Zealand homes.* Indoor Air, 2003. **13**(2): p. 128-135.
104. Bischof, W., et al., *Predictors of high endotoxin concentrations in the settled dust of German homes.* Indoor Air, 2002. **12**(1): p. 2-9.
105. Gereda, J.E., et al., *Metropolitan home living conditions associated with indoor endotoxin levels.* Journal of Allergy and Clinical Immunology, 2001. **107**(5): p. 790-796.
106. Vanlaar, C.H., et al., *Predictors of house-dust-mite allergen concentrations in dry regions in Australia.* Allergy, 2001. **56**(12): p. 1211-1215.
107. Johnston, J.D., et al., *Differential effects of air conditioning type on residential endotoxin levels in a semi-arid climate.* Indoor Air, 2017. **27**(5): p. 946-954.
108. Lemons, A.R., et al., *Microbial rRNA sequencing analysis of evaporative cooler indoor environments located in the Great Basin Desert region of the United States.* Environmental Science-Processes & Impacts, 2017. **19**(2): p. 101-110.
109. Ellingson, A.R., et al., *The Prevalence of Dermatophagoides Mite Allergen in Colorado Homes Utilizing Central Evaporative Coolers.* Journal of Allergy and Clinical Immunology, 1995. **96**(4): p. 473-479.
110. Johnston, J.D., et al., *Evaporative Cooler Use Influences Temporal Indoor Relative Humidity but Not Dust Mite Allergen Levels in Homes in a Semi-Arid Climate.* Plos One, 2016. **11**(1).
111. Prasad, C., et al., *Effect of evaporative coolers on skin test reactivity to dust mites and molds in a desert environment.* Allergy and Asthma Proceedings, 2009. **30**(6): p. 624-627.
112. Macher, J.M. and J.R. Girman, *Multiplication of Microorganisms in an Evaporative Air Cooler and Possible Indoor Air Contamination.* Environment International, 1990. **16**(3): p. 203-211.
113. Liu, A.H., *Something old, something new: indoor endotoxin, allergens and asthma.* Paediatr Respir Rev, 2004. **5 Suppl A**: p. S65-71.
114. Liu, A.H., *Revisiting the hygiene hypothesis for allergy and asthma.* J Allergy Clin Immunol, 2015. **136**(4): p. 860-5.
115. Gehring, U., et al., *Exposure to endotoxin decreases the risk of atopic eczema in infancy: a cohort study.* J Allergy Clin Immunol, 2001. **108**(5): p. 847-54.
116. Stein, M.M., et al., *Innate Immunity and Asthma Risk in Amish and Hutterite Farm Children.* New England Journal of Medicine, 2016. **375**(5): p. 411-421.
117. Thorne, P.S., et al., *Endotoxin exposure is a risk factor for asthma: the national survey of endotoxin in United States housing.* American journal of respiratory and critical care medicine, 2005. **172**(11): p. 1371-1377.

118. Michel, O., et al., *Severity of asthma is related to endotoxin in house dust.* American journal of respiratory and critical care medicine, 1996. **154**(6): p. 1641-1646.
119. Michel, O., et al., *Domestic endotoxin exposure and clinical severity of asthma.* Clinical & Experimental Allergy, 1991. **21**(4): p. 441-448.
120. Oluwole, O., et al., *The association between endotoxin and beta-(1 -> 3)-D-glucan in house dust with asthma severity among schoolchildren.* Respiratory Medicine, 2018. **138**: p. 38-46.
121. Rylander, R., *Investigations of the relationship between disease and airborne (1 -> 3)-beta-D-glucan in buildings.* Mediators of Inflammation, 1997. **6**(4): p. 275-277.
122. Thorn, J. and R. Rylander, *Airways inflammation and glucan in a rowhouse area.* American Journal of Respiratory and Critical Care Medicine, 1998. **157**(6): p. 1798-1803.
123. Douwes, J., et al., *(1 -> 3)-beta-D-glucan and endotoxin in house dust and peak flow variability in children.* American Journal of Respiratory and Critical Care Medicine, 2000. **162**(4): p. 1348-1354.
124. Rylander, R., et al., *Airways inflammation, atopy, and (1 -> 3)-beta-D-glucan exposures in two schools.* American Journal of Respiratory and Critical Care Medicine, 1998. **158**(5): p. 1685-1687.
125. Thorn, J., L. Beijer, and R. Rylander, *Airways inflammation and glucan exposure among household waste collectors.* American journal of industrial medicine, 1998. **33**(5): p. 463-470.
126. Cardet, J.C., et al., *Income is an independent risk factor for worse asthma outcomes.* Journal of Allergy and Clinical Immunology, 2018. **141**(2): p. 754-+.
127. Kozyrskyj, A.L., et al., *Association Between Socioeconomic Status and the Development of Asthma: Analyses of Income Trajectories.* American Journal of Public Health, 2010. **100**(3): p. 540-546.
128. Douwes, J., et al., *Measurement of beta(1->3)-glucans in occupational and home environments with an inhibition enzyme immunoassay.* Applied and Environmental Microbiology, 1996. **62**(9): p. 3176-3182.
129. Noss, I., et al., *beta-(1,3)-Glucan Exposure Assessment by Passive Airborne Dust Sampling and New Sensitive Immunoassays.* Applied and Environmental Microbiology, 2010. **76**(4): p. 1158-1167.
130. Beard, J.D., et al., *Carbon nanotube and nanofiber exposure and sputum and blood biomarkers of early effect among US workers.* Environment international, 2018. **116**: p. 214-228.
131. Lubin, J.H., et al., *Epidemiologic evaluation of measurement data in the presence of detection limits.* Environmental health perspectives, 2004. **112**(17): p. 1691-1696.
132. Schmidt-Weber, C.B., *Overview: The Paradox of Microbial Impact on the Immune System in Allergy Prevention and Exacerbation*, in *Allergy Prevention and Exacerbation*. 2017, Springer. p. 1-9.
133. Bach, J.-F., *The effect of infections on susceptibility to autoimmune and allergic diseases.* New England journal of medicine, 2002. **347**(12): p. 911-920.
134. Platts-Mills, T.A., et al., *Seasonal variation in dust mite and grass-pollen allergens in dust from the houses of patients with asthma.* Journal of Allergy and Clinical Immunology, 1987. **79**(5): p. 781-791.

135. Portnoy, J., et al., *Environmental assessment and exposure control of dust mites: a practice parameter.* Annals of Allergy Asthma & Immunology, 2013. **111**(6): p. 465-507.
136. Arbes Jr, S.J., et al., *House dust mite allergen in US beds: results from the First National Survey of Lead and Allergens in Housing.* Journal of Allergy and Clinical Immunology, 2003. **111**(2): p. 408-414.
137. Platts-Mills, T.A., et al., *Dust mite allergens and asthma—a worldwide problem.* Journal of Allergy and Clinical Immunology, 1989. **83**(2): p. 416-427.
138. Nitschke, M., et al., *A cohort study of indoor nitrogen dioxide and house dust mite exposure in asthmatic children.* Journal of occupational and environmental medicine, 2006. **48**(5): p. 462-469.
139. Vervloet, D., et al., *The Epidemiology of Allergy to the House Dust Mite.* Revue Des Maladies Respiratoires, 1991. **8**(1): p. 59-65.
140. Weiler, E., et al., *Dust allergens within rural northern Rocky Mountain residences.* Jacobs journal of allergy and immunology, 2015. **1**(2): p. 1.
141. Johnston, J.D., et al., *Prevalence of house dust mite allergens in low-income homes with evaporative coolers in a semiarid climate.* Archives of environmental & occupational health, 2018. **73**(1): p. 38-41.
142. Fisk, W., *Impact of ventilation and aircleaning on asthma.* Clearing the Air: Asthma and Indoor Air Exposures, 2000: p. 327-393.
143. Chen, Q. and L.M. Hildemann, *The Effects of Human Activities on Exposure to Particulate Matter and Bioaerosols in Residential Homes.* Environmental Science & Technology, 2009. **43**(13): p. 4641-4646.
144. Ege, M.J., *Good and Bad Farming: The Right Microbiome Protects from Allergy*, in *Allergy Prevention and Exacerbation*. 2017, Springer. p. 51-68.
145. Ege, M.J., et al., *Not all farming environments protect against the development of asthma and wheeze in children.* Journal of Allergy and Clinical Immunology, 2007. **119**(5): p. 1140-1147.
146. Choi, H., et al., *Residential culturable fungi,(1‐3, 1‐6)‐β‐d‐glucan, and ergosterol concentrations in dust are not associated with asthma, rhinitis, or eczema diagnoses in children.* Indoor Air, 2014. **24**(2): p. 158-170.
147. Maheswaran, D., et al., *Exposure to Beta-(1, 3)-D-glucan in house dust at age 7–10 is associated with airway hyperresponsiveness and atopic asthma by age 11–14.* PloS one, 2014. **9**(6): p. e98878.
148. Zhang, Z., et al., *β-Glucan exacerbates allergic asthma independent of fungal sensitization and promotes steroid-resistant TH2/TH17 responses.* Journal of Allergy and Clinical Immunology, 2017. **139**(1): p. 54-65. e8.
149. Reponen, T., et al., *High environmental relative moldiness index during infancy as a predictor of asthma at 7 years of age.* Annals of Allergy, Asthma & Immunology, 2011. **107**(2): p. 120-126.
150. Iossifova, Y.Y., et al., *Mold exposure during infancy as a predictor of potential asthma development.* Annals of Allergy, Asthma & Immunology, 2009. **102**(2): p. 131-137.
151. Reponen, T., et al., *Infant origins of childhood asthma associated with specific molds.* Journal of Allergy and Clinical Immunology, 2012. **130**(3): p. 639-644. e5.
152. Dannemiller, K.C., et al., *Next‐generation DNA sequencing reveals that low fungal diversity in house dust is associated with childhood asthma development.* Indoor air, 2014. **24**(3): p. 236-247.

153. Ege, M.J., et al., *Exposure to environmental microorganisms and childhood asthma.* New England Journal of Medicine, 2011. **364**(8): p. 701-709.
154. Von Hertzen, L., I. Hanski, and T. Haahtela, *Natural immunity: biodiversity loss and inflammatory diseases are two global megatrends that might be related.* EMBO reports, 2011. **12**(11): p. 1089-1093.
155. von Mutius, E., et al., *Exposure to endotoxin or other bacterial components might protect against the development of atopy.* Clin Exp Allergy, 2000. **30**(9): p. 1230-4.
156. Izadi, N., K.K. Brar, and B.J. Lanser, *Evaporative coolers are not associated with dust mite or mold sensitization in a large pediatric cohort.* Annals of Allergy, Asthma & Immunology, 2018. **120**(5): p. 542-543.
157. Aldous, M.B., et al., *Evaporative cooling and other home factors and lower respiratory tract illness during the first year of life.* American journal of epidemiology, 1996. **143**(5): p. 423-430.